UNIVERSITÀ DEGLI STUDI DI BARI

FACOLTÀ DI SCIENZE

MATEMATICHE, FISICHE E NATURALI

Corso di Laurea in Fisica

REPLICA TRICK IN A FINITE SIZE SPIN GLASS

Tesi di Laurea in Fisica Teorica

Relatori:

Prof. Saverio Pascazio,

Prof. Paolo Facchi

Laureando:

Marco Di Gennaro

22 settembre 2010

Contents

Introduction

Spin Glasses are magnetic alloys in which a great quantity of impurities is spread at random. The strength of the interactions between the magnetic moments of the atoms in the alloy is not constant and the interactions are sometimes "in conflict" with each other.

Due to its generality, spin glass is particularly convenient for the modelization of different kinds of disordered systems. Ideas and methods originating in the spin glass context have been fruitful in the study of structural glasses in condensed-matter physics, optimization in computer science, quantum information, econophysics, etc.

In the thermodynamic limit, no conventional long-range order can be established (neither ferromagnetic nor anti-ferromagnetic). Nevertheless, the system exhibits a new kind of order in which the spins are aligned in random directions.

There is a phase transition that separates the paramagnetic phase from a low-temperature phase of matter in which spins seem to remain out of equilibrium even if they are left to relax under constant experimental conditions for days

or weeks. This is a metastable phase that can be found, for example, in real glasses. This behavior is due to the fact that spins "freeze" according to extremely complex ordering patterns. In spite of this, it is believed that the equilibrium properties of their low-temperature phase control their non-equilibrium behavior. All these features can be interpreted simply if we suppose that an extremely large number of pure states (or phases) exist for very large systems.

Replicas have been proposed as a crucial tool in the study of spin glass systems [12], and a correct solution for the infinite spin glass has been found (Parisi's Replica Symmetry Breaking [7], [9], [8]) with a successful Ansatz (mean field approximation).

In this work, we shall analyze a finite size spin glass, for which the free energy will be found to be an analytic function. We begin studying the simplest non-trivial system, i.e., the system with $N = 3$ spins. The partition function can be computed exactly for this system but, however, this will become almost impossible when we have a finite size system with, for example, 10 spins.

Using the symmetric replica approach, we will show that good predictions for the free energy of the system can be obtained within the limit of low temperatures for an arbitrary value of N (number of spins), without explicitly computing the partition function.

Instead, the tool of replica symmetry breaking cannot be exploited since it is valid only in the thermodynamic limit.

This thesis is organized as follows. The spin glass model and the replica approach are introduced in the first chapter. We do not derive any equation of motion from the Hamiltonian. Rather, we investigate the equilibrium state. The concepts of *frustration* and *quenched average* are presented.

In the second chapter, the replica approach is applied to calculate the free energy density of the system. The results are compared with the real behavior of the system in various ranges of temperature.

In the third chapter, we present improvements of our technique and good predictions for the trend of the free energy for the $N = 3$ spin system.

The agreement between the exact results and our technique is considered in the fourth chapter. We obtain the exact β (inverse temperature) dependence and the analytical value of the energy ground state for the 3-spin system.

In the fifth chapter we illustrate a generalization of our approach, which yields to an efficient rule for the calculation of the free energy of an arbitrary N-spin system.

Chapter 1

Spin Glass

In this chapter, we present the spin glass model and concentrate on the calculation of the free energy. The focus will be on the properties of the model and on the different stages needed for an evaluation of the thermodynamic quantities that is physically consistent. We introduce the concepts of disorder and frustration, that mainly characterize the model. In the last section the replica symmetric approach is presented.

1.1 The model

A spin glass is a system composed of N dichotomic variables s_i:

$$\{s\} = (s_1, s_2, ..., s_N), \qquad s_i = \pm 1, \tag{1.1}$$

placed at the sites of a lattice, with i labeling the site of the lattice. Each couple of spins is connected by an edge and interact.

The Hamiltonian reads:

$$H_J(s) = -\sum_{i<j}^{N} J_{ij} s_i s_j + \sum_{i=1}^{N} h_i s_i. \tag{1.2}$$

In the first summation, each couple of spins is considered only once. J_{ij} denotes the interaction between spins i and j, while h_i is a magnetic field acting on spin i. To minimize the Hamiltonian (1.2), two spins tend to align themselves if J_{ij} is positive, yet, if $J_{ij} < 0$, they counteralign. Moreover, each spin tends to align to the magnetic field present in the site.

The spin glass behavior is much more complicated with respect to the Ising model ([3]) since, in the Hamiltonian (1.2) , the J_{ij}'s are random variables distributed according to some distribution function $P(J)$, while in the Ising model, the coupling is the same for each couple of neighbor spins. For an Ising model, this feature of the interaction leads to the presence of two different phases: a paramagnetic phase in which spins are "randomized"with local magnetization $m_i = \langle s_i \rangle$ different from zero only if a magnetic field is present and a ferromagnetic phase where the system assumes a definite value for the global magnetization $(\frac{1}{N}\sum_i m_i)$[1]. A phase transition takes place when the temperature T becomes smaller with respect to a critical value T_c and the magnetic field is set to zero. All the spins, in this case, assume the same

[1]Here $\langle \dots \rangle$ denotes the thermal average

direction (the limit of vanishing magnetic field in eq.(1.2) should be taken after having reached $T < T_c$).

The physical motivation for working here with a random Hamiltonian is to model the effects of impurities in the magnetic alloy. The distribution function of the couplings $P(J)$ is the feature that distinguishes various models.

In the literature one can find different kinds of probability distribution function, which can be distinguished if they are short-ranged or long-ranged [5].

If all spins interact with each other, the interaction of the model will have an infinite range, otherwise, if J_{ij} is different from zero only for pairs of nearby spins the model will have a short range interaction. We will use a long range interaction for our computations, in particular the so called Sherrington-Kirkpatrick (SK) model [12] [13] , in which all the J_{ij}'s have the same Gaussian probability distribution:

$$P(J_{ij}) = \left(\frac{1}{2\pi\sigma^2}\right)^{1/2} \exp\left\{-\frac{J_{ij}^2}{2\sigma^2}\right\}. \tag{1.3}$$

In some spin glasses, the spins can also take other values besides ± 1 (Ising spins) and the energy has a form different from eq.(1.2).

Our thermodynamic quantities shall depend on the J_{ij}'s configuration. All the results achieved depend on the characteristic of the probability distribution function $P(J)$. Let introduce the partition function for our model:

$$Z_J(\beta) = \sum_{\{s\}} e^{-\beta H_J(s)}. \tag{1.4}$$

The sum over $\{s\}$ runs over all the configurations of the set $(s_1, s_2, \dots s_N)$. Since $s_i = \pm 1$ we have 2^N total spin configurations. The free energy density is:

$$f_J(\beta) = -\frac{1}{\beta N} \ln \left(Z_J(\beta) \right). \tag{1.5}$$

The subscript J in equations (1.4) and (1.5) means that these quantities are computed by choosing a fixed realization of the interaction parameters J_{ij} in the Hamiltonian (1.2).

Physically, the necessity of computing the free energy at fixed J_{ij}'s arise because the evolution of the J_{ij}'s configuration occurs so slowly to appear "frozen"during the observation [2]. Thus there are two different time scales that are relevant for the dynamics of the whole model: the time scale relative to the motion of the impurities and the time scale relative to the spin dynamics that is much shorter with respect to the former. Hence, any back-reaction of the spins over the coupling constants will not be considered and we can consider the set of the J_{ij} as static.

To hold this feature in our mathematical model, in the following, we shall distinguish between "thermal "and "quenched "variables according to their relaxation time.

1.2 Disorder

From equations (1.4) and (1.5) we see that both $Z_J(\beta)$ and $f_J(\beta)$ depend on the set of control parameters $\{J\}$:

$$\{J\} = (J_{12}, J_{23}, \ldots, J_{1N}, J_{23}, \ldots, J_{N-1\,N}),$$

besides on the spins configuration $\{s\}$. Since we are using an infinite range model, each spin interacts with all the others and the number of couplings is equal to the number of pairs of spins, i.e. $\frac{N(N-1)}{2}$.

A correct average on our *ensemble* implies a double averaging procedure. For any arbitrary observable $O_J(s)$ (function of the spins and the coupling constants configuration), we shall first compute the thermal average, by defining the probability distribution for a spins configuration with the Boltzmann weight at temperature $T = \frac{1}{k_B\beta}$:

$$O_J = \langle O_J(s) \rangle = \frac{1}{Z_J(\beta)} \sum_{\{s\}} e^{-\beta H_J(s)} O_J(s). \tag{1.6}$$

Subsequently, the average over the coupling constants distribution (the "quenched average"hereafter) has to be taken:

$$\overline{O_J} = \prod_{i<k} \int dJ_{ik} P(J_{ik}) O_J. \tag{1.7}$$

The J_{ij}'s probability distribution function $P(J)$ (1.3) should be chosen here in such a way that the quenched free energy density $f(\beta) = \overline{f_J(\beta)}$ be independent of the number of spins, and the free energy $F(\beta) = Nf(\beta)$ be an extensive quantity. This result can be achieved by choosing the standard deviation in (1.3) in such a way taht:

$$\overline{J_{ik}} = 0, \qquad \overline{J_{ik}^2} = \frac{1}{N}, \qquad J_{ik} = J_{ki}, \tag{1.8}$$

where the average $\overline{(\dots)}$ has been defined in eq.(1.7). To obtain eq.(1.8) we see that:

$$\begin{aligned} \overline{J_{ik}^2} &= \int dJ_{ik} P(J_{ik}) J_{ik}^2 \\ &= \sqrt{\frac{1}{2\pi\sigma^2}} \int_{-\infty}^{\infty} dJ_{ik} e^{-\frac{J_{ik}^2}{2\sigma^2}} J_{ik}^2 = \sigma^2, \end{aligned} \tag{1.9}$$

having utilized:

$$\int_{-\infty}^{\infty} y^2 e^{-ay^2} dy = \sqrt{\frac{\pi}{a}} \left(\frac{1}{2a}\right). \tag{1.10}$$

We then will set:

$$\sigma^2 = \frac{1}{N} \tag{1.11}$$

in eq.(1.3).

In the thermodynamic limit the total energy $F(\beta)$ results to be proportional to N. This can be obtained with the replica symmetric breaking pattern, within the $N \to \infty$ limit: [4], [3], [5]. In this thesis we obtain the same result for a finite size system, without breaking the replica symmetry.

1.3 Symmetries and Frustration

We can highlight two kind of symmetries for a spin glass described by the Hamiltonian (1.2) when the magnetic field is zero:

- with $h = 0$, $H(s)$ becomes a quadratic form of the spins and it results to be invariant under the action of the spin-flip operator P, which acts as:

$$P(s_i) = -s_i, \quad \forall i. \tag{1.12}$$

  This is a global symmetry, broken if a magnetic field is present.

- (1.2) with $h = 0$ is left invariant under

$$\begin{cases} s_i \to -s_i \\ J_{ij} \to -J_{ij} \end{cases} \quad \forall j \text{ adjacent to } i, \tag{1.13}$$

The simplest model in which this symmetry is evident is $N = 3$. Eq.(1.2) in this case becomes (by taking $h_i = 0 \quad \forall i$):

$$H_J(s) = -\sum_{i<j}^{3} J_{ij} s_i s_j = -\sum_{i}^{3} J_i s_i s_{i+1}, \tag{1.14}$$

where we have used the boundary condition $s_4 = s_1$ and have called:

$$J_{ij} = J_{i,i+1} \equiv J_i,$$

without ambiguity, since the spins are all firsts neighbors and we have chosen periodic boundary conditions.

If we take $J_i = J$ and $s_i = 1$, $\forall i$, the energy of the system would be equal to $-3J$. By reversing the sign of one spin and its two adjacent couplings we still have $E = -3J$ (see Fig. 1.1). This symmetry is a peculiarity of a spin

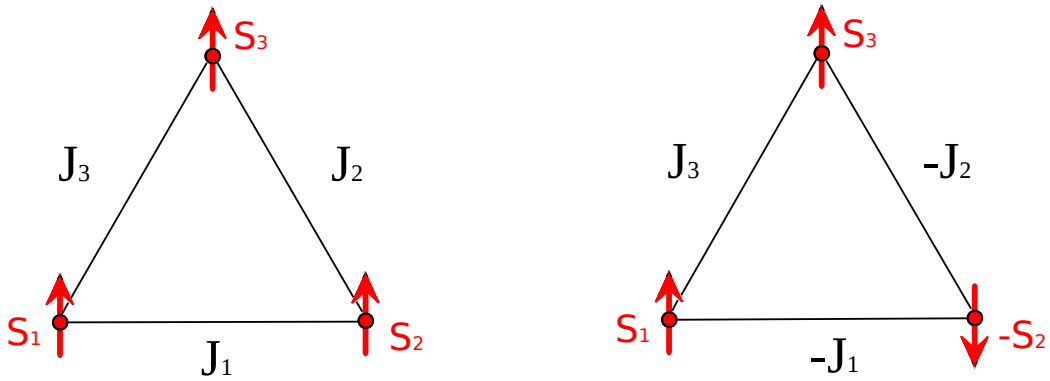

Figure 1.1: The simplest non-trivial spin glass is obtained for $N = 3$: it is described by the Hamiltonian (1.14) which results invariant under (1.13).
In this figure, we show two possible configurations of the $N = 3$ spin system. They have the same energy and can be obtained by applying (1.13).

glass and arises since the coupling constant are not fixed in the Hamiltonian. The ground state of the system gains a great level of degeneracy (the same operation of reversion can be carried out for each of the other two spins, thus, for a $N = 3$ spins system we have 6 equivalent ground states).

It is not possible, however, to place the couplings in an arbitrary way: we in fact encounter the problem of frustration, first introduced by *G. Touluse* in [16].

This problem arises when we choose the set of J_{ij}'s in such a way that the

sign of their product is negative. In this case, we run into the impossibility for the couplings to be all satisfied at the same time.

To satisfy a coupling (for example J_{ij}) means to dispose its adjacent spins (here s_i and s_j) in such a way that their product (i.e. $J_{ij}s_is_j$) results minimized. We can see what happens, as an example, with 3 spins by choosing in the Hamiltonian (1.16) the following set of couplings:

$$\{J_i\} = (J_1, J_2, J_3) = (1, -1, 1), \tag{1.15}$$

$$\begin{aligned} H_J(s) &= -J_1 s_1 s_2 - J_2 s_2 s_3 - J_3 s_3 s_1 = \\ &= -s_1 s_2 + s_2 s_3 - s_3 s_1. \end{aligned} \tag{1.16}$$

Thus, by fixing the value of one spins (for example $s_1 = 1$), we should take $s_2 = 1$ and $s_3 = 1$ to minimize the first and the third term of the Hamiltonian, but now, with this choice, the the second term results to be not minimized. The same happens with each other choice of the spin's set. We conclude that there is no spin configuration which simultaneously minimizes each term in the Hamiltonian (1.16).

In Fig. 1.2 we show the 3-spins chain, with a frustrated interaction. We set $s_1 = 1$ and now, running the chain clockwise, we put $s_3 = 1$ according to J_3. There isn't now any way of placing s_2 and satisfying both J_2 and J_1.

The same thing happens if we run the chain in a counterclockwise sense or if we begin by placing $s_1 = -1$.

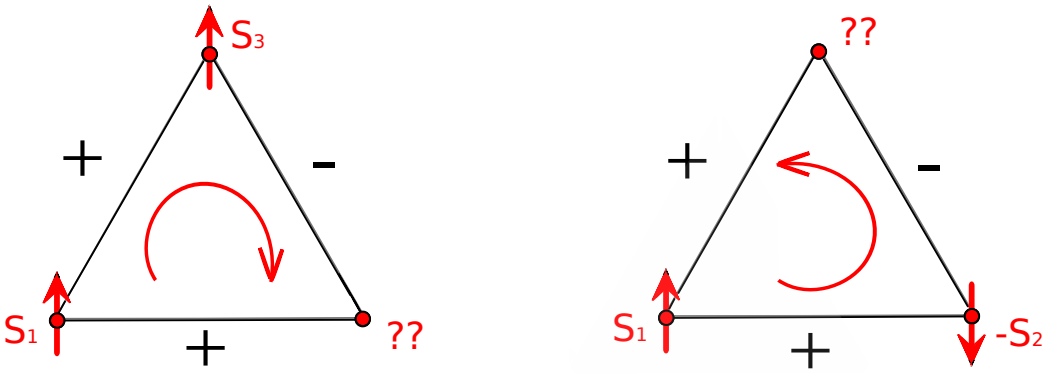

Figure 1.2: The phenomena of frustration exists for the $N = 3$ spins system. Since the product of the three couplings in figure has negative sign we cannot place all the spins in such a way to "satisfy" all the couplings, i.e., all the terms in the Hamiltonian (1.16) cannot be simultaneously minimized by any choice of the spin's configuration.

More generally, given a closed spin chain c built on the lattice, we can define the frustration function:

$$\Phi = \prod_c \text{sign}\left(J_{ij}\right), \tag{1.17}$$

where the product runs over all the edges belonging to the circuit c: the system is frustrated if $\Phi = -1$. We can imagine that in an N-vertices lattice spin A sends a message to the spin B placed at a certain distance. The message contains information about the orientation that B should assume to minimize the energy according to the orientation of A. This message can choose different paths to reach B and the information contained is modified according to the path followed. So really, B receives a great number of messages, and cannot decide which position is the best.

Disorder is the central feature of the model. Sometimes however, it results not to be so important. It can be eliminated with a redefinition of the variables as it happens in the "Mattice magnet"[3], in which the couplings are defined in the following way:

$$J_{ij} = \xi_i \xi_j, \tag{1.18}$$

where $\xi_i = \pm 1$ with equal probability. In this case, it is enough to substitute $s_i \to \xi_i s_i$ to recover an Ising model. On the contrary, "serious"disorder cannot be eliminated and is present only if also frustration is present [2].

1.4 The replica approach

According to Sec. 1.2, to give a physically consistent formula for the free energy, we must rewrite eq.(1.5) using the quenched average.

$$f(\beta) = \overline{f_J(\beta)} = \int \prod_{i<k} dJ_{ik} P(J_{ik}) f_J(\beta) = -\frac{1}{\beta N} \overline{\ln(Z_J(\beta))}, \tag{1.19}$$

The term $\frac{1}{\beta N}$ does not depends on the realization of the J_{ij}'s, thus we can bring it out from the integral over the $J'_{ij}s$. We have to deal with the mean of a logarithm that, in all relevant situations, is impossible to solve analytically. We try to find an alternative way which enables us to simplify this expression. In a nutshell, we try to get the quenched average of $f_J(\beta)$ from the partition function of a set of n uncoupled copies of the initial system, each with the

same partition function. We observe that:

$$x^n = \mathrm{e}^{n \ln x}, \tag{1.20}$$

thus, for $n \to 0$

$$\mathrm{e}^{n \ln x} \simeq 1 + n \ \ln x \Rightarrow \ln \ x = \lim_{n \to 0} \frac{x^n - 1}{n}, \tag{1.21}$$

and this holds independently of the value of x. We can write:

$$\overline{\ln(Z_J(\beta))} = \lim_{n \to 0} \frac{\overline{Z_J(\beta)^n - 1}}{n} = \lim_{n \to 0} \frac{\overline{Z_J(\beta)^n} - 1}{n}. \tag{1.22}$$

Using this "trick"and the well known approximation

$$nx \simeq \ln(1 + nx), \quad \text{for } nx \ll 1,$$

for $\overline{\ln(Z_J(\beta))}$ we obtain:

$$n\overline{\ln(Z_J(\beta))} \simeq \ln(1 + n\overline{\ln(Z_J(\beta))}), \quad \text{for } n \to 0. \tag{1.23}$$

Using now eq.(1.22)

$$\begin{aligned} \overline{\ln(Z_J(\beta))} &= \lim_{n \to 0} \frac{1}{n} \ln(1 + n\overline{\ln(Z_J(\beta))}) \\ &= \lim_{n \to 0} \frac{1}{n} \ln \left[1 + n \left(\frac{\overline{Z_J(\beta)^n} - 1}{n} \right) \right] = \lim_{n \to 0} \frac{1}{n} \ln(\overline{Z_J(\beta)^n}), \end{aligned} \tag{1.24}$$

and

$$\overline{f_J(\beta)} = -\frac{1}{\beta N}\lim_{n\to 0}\frac{1}{n}\ln(\overline{Z_J(\beta)^n}). \tag{1.25}$$

Now, instead of the mean of a logarithm, we have the logarithm of an averaged quantity that is much easier to compute. We should solve a certain number of Gaussian integrals and then take the logarithm of the result.

For n integer we can think that we are dealing with n replicas of the systems, each one with an identical partition function. The partition function of the whole system will be the n^{th} power of the partition function eq.(1.4):

$$Z_J(\beta)^n = \sum_{\{s^1\}}\sum_{\{s^2\}}\cdots\sum_{\{s^n\}} e^{(-\sum_{a=1}^{n}\beta H_J(s^a))}. \tag{1.26}$$

This means that the couplings realization is the same for each virtual system. Now the variables s_i^a carry two index, the upper one denoting the replica and varing from 1 to n, the lower one denoting the site and varing from 1 to N. In two different replicas of the system, between two fixed vertices of the lattice $\{i, j\}$, the couple of spins can assume 4 configurations:

$$\{s_i, s_j\} = \{\Uparrow; \uparrow\downarrow; \downarrow\uparrow; \Downarrow\},$$

but the value of the couplings J_{ij} between the spins is always the same.

It is necessary to understand that we must mediate between the two pictures presented, i.e. the physical idea of n non interacting replicas of the system and the mathematical necessity of taking the limit $n \to 0$ in equations (1.22)

and (1.25).

In the following chapter, we will analyze the $N = 3$ spin system, for which it is possible to perform some explicit calculation. We will understand how the many-replicas system behaves and how we can intend the $n \to 0$ limit.

Chapter 2

Finite-Size Spin Glasses

In this chapter, we analyze the simplest non trivial spin glass, i.e. the $N = 3$ spin system. The replica trick is exploited for the computation of the partition function (eq.(1.23)). The $n \to 0$ limit (being n the replica's index) is studied with a polynomial interpolation, in order to achieve a form of the free energy density that is consistent with eq.(1.25).
The results obtained are compared with numerical simulations and some attempts to improve our results are introduced.

2.1 The free energy

As told in Sec. 1.3, the simplest non-trivial spin glass is the 3-spin system. Let us consider the particular form of the Hamiltonian (1.2)

$$H_J(s) = \sum_{i=1}^{3} J_i s_i s_{i+1}, \tag{2.1}$$

with $s_4 \equiv s_1$, with magnetic field h_i null on each site and with:

$$J_{ij} = J_{i,i+1} \equiv J_i. \tag{2.2}$$

Since the magnetic field is equal to zero, the Hamiltonian (2.1) is symmetric with respect to the spin flip operator P introduced in Chapter 1 with eq.(1.12). Thus, although the total number of spin configurations is $2^N = 8$, we have that only $2^{N-1} = 4$ of them are relevant, and this makes possible some explicit computation. The partition function reads:

$$\begin{aligned} Z_J(\beta) = \sum_{\{s\}} e^{-\beta H_J(s)} = 2 \big(& e^{-\beta(J_1+J_2+J_3)} + e^{-\beta(J_1-J_2-J_3)} \\ & + e^{-\beta(-J_1-J_2+J_3)} + e^{-\beta(-J_1+J_2-J_3)} \big), \end{aligned} \tag{2.3}$$

where $\{s\}$ denotes the sum over all the spin configurations and with $H_J(s)$ introduced in eq.(2.1).

The quenched free energy density of the system is given by:

$$\overline{f_J(\beta)} = -\frac{1}{\beta N}\overline{\ln(Z_J(\beta))}, \tag{2.4}$$

where N is the number of spins and the symbol $\overline{(\dots)}$ denotes the quenched average, introduced in eq.(1.7) in Sec. 1.2. The couplings probability distribution function for the $N = 3$ spin system, defined in eq.(1.3), reads:

$$P(\vec{J}) = \prod_{i=1}^{3} P(J_i) = \left(\frac{1}{2\pi\sigma^2}\right)^{\frac{3}{2}} e^{-\frac{1}{2\sigma^2}(J_1^2+J_2^2+J_3^2)}, \tag{2.5}$$

Where $\vec{J} = (J_1, J_2, J_3)$[1]. We note that with 3 spins we have no difference between short-range and long-range model (cfr. Sec. 1.1), since all the spins are neighbors.

According to eq.(1.7) and eq.(2.3), the quenched average of $\ln(Z_J(\beta))$ is:

$$\begin{aligned}\overline{\ln(Z_J(\beta))} &= \prod_{i=1}^{3}\int dJ_i P(J_i)\left(\ln(Z_J(\beta))\right) = \\ &= \int d\vec{J} P(\vec{J}) \ln\left(\sum_{\{s\}} e^{-\beta H_J(s)}\right).\end{aligned} \tag{2.6}$$

The behavior of $\overline{\ln(Z_J(\beta))}$ vs. β in displayed in Fig. 2.1. Its trend is linear when $\beta \gtrsim 1$. This feature can be explained if we study the $\beta \to \infty$ limit of $\overline{\ln(Z_J(\beta))}$. Indeed, since our system has a finite size, the free energy is an analytical function, i.e. it is a smooth function everywhere. The Hamiltonian

[1] we shall set $\sigma^2 = \frac{1}{3}$ at the end of the calculation, as required in(1.8)

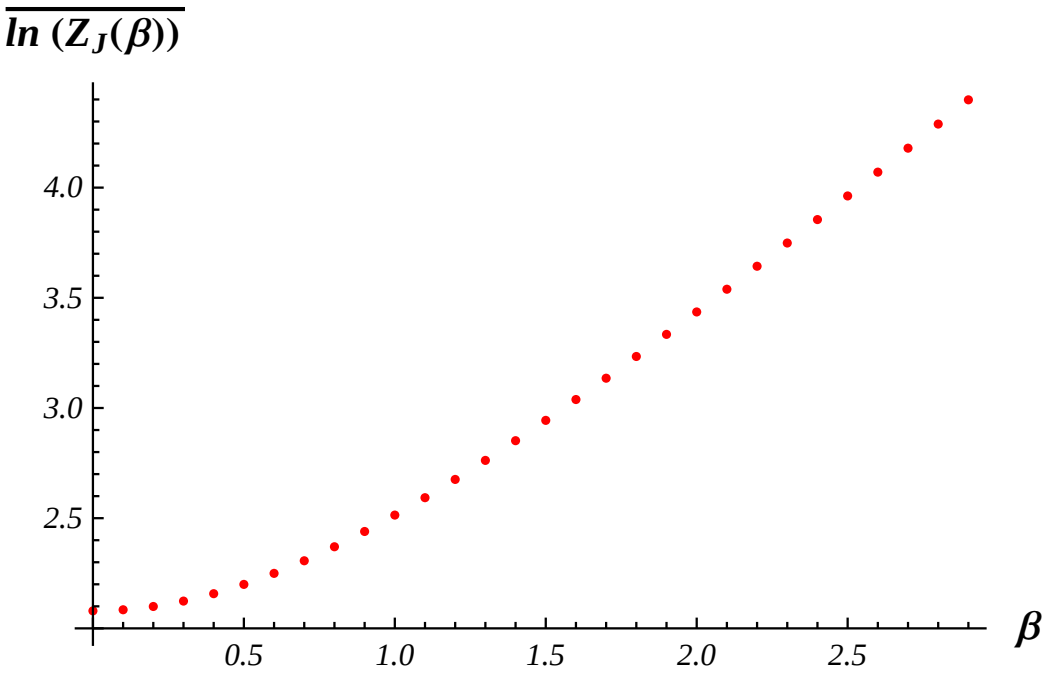

Figure 2.1: The red points are the values numerically computed for $\overline{\ln(Z_J(\beta))}$ (eq.(2.6)). The behavior is linear for $\beta \gtrsim 1$, and the limit slope for $\beta \to \infty$ is the value of the energy ground state according to (2.8).

(2.1) has a well defined minimum [2]:

$$E_0 = \overline{H_0} = \overline{\min_{\{s\}}[H_J(s)]}, \tag{2.7}$$

thus, we can approximate the sum over all the spin configurations in the partition function with the most important term, writing:

$$\overline{\ln(Z_J(\beta))} = \overline{\ln \sum_{\{s\}} e^{-\beta H_J(s)}} \simeq \overline{\ln e^{-\beta H_0}} = -\beta E_0. \tag{2.8}$$

Thus, when $\beta \to \infty$, the system reaches its ground state and, from (2.4), the free energy density reaches a constant value:

$$\lim_{\beta\to\infty} \overline{f_J(\beta)} = -\frac{1}{N} \lim_{\beta\to\infty} \frac{\overline{\ln(Z_J(\beta))}}{\beta} = \frac{1}{3} E_0, \tag{2.9}$$

having set $N = 3$. Therefore, the limit slope of $\overline{\ln(Z_J(\beta))}$ in Fig. 2.1 (for $\beta \gtrsim 1$) is E_0.

The behavior of the quenched free energy density is shown in Fig. 2.2, according to a numerical integration. As we expected, when β increases, $\overline{f_J(\beta)}$ reaches a *plateau*. This properties arises from the behavior of $\overline{\ln(Z_J(\beta))}$.

[2] See Sec. 4.1 for the exact calculation of E_0.

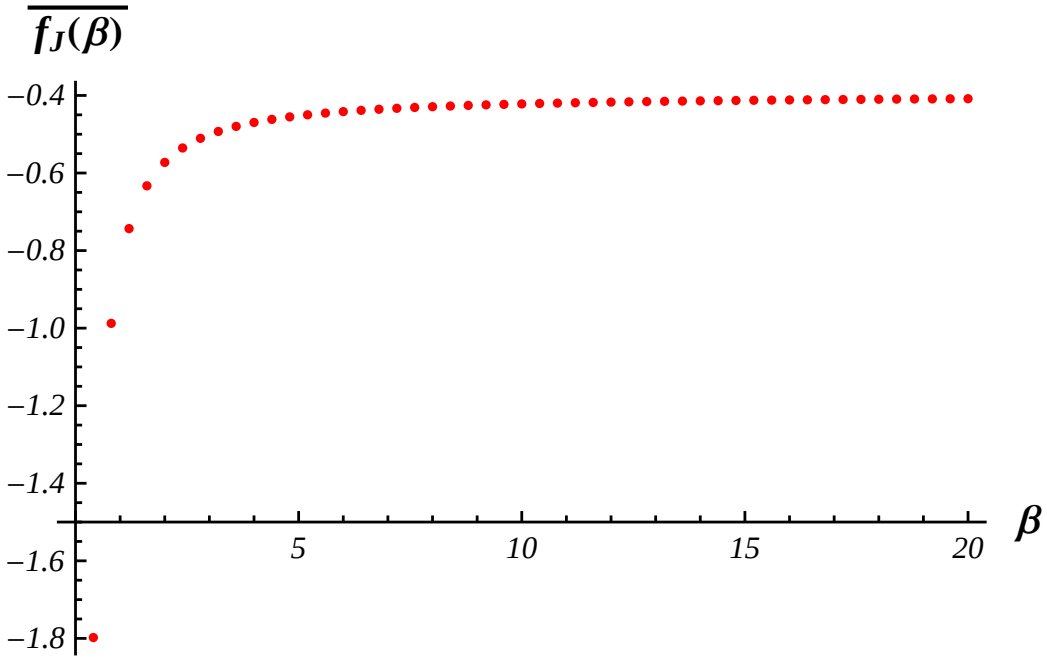

Figure 2.2: The red points represent the values of the quenched free energy density $\overline{f_J(\beta)}$, numerically computed using equations (2.4) and (2.6). The convergence to an equilibrium state is manifest.

2.2 The replica approach

We write the replica approximation eq.(1.25) for the quenched free energy density of our system:

$$\overline{f_J(\beta)} = -\frac{1}{N\beta}\lim_{n\to 0}\frac{1}{n}\ln\overline{Z_J(\beta)^n}. \tag{2.10}$$

Let us introduce a new quantity, that will be of central interest in this work, by scaling the free energy density respect to $\frac{1}{\beta}$ in the replica approximation. We define the "pressure":

$$g_n(\beta) \equiv \frac{1}{n}\ln\overline{Z_J(\beta)^n}. \tag{2.11}$$

The free energy density reads:

$$\overline{f_J(\beta)} = -\frac{1}{N\beta}\lim_{n\to 0} g_n(\beta). \tag{2.12}$$

In the next calculations we shall set $N = 3$ in eq.(2.10) and eq.(2.12).
As a first step, we shall compute the n^{th} power of the partition function $Z_J(\beta)$. From eq.(2.3), we have:

$$\begin{aligned} Z_J(\beta)^n =& \left[\sum_{\{s\}} \mathrm{e}^{-\beta H_J(s)}\right]^n \\ =& 2^n \left[\mathrm{e}^{-\beta(J_1+J_2+J_3)} + \mathrm{e}^{-\beta(J_1-J_2-J_3)}\right. \\ &\left. + + \mathrm{e}^{-\beta(-J_1-J_2+J_3)} + \mathrm{e}^{-\beta(-J_1+J_2-J_3)}\right]^n. \end{aligned} \tag{2.13}$$

The n^{th} power of a polynomial made of four terms can be calculated using the Multinomial Theorem (see Appendix (A.2)). In our case, the term in square brackets in the previous equation becomes:

$$\begin{aligned}\left[\mathrm{e}^{-\beta(J_1+J_2+J_3)} + \mathrm{e}^{-\beta(J_1-J_2-J_3)} + \mathrm{e}^{-\beta(-J_1-J_2+J_3)} + \mathrm{e}^{-\beta(-J_1+J_2-J_3)}\right]^n \\ = \sum_{|\vec{K}|=n} \frac{n!}{k_1!k_2!k_3!k_4!} \left[\mathrm{e}^{-\beta(J_1+J_2+J_3)k_1} \mathrm{e}^{-\beta(J_1-J_2-J_3)k_2}\right. \\ \left. \times\, \mathrm{e}^{-\beta(-J_1-J_2+J_3)k_3} \mathrm{e}^{-\beta(-J_1+J_2-J_3)k_4}\right],\end{aligned} \tag{2.14}$$

where we have introduced the vector $\vec{K} = (k_1, k_2, k_3, k_4)$ and the summation is carried over all the configuration of $\vec{K}$'s components such that:

$$|\vec{K}| = k_1 + k_2 + k_3 + k_4 = n. \tag{2.15}$$

This condition is satisfied introducing a new vector $\vec{k} = (k_1, k_2, k_3)$ such that:

$$|\vec{k}| = k_1 + k_2 + k_3 = n - k_4 \leq n. \tag{2.16}$$

Thus, eq.(2.14) becomes:

$$\begin{aligned}
&\left[\mathrm{e}^{-\beta(J_1+J_2+J_3)}+\ \mathrm{e}^{-\beta(J_1-J_2-J_3)}+\mathrm{e}^{-\beta(-J_1-J_2+J_3)}+\mathrm{e}^{-\beta(-J_1+J_2-J_3)}\right]^n \\
&\quad=\sum_{|\vec{k}|\leq n}\frac{n!}{k_1!k_2!k_3!(n-k_1-k_2-k_3!)}\left[\mathrm{e}^{-\beta(J_1+J_2+J_3)k_1}\right. \\
&\qquad\left.\times\ \mathrm{e}^{-\beta(J_1-J_2-J_3)k_2}\mathrm{e}^{-\beta(-J_1-J_2+J_3)k_3}\mathrm{e}^{-\beta(-J_1+J_2-J_3)(n-|\vec{k}|)}\right] \\
&\quad=\sum_{|\vec{k}|\leq n}\binom{n}{\vec{k}}\left[\mathrm{e}^{-\beta(J_1+J_2+J_3)k_1}\mathrm{e}^{-\beta(J_1-J_2-J_3)k_2}\right. \\
&\qquad\left.\times\ \mathrm{e}^{-\beta(-J_1-J_2+J_3)k_3}\mathrm{e}^{-\beta(-J_1+J_2-J_3)(n-|\vec{k}|)}\right] \\
&\quad=\sum_{|\vec{k}|\leq n}\binom{n}{\vec{k}}\mathrm{e}^{-\beta J_1(n-2k_2-2k_3)}\mathrm{e}^{-\beta J_2(n-2k_1-2k_2)}\mathrm{e}^{-\beta J_3(n-2k_1-2k_3)}.
\end{aligned} \tag{2.17}$$

Where, in the last line we have rearranged the various terms in the exponentials. The quenched n^{th} power of the partition function is then:

$$\begin{aligned}
\overline{Z_J(\beta)^n}&=\int d\vec{J}P(\vec{J})\left[Z_J(\beta)\right]^n=2^n\sum_{|\vec{k}|\leq n}\binom{n}{\vec{k}} \\
&\quad\times\int d\vec{J}P(\vec{J})\left(\mathrm{e}^{-\beta J_1(n-2k_2-2k_3)}\mathrm{e}^{-\beta J_2(n-2k_1-2k_2)}\mathrm{e}^{-\beta J_3(n-2k_1-2k_3)}\right).
\end{aligned} \tag{2.18}$$

It is now straightforward, by using the Gaussian formula:

$$\int_{-\infty}^{\infty}e^{-ay^2+by}dy=\sqrt{\frac{\pi}{a}}e^{\frac{b^2}{4a}}, \tag{2.19}$$

to integrate eq.(2.18), which yields:

$$\overline{Z_J(\beta)^n} = 2^n \sum_{|k|\leq n} \binom{n}{\vec{k}} \mathrm{e}^{\frac{\beta^2\sigma^2}{2} r^2(n,\vec{k})}, \tag{2.20}$$

where

$$\begin{aligned} r^2(n,\vec{k}) =& (n-2k_1-2k_2)^2 + \\ & (n-2k_1-2k_3)^2 + (n-2k_2-2k_3)^2. \end{aligned} \tag{2.21}$$

The pressure $g_n(\beta)$ can be expressed as follows:

$$g_n(\beta) = \frac{1}{n} \ln \left\{ 2^n \sum_{|k|\leq n} \binom{n}{\vec{k}} \mathrm{e}^{\frac{\beta^2\sigma^2}{2} r^2(n,\vec{k})} \right\}. \tag{2.22}$$

Fig. 2.3 shows the behavior of the pressure when n varies and for $\beta = 1$. All the points are on a straight line except for the former ones. These are very important points for us, since we are interested in the $n \to 0$ limit.

Mathematically it is difficult to define such a limit for $g_n(\beta)$, since $n \in \mathbb{N}$ and we do not have an accumulation point for a discrete variable. We can try to get some information about this limit by providing an analytic continuation of the function $g_n(\beta)$.

We shall look for a continuous function of a variable $x \in \mathbb{R}$, that takes the same values of $g_n(\beta)$ when $x = n$. With a continuous variable, it is possible to perform the limit.

However, we have different ways of interpolating our points. We exclude

the linear interpolation, indeed, we see from Fig. 2.3 that it would be not enough, since the points are not on a straight line. Instead, we will exploit a polynomial interpolation, which has the property of be unique [15]. We must keep in mind that, when $x = 0$, our function should look like the numeric results obtained for $\overline{\ln(Z_J(\beta))}$ (i.e. Fig. 2.1), since looking at eq.(1.23) and to eq.(2.11) we obtain:

$$\overline{\ln(Z_J(\beta))} = \lim_{n\to 0} g_n(\beta). \tag{2.23}$$

Our goal is to find a rule that allows us to get an estimation of $\overline{\ln(Z_J(\beta))}$ for a generic N-spin system, without the explicit computation of the partition function.

2.3 Polynomial interpolation

For a generic function $g(x)$, whose values are known only at a discrete set of values $\{x\} = (x_1, x_2, \dots x_m)$, it exists a unique polynomial of minimum degree $m-1$, which interpolates the set of points $g(x_i)$ (with $i = 1 \dots m$) [15]. This polynomial is given by the equation:

$$Q_m(x) = \sum_{j=1}^{m} \prod_{\substack{i=1 \\ i\neq j}}^{m} \frac{(x - x_i)}{(x_j - x_i)} g(x_j). \tag{2.24}$$

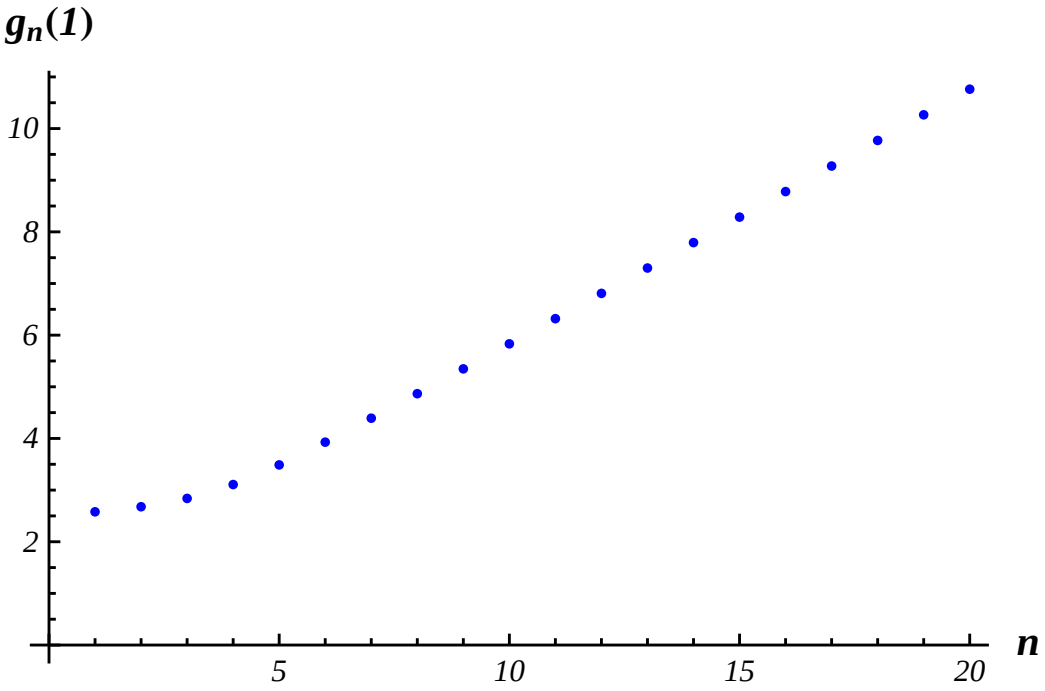

Figure 2.3: The blue points represent the value of the pressure $g_n(\beta)$, defined in eq.(2.11), computed for $\beta = 1$ and $\sigma^2 = \frac{1}{N} = \frac{1}{3}$ as the replica index n grows from 1 to 20. Almost all the points are essentially on a straight line, apart form the first four.

If we put $x = x_k$, the result will be trivially $Q_m(x_k) = g(x_k)$.
For the present case, we use $x_i = i$ and $g(x_k) = g_k(\beta)$ defined in (2.11), thus, the polynomials are functions of β and x, and read:

$$Q_m(x, \beta) = \sum_{j=1}^{m} g_j(\beta) \prod_{\substack{i=1 \\ i \neq j}}^{m} \frac{(x - i)}{(j - i)}. \tag{2.25}$$

Notice that $Q_m(x, \beta)$ depends on m replicas only. Indeed, we see from Fig. 2.4 that it intercepts only the former m points of the pressure ($Q_2(x, \beta)$ interpolates the first two points, $Q_4(x, \beta)$ interpolates the first four points and so on...). What we need is $g_0(\beta)$, hence we see how does $Q_m(x, \beta)$ behaves if we set $x = 0$.

2.4 The $x \to 0$ limit

In this section, we analyze the behavior of $Q_m(x, \beta)$ introduced with eq.(2.25), by setting $x = 0$:

$$Q_m(0, \beta) = \sum_{j=1}^{m} \prod_{\substack{i=1 \\ i \neq j}}^{m} \frac{-i}{j - i} g_j(\beta) = \sum_{j=1}^{m} \frac{\prod_{i=1, i \neq j}^{m} (-i)}{\prod_{i=1, i \neq j}^{m} (j - i)} g_j(\beta). \tag{2.26}$$

This expression can be handled by looking separately at the numerator:

$$\prod_{\substack{i=1 \\ i \neq j}}^{m} (-i) = (-1)^{m-1} \prod_{\substack{i=1 \\ i \neq j}}^{m} i = (-1)^{m-1} \frac{m!}{j}, \tag{2.27}$$

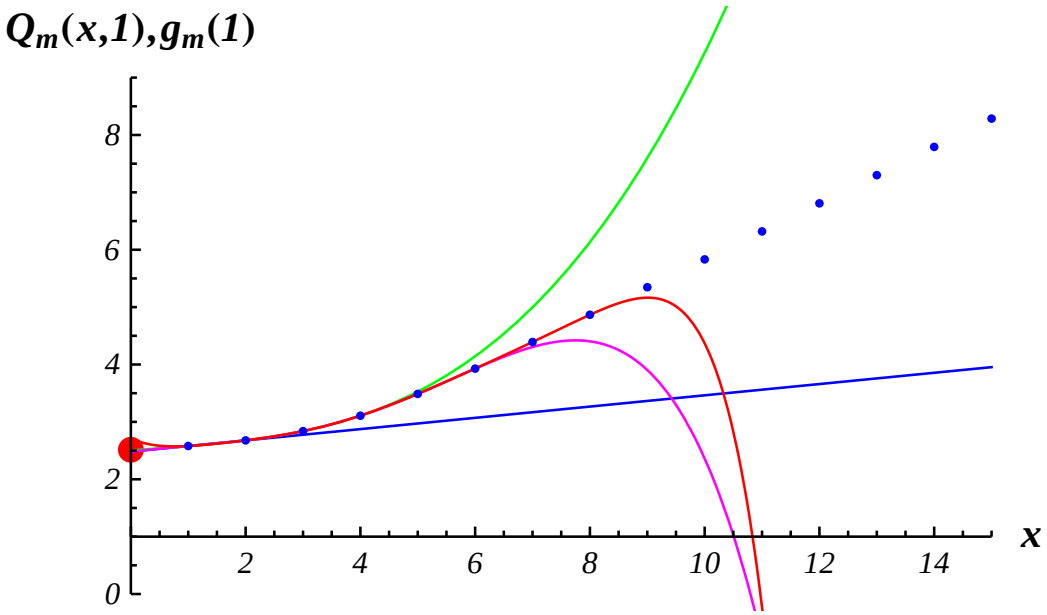

Figure 2.4: In this figure we compare three quantities, all calculated by setting $\beta = 1$.
The blue points represent the pressure $g_n(\beta)$ (as in Fig(2.3)). The red point is the exact value of $\overline{\ln(Z_J(\beta))}$ (eq.(2.6)).
The solid lines represent four polynomials. The blue line is $Q_2(x, \beta)$, it interpolates the firsts two replicas. The green line is $Q_4(x, \beta)$, the violet line is $Q_6(x, \beta)$ and the red line is $Q_8(x, \beta)$. They interpolate the firsts 4, 6, and 8 blue points, i.e. all the replicas which goes from 1 to the value of their degree.

and at the denominator:

$$\begin{aligned}\prod_{\substack{i=1\\ i\neq j}}^{m}(j-i) &= [(j-1)(j-2)\dots 2\cdot 1]\,[(-1)(-2)\dots(j-m)] = \\ &= [(j-1)(j-2)\dots 2\cdot 1]\,(-1)^{m-j}\,[1\cdot 2\dots(m-j)] \\ &= (-1)^{m-j}(j-1)!(m-j)!\end{aligned} \tag{2.28}$$

Merging these results, the final expression for the polynomial interpolation at 0 of the pressure $g_m(\beta)$ is:

$$\begin{aligned}Q_m(0,\beta) &= \sum_{j=1}^{m}(-1)^{m-1}\frac{m!}{j}\frac{1}{(-1)^{m-j}(j-1)!(m-j)!}g_j(\beta) = \\ &= \sum_{j=1}^{m}(-1)^{m-1-m+j}\frac{m!}{j}\frac{1}{(j-1)!(m-j)!}g_j(\beta) = \\ &= \sum_{j=1}^{m}(-1)^{j-1}\frac{m!}{j!(m-j)!}g_j(\beta) = \\ &= \sum_{j=1}^{m}(-1)^{j-1}\binom{m}{j}g_j(\beta).\end{aligned} \tag{2.29}$$

Fig. 2.5 shows the behavior of a set of $Q_m(0,\beta)$ superimposed to $\overline{\ln(Z_J(\beta))}$ (Fig. 2.1) as β varies. The degree of the polynomials, m, is taken as variable parameter. Three different kinds of agreement can be noted between $\overline{\ln(Z_J(\beta))}$ and the set of polynomials as β varies.

For $\beta = 0$, all the polynomials are found to be superimposed among themselves

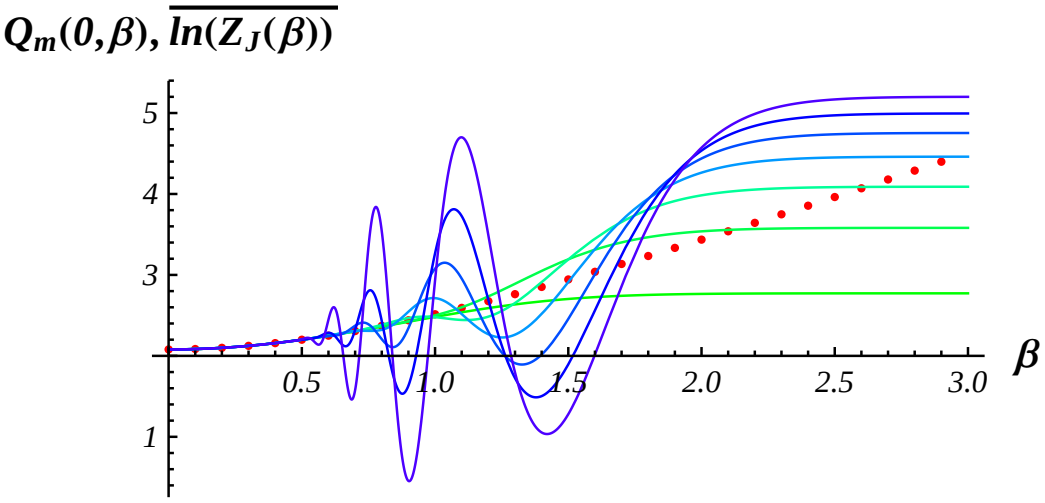

Figure 2.5: The solid curves represent some of the polynomials $Q_m(x,\beta)$, calculated for $m = \{2,4,6,8,10,12,14\}$ and $x = 0$. The red points, as in Fig. 2.1, represent $\overline{\ln(Z_J(\beta))}$ computed with eq.(2.6). For $\beta \lesssim 0.5$ the polynomials are in agreement with $\overline{\ln(Z_J(\beta))}$. For $0.5 \lesssim \beta \lesssim 2$ the polynomials $Q_m(0,\beta)$ show some oscillations and, for $\beta \gtrsim 2$, they saturate while $\overline{\ln(Z_J(\beta))}$ grows.

and with $\overline{\ln(Z_J(\beta))}$. Indeed, we can show that, by setting $\beta = 0$ we have:

$$\overline{\ln(Z_J(\beta))} = Q_m(0,0). \tag{2.30}$$

We shall now show that (2.30) is true. If we set $\beta = 0$ in eq.(2.3), we have that all the exponential in the sum over the spin configurations go to one, then the partition function $Z_J(\beta)$ reduces to the number of configurations of the system. From (2.6), $\overline{\ln(Z_J(\beta))}$ becomes:

$$\overline{\ln(Z_J(0))} = \int d\vec{J} P(\vec{J}) \ln\left(\sum_{\{s\}} 1\right) = \ln(8) \int d\vec{J} P(\vec{J}) = \ln(8), \tag{2.31}$$

since the spin configurations are $2^3 = 8$ and the probability distribution function, $P(\vec{J})$, is normalized.

By setting $\beta = 0$, we get the same value for the polynomials $Q_m(x, \beta)$. Indeed, also the pressure $g_n(\beta)$ depends on the partition function (eq.(2.11)). For $\beta = 0$ it reduces to:

$$g_n(0) = \frac{1}{n} \ln \overline{Z_J(\beta)^n} = \frac{1}{n} \ln(8^n) = \ln(8). \tag{2.32}$$

It follows, from (2.25) that:

$$Q_m(0,0) = \sum_{j=1}^{m} (-1)^{j-1} \binom{m}{j} g_j(0) = \ln(8) \sum_{j=1}^{m} (-1)^{j-1} = \ln(8), \tag{2.33}$$

since the summation over j in the previous equation gives one. This can be shown by using the Binomial Theorem (see Appendix (A.1)):

$$\begin{aligned} (1-1)^n = \sum_{j=0}^{n} \binom{m}{j} (-1)^j (1)^{m-j} = 0 \Rightarrow \\ \Rightarrow \sum_{j=1}^{n} \binom{m}{j} (-1)^j = -1 \Rightarrow \sum_{j=1}^{n} \binom{m}{j} (-1)^{j-1} = 1. \end{aligned} \tag{2.34}$$

Thus, both the polynomials and $\overline{\ln(Z_J(\beta))}$ converge to $\ln(8)$ when $\beta \to 0$. Important differences between the behavior of $\overline{\ln(Z_J(\beta))}$ and the set of $Q_m(0,\beta)$ appear for $\beta \gtrsim 0.5$. In fact, in the low β region, we have some oscillations of the polynomials and these grow in intensity as the degree m of the polynomials raises. For $\beta \to \infty$ instead, the agreement totally fails, since $\overline{\ln(Z_J(\beta))}$ has a linear dependence [3] on β, while, each polynomial reaches a *plateau*, whose value depends only on the degree m of the polynomial.

We should look for a way of refining the interpolation, avoiding the presence of the oscillations, and above all, improving the agreement in the low temperature region, i.e. within the $\beta \to \infty$ limit, since it is the region we are more interested in.

In the next chapters, we shall achieve these requirements by analyzing the polynomials $Q_m(x,\beta)$ for a value of $x \neq 0$. In the following section instead, we will present other interesting features of the polynomials computed for $x = 0$.

[3] We remind that the slope of this line is the ground state energy of the system

2.5 Polynomials' features

In this section, different calculations that have been carried out on the polynomials $Q_m(x, \beta)$, introduced in (2.25), are presented.

Fig. 2.6 is a "zoom" close to the origin of Fig. 2.4, which represents the superposition of some of the polynomials $Q_m(x, \beta)$ with the pressure $g_n(\beta)$ introduced with (2.11). The value of β is fixed to 1, and we see what happens by changing the value of m. The red point is the numerical value of $\overline{\ln(Z_J(\beta))}$ computed using (2.6), the blue point is the pressure $g_n(\beta)$ computed for $n = 1$, while the solid lines are the polynomials $Q_m(0, \beta)$. Looking at this figure, an oscillation of the value of $Q_m(0, \beta)$ around the real value of $\overline{\ln(Z_J(\beta))}$ when m increased can be noted. We shall analyze this oscillation, in order to understand if its amplitude is constant, or damped when m grows.

In Fig. 2.7, we show this oscillation.

We set $\beta = 0.25$, $x = 0$ and we plot the absolute value of $Q_m(0, 0.25)$ whem m varies. The red point represent, as before, the numerical value of $\overline{\ln(Z_J(\beta))}$, computed at $\beta = 0.25$. The other points represent the value assumed by $Q_m(0, \beta)$ when m varies, with $\beta = 0.25$. The blue points represent the values of $Q_m(0, \beta) > 0$, while, the green points are the absolute value of $Q_m(0, \beta)$ when it assumes negative values. They are nothing else that the intercept on the vertical axis of the various polynomials plotted in Fig(2.6)).

The value of β has be chosen equal to 0.25 in this figure in order to achieve values of m near 100. A similar behavior occurs for other values of β.

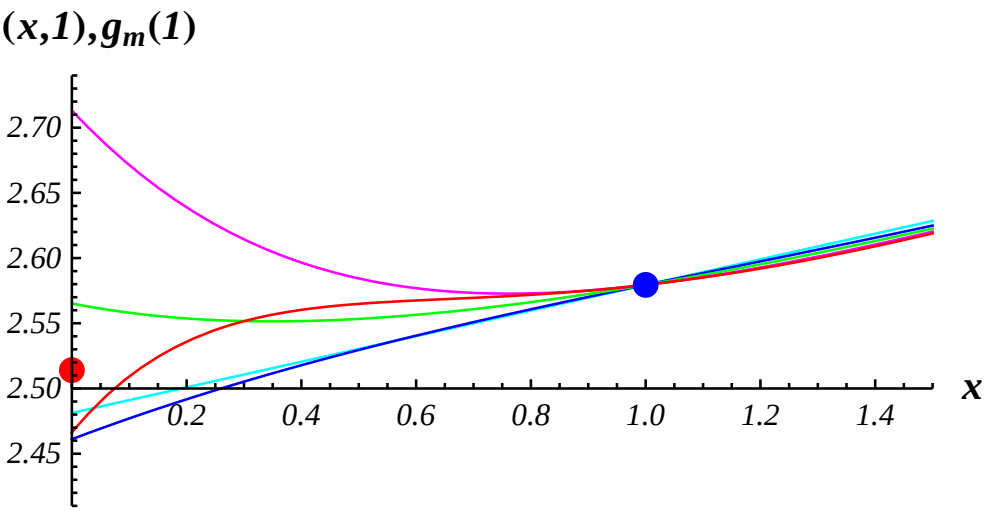

Figure 2.6: This figure represents a particular of Fig. 2.4, zoomed on about the origin. The value of β is set to 1. As before, the red point is $\overline{\ln(Z_J(\beta))}$ eq.(2.6), the blue point is the pressure $g_n(\beta)$ (2.22) computed for $n = 1$. The solid lines are various polynomials. The sky blue is the 2^{nd} polynomial, the blue is the 5^{th}, the green is the 7^{th}, the violet is the 8^{th}, the red is the 15^{th}. The value of $Q_m(x, \beta)$ when $x = 0$ oscillate around the value of $\overline{\ln(Z_J(\beta))}$ as m is increased.

The oscillation is present and grows exponentially in intensity with a mean compatible with $\overline{\ln(Z_J(\beta))}$.

Another feature of the class of polynomials $Q_m(x, \beta)$ can be noted by fixing $x = 0$ and by varying the value of β. Let us "zoom" close to the region in which the oscillations are present in Fig. 2.5.

We are referring to Fig. 2.8, that is a particular of Fig. 2.5 around the value $\beta = 1.5$. Three polynomials are shown: the green line is $Q_5(0, \beta)$, the sky blue line is $Q_7(0, \beta)$ and the blue line is $Q_9(0, \beta)$. They cross $\overline{\ln(Z_J(\beta))}$ respectively at $\beta = 1.26$, $\beta = 1.44$, and $\beta = 1.56$.

It seems that, for any value of β, there exists a polynomial which approximates

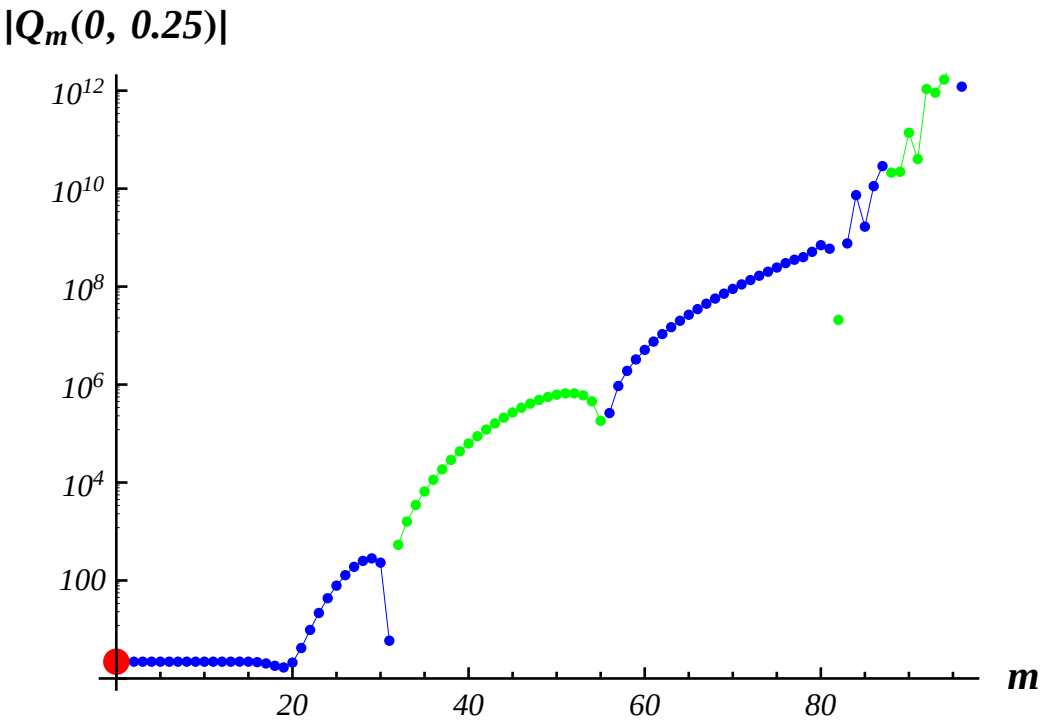

Figure 2.7: The red point is the value of $\overline{\ln(Z_J(\beta))}$ calculated for $\beta = 0.25$. The other points are the absolute value of the polynomials $Q_m(x, \beta)$ computed in $x = 0$ and $\beta = 0.25$, with m varying from 1 to 100. The difference between the blue and the green points is the sign: the blue points represent the value of $Q_m(x, \beta) > 0$ while the values of $Q_m(0, \beta) < 0$ are represented by the green points. The values of $Q_m(0, 0.25)$ are comparable with the value of $\overline{\ln(Z_J(\beta))}$ in the low m zone, while the intensity of the oscillation grows exponentially in intensity when m raises.

the value of $\overline{\ln(Z_J(\beta))}$ better than the others (we can call it $Q_{m_{BP}}(0,\beta)$, where BP stands for "best polynomial").

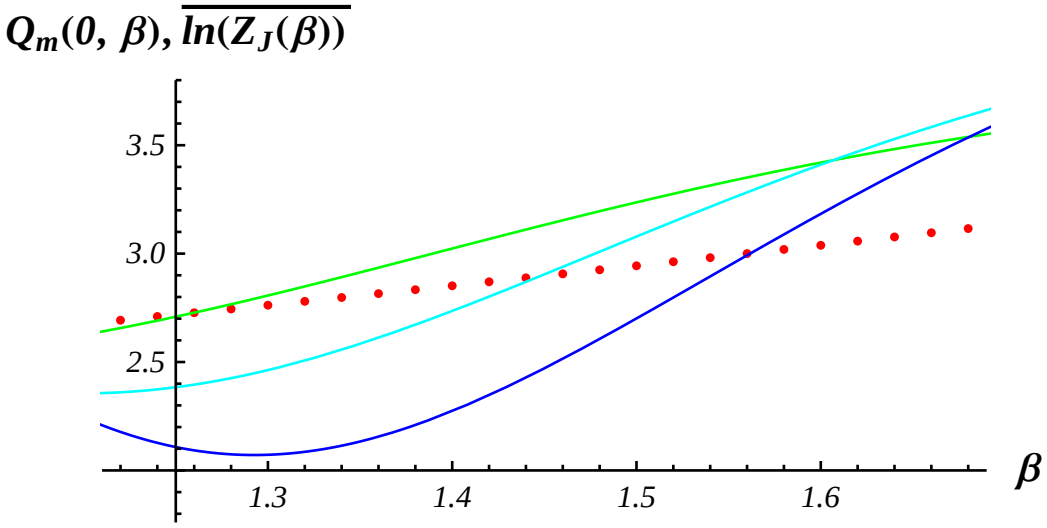

Figure 2.8: We "zoom" Fig. 2.5 about $\beta = 1.5$. The green line is the 5^{th} polynomial $Q_5(0,\beta)$, the sky blue line is $Q_7(0,\beta)$ and the blue line is $Q_9(0,\beta)$. As in Fig. 2.1, the red points represent the values of $\overline{\ln(Z_J(\beta))}$.

Can we expect that this feature happens with a regular behavior? And can we make some guess about the dependence of the degree of the polynomial found on β? We should look for a function of the form $m_{BP} = m_{BP}(\beta)$.

In Fig. 2.9, for various value of β, we plot the degree of the polynomial which satisfies the following propriety:

$$m_{BP}(\beta) = \min_m\{1 \le m \le 100 \,\Big|\, |\overline{\ln(Z)} - Q_{m_{BP}}(x,\beta)| \le |\overline{\ln(Z)} - Q_m(x,\beta)|\}.^4 \tag{2.35}$$

[4] In this expression we have written, for simplicity, $\overline{\ln(Z)}$ instead of $\overline{\ln(Z_J(\beta))}$

We have computed the values of $\overline{\ln(Z_J(\beta))}$ for $\beta \in [0, 5]$ and, increasing the value of β of 0.1 each time, we have found the polynomial which assumes a value closer to the numerical value of $\overline{\ln(Z_J(\beta))}$. After an initial, irregular behavior, the dependence seems to become polynomial for large β.

Nevertheless, to obtain the correct form of $m_{BP}(\beta)$, we should analyze all the $m \in \mathbb{N}$. Instead, in eq.(2.35) and Fig. 2.9 we have analyzed just the polynomials with $1 \leq m \leq 100$.

Moreover, if we suppose that $m_{BP}(\beta)$ is a polynomial in the variable β, we have that, if $\beta \to \infty$, also $m_{BP}(\beta) \to \infty$.

Thus, we should take a polynomial with degree infinity to get the value of the ground state free energy, which is achieved for $\beta \to \infty$.

All these features could be explained by studying the analytic continuation of the polynomials $Q_m(x, \beta)$ in the complex plane. We can suppose that, in the plane of complex β, there exists a polynomial that assumes a value equal to the value of $\overline{\ln(Z_J(\beta))}$ for each value of the real part of β. In the next chapter, we shall better analyze the features of the polynomials $Q_m(x, \beta)$, and try to obtain a more efficient agreement with respect to $\overline{\ln(Z_J(\beta))}$ by exploring the $x \neq 0$ zone.

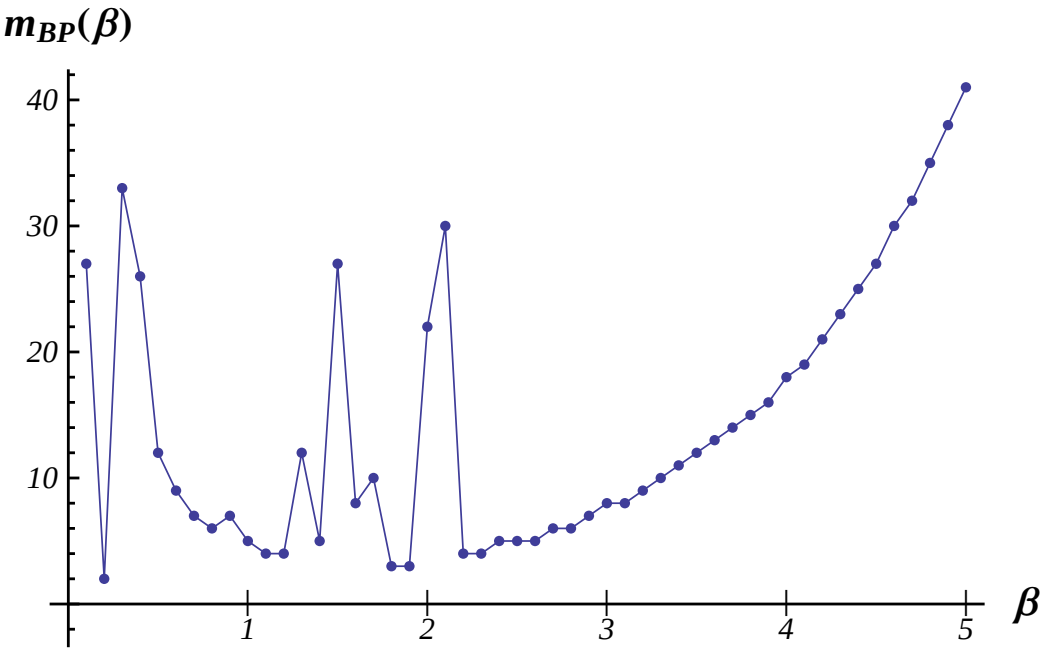

Figure 2.9: The blue points represent, for various value of β, the degree m_{BP} of the polynomial $Q_m(x, \beta)$ which minimizes the difference $|Q_m(x, \beta) - \overline{\ln(Z_J(\beta))}|$. The set of m's analyzed is between 1 and 100.

Chapter 3

Low-Temperature Behavior

In the previous chapter, the polynomials $Q_m(x, \beta)$ were introduced (eq.(2.25)), as interpolating polynomials of the pressure $g_n(\beta)$ (2.11) (see Sec. 2.3). In Sec. 2.4, we have analyzed the behavior of $Q_m(x, \beta)$ when $x = 0$. As discussed at the end of Sec. 2.4, the polynomials $Q_m(x, \beta)$ computed at $x = 0$ present some features (oscillations for low values of β and a *plateau* reached for large values of β) that should be corrected in order to obtain a good agreement of $Q_m(x, \beta)$ with $\overline{\ln(Z_J(\beta))}$ (eq.(2.6)).

In this chapter, we shall study the behavior of the polynomials $Q_m(x, \beta)$ when $x \neq 0$, and compare it with $\overline{\ln(Z_J(\beta))}$.

We are going to show that, for large values of β, we have succeeded in reproducing the trend of $\overline{\ln(Z_J(\beta))}$ (eq.(2.6)) with $Q_m(x, \beta)$.

3.1 Behavior at $x \neq 0$

In Chapter 2, we have analyzed the behavior of the polynomials $Q_m(x, \beta)$ (eq.(2.25)) when $x = 0$ (see Fig. 2.5) or with β fixed at a constant value (Fig. 2.4 and Fig. 2.6). A look at the plane (x, β) can give us some interesting insights about the shape of the polynomials.

The polynomial $Q_{14}(x, \beta)$ is shown in Fig. 3.1, when both x and β vary. In this figure, it can be noted that the oscillations of the polynomials, that are present at $x = 0$, disappear when x is sufficiently large. Moreover, the *plateau* reached by the polynomials for $\beta \gtrsim 1$ in Fig. 2.5 disappears as x increases.

In figures 3.2 and 3.3, the solid curves are the values of the polynomials $Q_m(x, \beta)$, computed for $x = 0.5$ and $x = 1$, respectively, as β varies and for various values of m. The red points represent the values of $\overline{\ln(Z_J(\beta))}$, as showed in Fig. 2.1. Looking in sequence at Fig. 2.5 and Fig. 3.2, we note that, when the value of x increases, the polynomials get closer among themselves and the *plateaux* reached by $Q_m(x, \beta)$ for large β when $x = 0$, disappear.

In Fig. 3.3, the polynomials $Q_m(x, \beta)$ are evaluated at $x = 1$ and, independently from the degree of the polynomials m, they perfectly coincide. The same happens for the polynomials of higher degrees, for larger values of x.

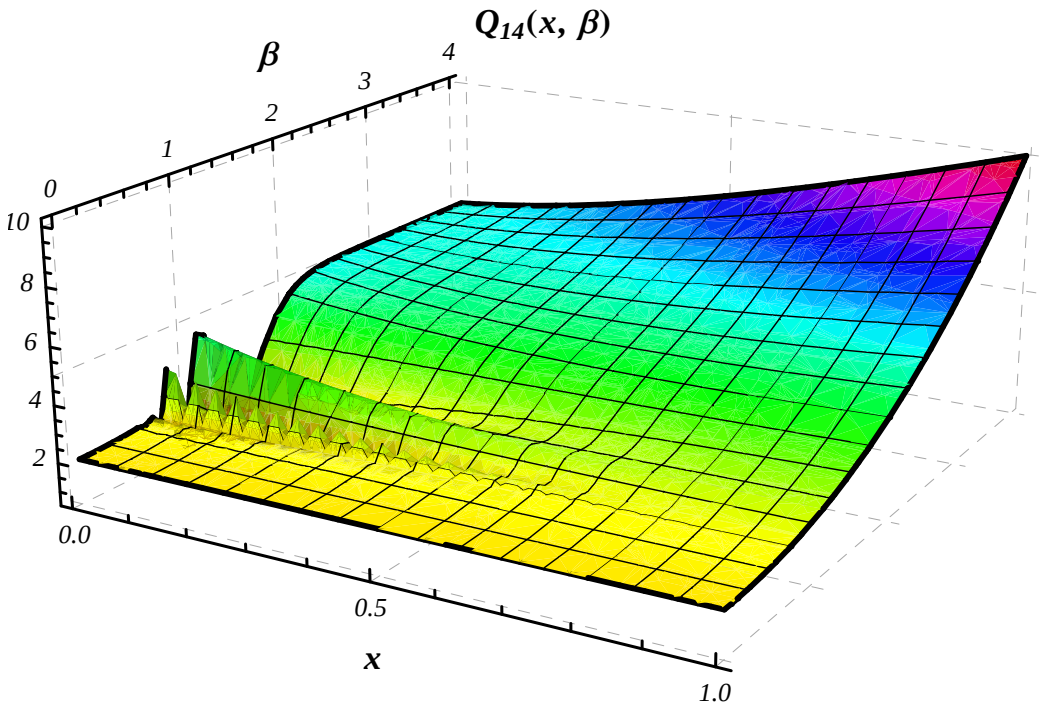

Figure 3.1: In this figure, $Q_{14}(x, \beta)$ defined in eq.(2.25), is shown. The intersection of this surface with the plane $x = 0$ corresponds to the solid line with the highest oscillation showed in Fig. 2.5, representing $Q_{14}(0, \beta)$. Here, both the oscillations and the *plateau* present at $x = 0$ disappear when $x \gtrsim 0.5$.

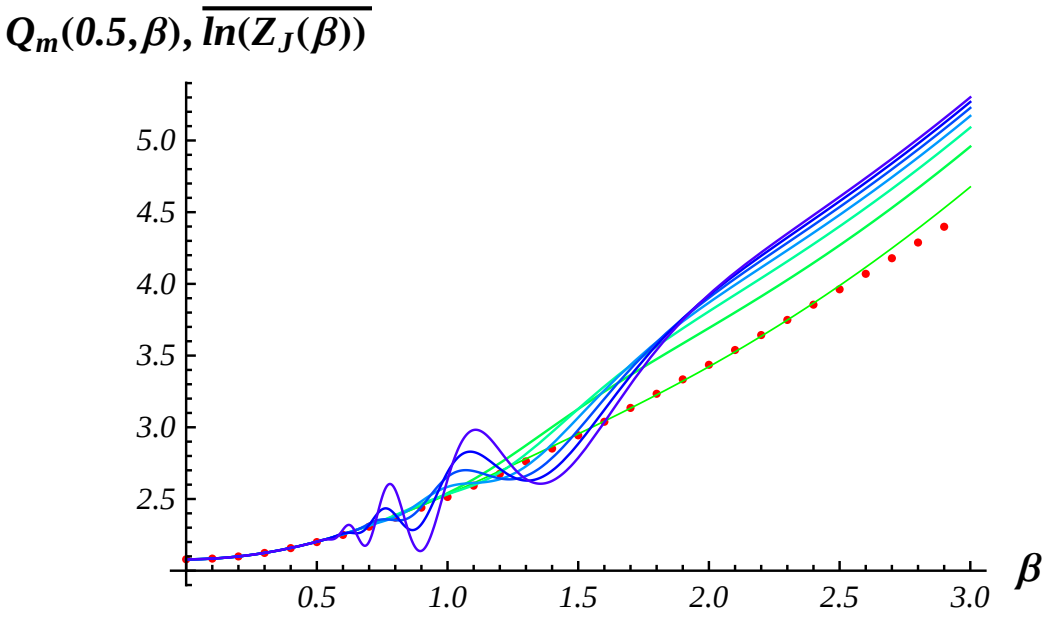

Figure 3.2: The red points are the values of $\overline{\ln(Z_J(\beta))}$, numerically computed from eq.(2.6) and showed in Fig. 2.1. The solid lines are the values of $Q_m(x,\beta)$ for $x = 0.5$. Here $m = \{2, 4, 6, 8, 10, 12, 14\}$.
Polynomials' oscillations present in Fig. 2.5 are still evident for the polynomials of higher degree, while the *plateaux* reached in Fig. 2.5 for $\beta \gtrsim 2$ have disappeared.

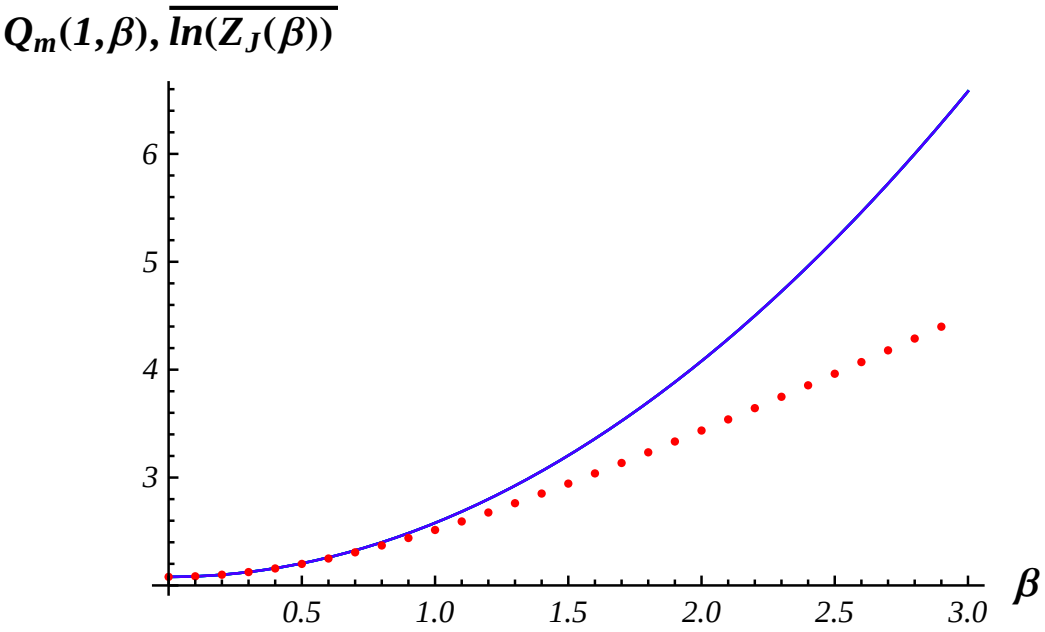

Figure 3.3: As in Fig. 3.2, the red points represent the values of $\overline{\ln(Z_J(\beta))}$ (eq.(2.6) and Fig. 2.1). The solid lines are the values of $Q_m(x,\beta)$ for $x = 1$. Here $m = \{2, 4, 6, 8, 10, 12, 14\}$. The polynomials plotted in Fig. 2.5 and Fig. 3.2 coincide, independently on their degree m.

3.2 Exact intersecting region

In this section, we endeavor to improve the agreement between $Q_m(x,\beta)$ and $\overline{\ln(Z_J(\beta))}$. In Fig. 3.3, the behavior of the polynomials $Q_m(x,\beta)$ for $x = 1$ and small β is in good agreement with $\overline{\ln(Z_J(\beta))}$, however, it continues to fail for $\beta \to \infty$.

Let us compare the function $\overline{\ln(Z_J(\beta))}$ with the polynomials $Q_m(x,\beta)$ in the plane (x,β), and find where the following equation is satisfied:

$$Q_m(x,\beta) = \overline{\ln(Z_J(\beta))}. \tag{3.1}$$

In Fig. 3.4, the red surface is $\overline{\ln(Z_J(\beta))}$, while, the rainbow-shaded surface is the 5^{th} polynomial $Q_5(x,\beta)$. The two surfaces intersect along a curve that becomes closer to the $x = 0$ plane when β increases. This curve represents the values of $x = x_m(\beta)$ where eq.(3.1) is satisfied.

By plotting the intersection curve on the (x,β) plane, it can be observed that $x_m(\beta)$ tends to the $x = 0$ plane when the temperature is lowered (i.e. when β is increased). This is shown in Fig. 3.5. We try to fit the function $x = x_m(\beta)$ by:

$$x_m(\beta) = \frac{\epsilon_m}{\sigma\beta + \eta_m}, \tag{3.2}$$

where two constants ϵ_m and η_m are introduced and $\sigma = \frac{1}{\sqrt{3}}$ from eq.(1.11). When the temperature is sufficiently low, we can use $Q_m(x,\beta)$ with $x = x_m(\beta)$, given by eq.(3.2), to obtain the asymptotic value of $\overline{\ln(Z_J(\beta))}$ for large β. We

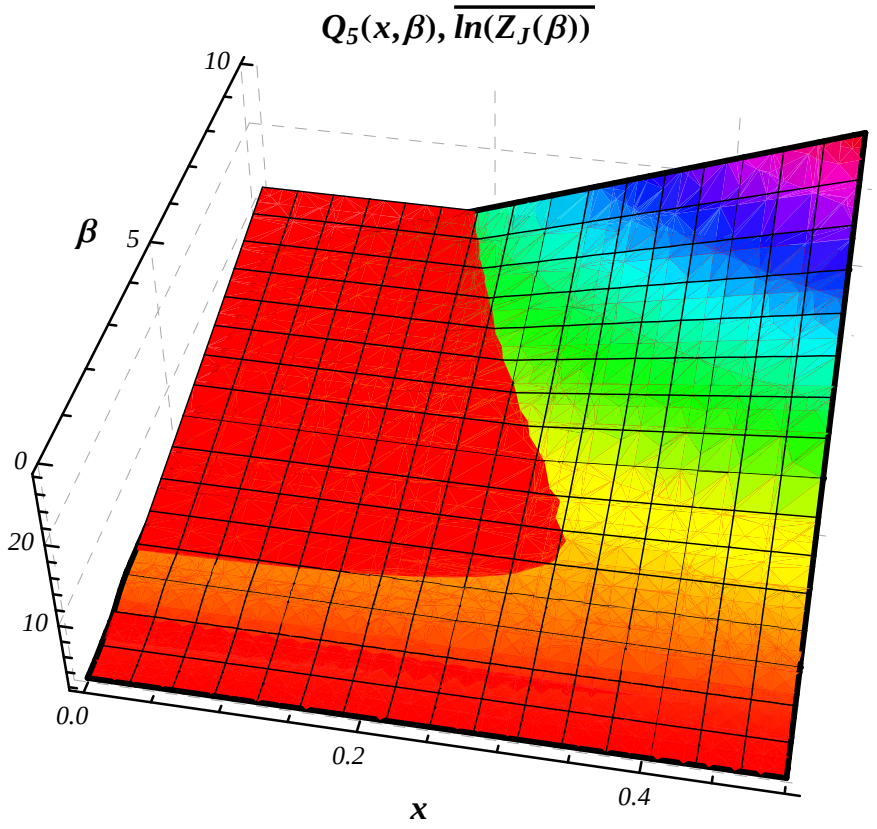

Figure 3.4: The red surface is $\overline{\ln(Z_J(\beta)}$, the rainbow-shaded surface is the 5^{th} polynomial $Q_5(x,\beta)$. The intersection curve (i.e. $x_m(\beta)$ given by eq.(3.3)) gets closer to $x = 0$ as β increases.

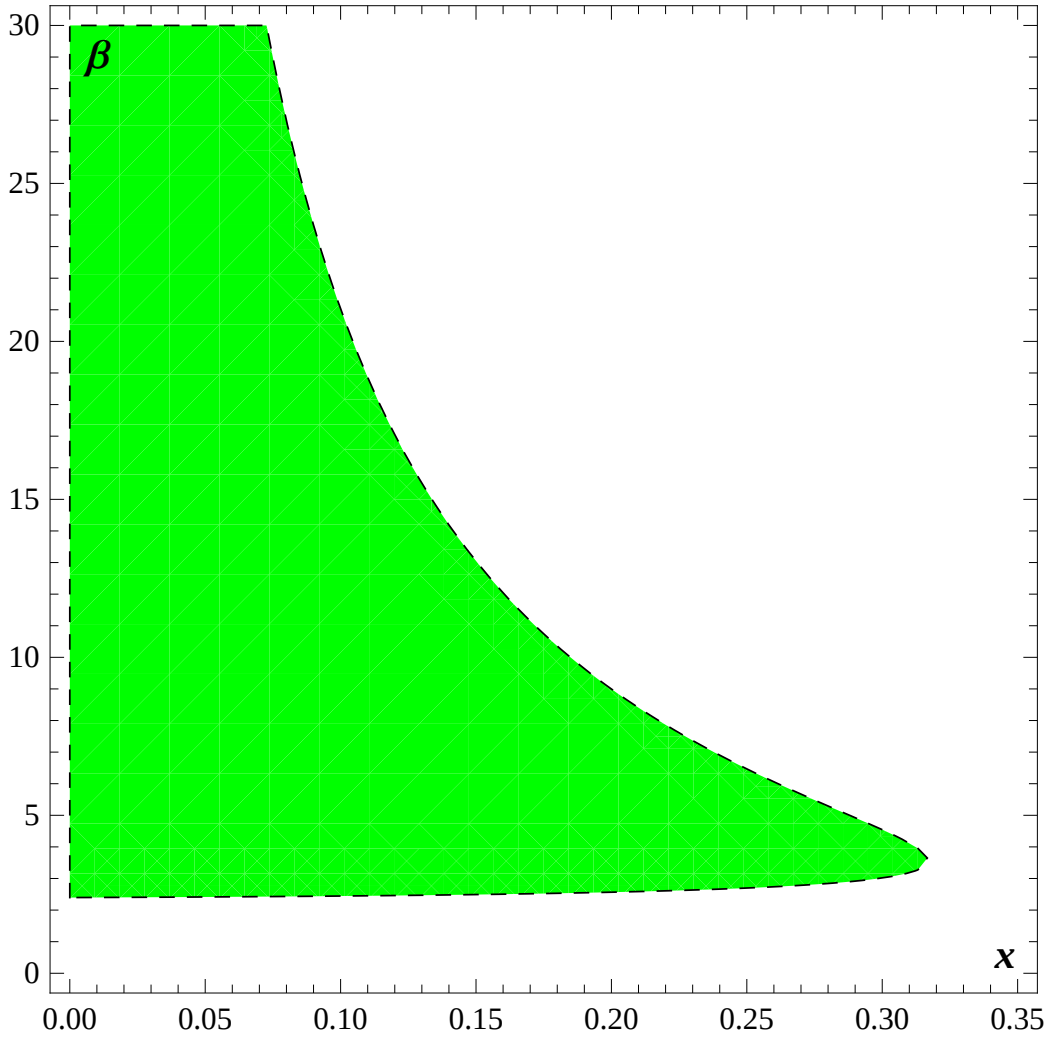

Figure 3.5: The green zone represents the region where $Q_5(x,\beta) < \overline{\ln(Z_J(\beta))}$ and, vice versa in the rest of the plane we have $Q_5(x,\beta) > \overline{\ln(Z_J(\beta))}$. The dashed line which separes the two zone is $x_5(\beta)$, solution of eq.(3.1) for $m = 5$.

shall analyze this possibility in the rest of the thesis.

Numerical analysis on polynomials of different degrees show that the two constants ϵ_m and η_m do not depend on the degree of the polynomial used, thus, hereafter, we shall omit the subscript m in the notation. Eq (3.2) becomes:

$$x_m(\beta) = x(\beta) = \frac{\epsilon}{\sigma\beta + \eta} = \frac{\tilde{\epsilon}}{\beta + \tilde{\eta}}, \tag{3.3}$$

where the constants are fitted by:

$$\epsilon = 1.37, \quad \eta = 1.55. \tag{3.4}$$

while the constants $\tilde{\epsilon}$ and $\tilde{\eta}$ are rescaled with respect to the standard deviation $\sigma = \frac{1}{\sqrt{3}}$:

$$\tilde{\epsilon} = \frac{\epsilon}{\sigma} = \sqrt{3}\epsilon = 2.38, \tag{3.5a}$$

$$\tilde{\eta} = \frac{\eta}{\sigma} = \sqrt{3}\eta = 2.70. \tag{3.5b}$$

We expect that these two constants are independent on the dimension of the system. These quantities will be used in Chapter 5, where a generalization of our approach to a N-spin system will be presented.

3.3 First order approximation

By using the function $x(\beta)$, introduced in eq.(3.3), we now can express $\overline{\ln(Z_J(\beta))}$ in terms of the polynomials $Q_m(x,\beta)$:

$$\overline{\ln(Z_J(\beta))} = Q_m(x(\beta),\beta). \tag{3.6}$$

Looking at the definition (2.25), given for $Q_m(x,\beta)$, we can write our polynomials in an equivalent way:

$$Q_m(x,\beta) = \sum_{j=1}^{m} g_j(\beta) \prod_{\substack{i=1 \\ i\neq j}}^{m} \frac{(x-i)}{(j-i)} = \sum_{j=1}^{m} g_j(\beta) h_{j,m}(x), \tag{3.7}$$

where we introduced the polynomials of degree $m-1$:

$$h_{j,m}(x) = \prod_{\substack{i=1 \\ i\neq j}}^{m} \frac{(x-i)}{(j-i)}. \tag{3.8}$$

$Q_m(x,\beta)$ is then the sum of m terms, each of them being the product of a function depending only on β (i.e. $g_j(\beta)$) and a polynomial depending only on x, i.e. $h_{j,m}(x)$. Since $h_{j,m}(x)$ is a polynomial of degree $m-1$ in x, $Q_m(x,\beta)$ can be written in the following way:

$$Q_m(\beta,x) = \sum_{i=0}^{m-1} c_i^{(m)}(\beta) x^i = c_0^{(m)} + c_1^{(m)} x + \ldots + c_{m-1}^{(m)} x^{m-1}, \tag{3.9}$$

having denoted with $c_i^{(m)}(\beta)$ the coefficients of the term of i^{th} degree in x of the polynomial. They can be expressed as the i^{th} derivative of the polynomial with respect to x:

$$c_i^{(m)}(\beta) = \left.\frac{\partial^i Q_m(\beta, x)}{\partial x^i}\right|_{x=0} = \sum_{j=1}^{m} g_j(\beta) \left.\frac{\partial^i h_{j,m}(x)}{\partial x^i}\right|_{x=0}. \tag{3.10}$$

Here $i = 0, 1, \ldots, m-1$. By taking $i = 0$, we note that $c_0^{(m)}(\beta) = Q_m(0, \beta)$, already treated in eq.(2.26). These functions have a well understood behavior (cfr. Sec(2.4)): in the limit $\beta \to 0$ they tend to the numerical value of $\overline{\ln(Z_J(\beta))}$ computed for $\beta = 0$ (see eq.(2.33)), while, as β increases, they reach a constant value which depends only on the degree of the polynomial and that we call $c_0^{(m)}$:

$$\begin{cases} \lim_{\beta \to 0} c_0^{(m)}(\beta) = Q_m(0,0) = \ln(8), \\ \lim_{\beta \to \infty} c_0^{(m)}(\beta) = c_0^{(m)}. \end{cases} \tag{3.11}$$

Let us focus on the first order coefficient $c_1^{(m)}(\beta)$. The derivative of $h_{j,m}(x)$ (eq:(3.8)) with respect to x is:

$$\begin{aligned} h'_{j,m}(x) = \frac{\partial h_{j,m}(x)}{\partial x} &= \frac{\partial}{\partial x} \prod_{\substack{i=1 \\ i\neq j}}^{m} \frac{(x-i)}{(j-i)} \\ &= \frac{1}{\prod_{\substack{i=1 \\ i\neq j}}^{m}(j-i)} \frac{\partial}{\partial x} \left(\prod_{\substack{i=1 \\ i\neq j}}^{m} (x-i) \right) \\ &= \frac{1}{\prod_{\substack{i=1 \\ i\neq j}}^{m}(j-i)} \sum_{\substack{k=1 \\ i\neq j}}^{m} \left(\prod_{\substack{i=1 \\ i\neq j \\ i\neq k}}^{m} (x-i) \right). \end{aligned} \tag{3.12}$$

The first order coefficient is obtained from eq.(3.10) and eq.(3.12), setting $x = 0$:

$$c_1^{(m)}(\beta) = \left. \frac{\partial Q_m(\beta, x)}{\partial x} \right|_{x=0} = \sum_{j=1}^{m} \frac{g_j(\beta)}{\prod_{\substack{i=1 \\ i\neq j}}^{m}(j-i)} \left(\sum_{\substack{k=1 \\ i\neq j}}^{m} \prod_{\substack{i=1 \\ i\neq j \\ i\neq k}}^{m} (-i) \right). \tag{3.13}$$

The second order coefficient $c_2^{(m)}(\beta)$ in the expansion (3.9) will be analyzed in the next section. Numerical analysis show that its contribution can be neglected, thus our polynomial $Q_m(x, \beta)$ have a dependence on x that is almost linear. We argue that, the first order approximation in x of $Q_m(x(\beta), \beta)$ will give a good estimation of $\overline{\ln(Z_J(\beta))}$. In the rest of this section we shall then analyze the approximation of the polynomials $Q_m(x(\beta), \beta)$ at the first order

in x:

$$Q_m(x,\beta) \simeq c_0^{(m)}(\beta) + c_1^{(m)}(\beta)x, \tag{3.14}$$

with:

$$\begin{aligned} c_0^{(m)}(\beta) &= Q_m(0,\beta) \quad \text{and} \\ c_1^{(m)}(\beta) &= \sum_{j=1}^{m} g_j(\beta) h'_{j,m}(0). \end{aligned} \tag{3.15}$$

We now shall replace the value of x in eq.(3.9) with the value obtained with eq.(3.3):

$$x(\beta) = \frac{\epsilon}{\sigma\beta + \eta},$$

In this way, from equations (3.6), (3.14) and (3.3) we obtain an approximation for $\overline{\ln(Z_J(\beta))}$:

$$\begin{aligned} \overline{\ln(Z_J(\beta))} &= Q(x(\beta),\beta) \\ &\simeq c_0^{(m)}(\beta) + c_1^{(m)}(\beta)x(\beta) \\ &= c_0^{(m)}(\beta) + c_1^{(m)}(\beta)\frac{\epsilon}{\sigma\beta + \eta}. \end{aligned} \tag{3.16}$$

Moreover, if $\beta \gg 1$ we can write the asymptotic approximation of $\overline{\ln(Z_J(\beta))}$ by neglecting η ($\eta = 1.55$ from (3.4)) and by taking the limit of $c_0^{(m)}(\beta)$ from the second of equations (3.11). The previous expression becomes:

$$\overline{\ln(Z_J(\beta))} \sim c_0^{(m)} + c_1^{(m)}(\beta)\,\frac{\epsilon}{\sigma\beta} \tag{3.17}$$

We call $\Theta_m(\beta)$ the asymptotic limit of $\overline{\ln(Z_J(\beta))}$:

$$\Theta_m(\beta) \equiv c_0^{(m)} + c_1^{(m)}(\beta)\frac{\epsilon}{\sigma\beta}, \tag{3.18}$$

with $c_0^{(m)}$ and $c_1^{(m)}(\beta)$ introduced respectively in the second equation of (3.11) and in (3.13). Thus, we summarize:

$$\overline{\ln(Z_J(\beta))} \sim \Theta_m(\beta), \quad \text{for } \beta \text{ large.} \tag{3.19}$$

In Fig. 3.6 we compare the values of $\overline{\ln(Z_J(\beta))}$, numerically obtained from eq.(2.6), with its approximation (3.19). We remark that, as already stated in Sec. 2.1, we are interested in the value of the ground state energy, which can be obtained from the limit slope of $\overline{\ln(Z_J(\beta))}$ for large β. Thus, we are interested only in the first order term of eq.(3.19). We want to understand the dependence of the coefficient $c_1^{(m)}(\beta)$ on β. In the next section we shall provide some numeric result. The explicit dependence of $c_1^{(m)}$ on β will be obtained in the next chapter.

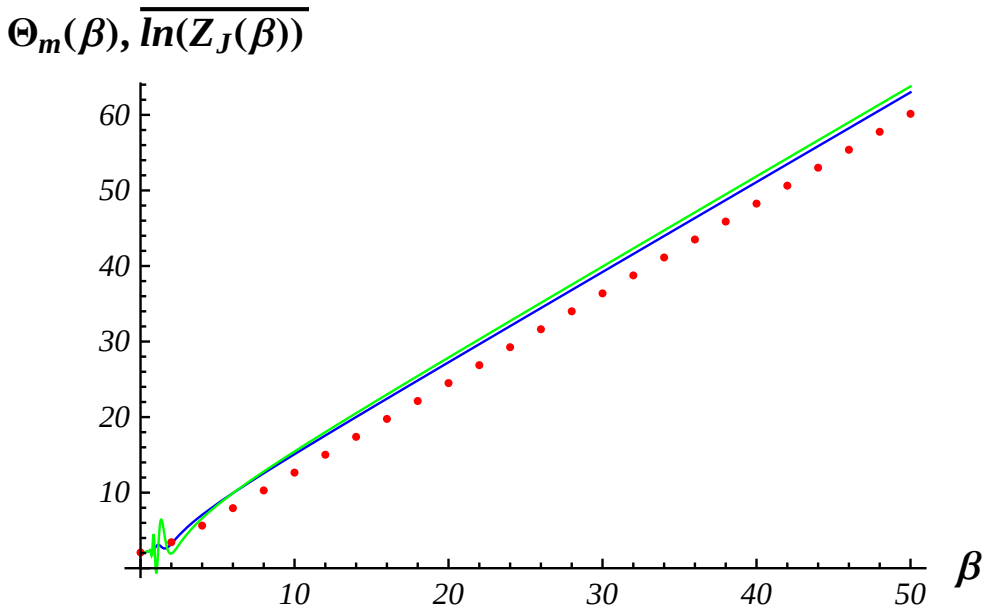

Figure 3.6: The blue line represents $\Theta_5(\beta)$, while the green line is $\Theta_{10}(\beta)$, both obtained from eq.(3.18). The red points are the numerical values of $\overline{\ln(Z_J(\beta))}$ (Fig. 2.1). The slope is the same for all the curves. We can obtain the value of the energy ground state E_0, introduced in (2.8), from the angular coefficient of the solid curve (for $\beta \gg 1$) and we expect that this is independent on the value of m.

3.4 The β dependence

Let us consider how the first two coefficients $c_0^{(m)}(\beta)$ and $c_1^{(m)}(\beta)$ in eq.(3.18) depend on β. As already noted in the previous section we have:

$$c_0^{(m)}(\beta) = Q_m(0, \beta), \tag{3.20}$$

with:

$$\begin{cases} \lim_{\beta \to 0} c_0^{(m)}(\beta) = \ln(8) \\ \lim_{\beta \to \infty} c_0^{(m)}(\beta) = c_0^{(m)}, \end{cases} \tag{3.21}$$

$c_0^{(m)}(\beta)$ takes a finite value both within the $\beta \to 0$ and the $\beta \to \infty$ limits. The behavior of these coefficients (for $m = \{5, 10\}$) is shown in Fig. 3.7. Instead, the first order coefficient $c_1^{(m)}(\beta)$, according to numerical simulations, has a quadratic dependence on β. The function $\frac{1}{\beta} c_1^{(m)}(\beta)$ results then linear in β. We present the behavior of two first order coefficients (for $m = 5$ and $m = 10$) in Fig 3.8 and the same coefficients divided by β in Fig. 3.9. The term $\frac{1}{\beta} c_1^{(m)}(\beta)$ will be important in the limit $\beta \to \infty$.

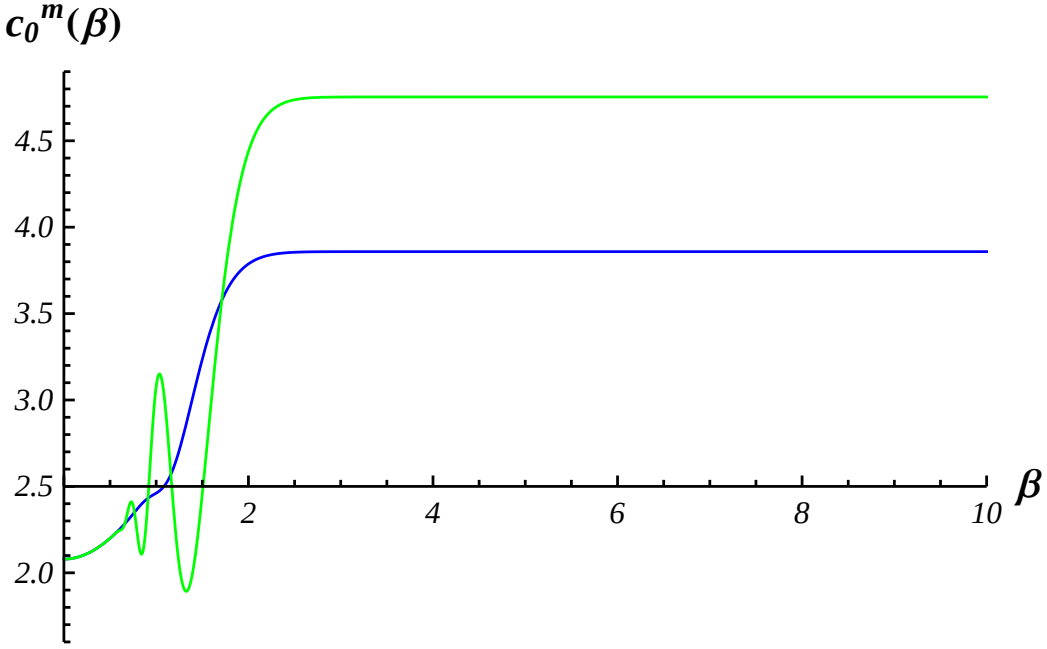

Figure 3.7: The solid curves represent the values of $c_0^{(5)}(\beta)$ (blue curve) and $c_0^{(10)}(\beta)$ (green curve), both calculated from eq.(2.29)

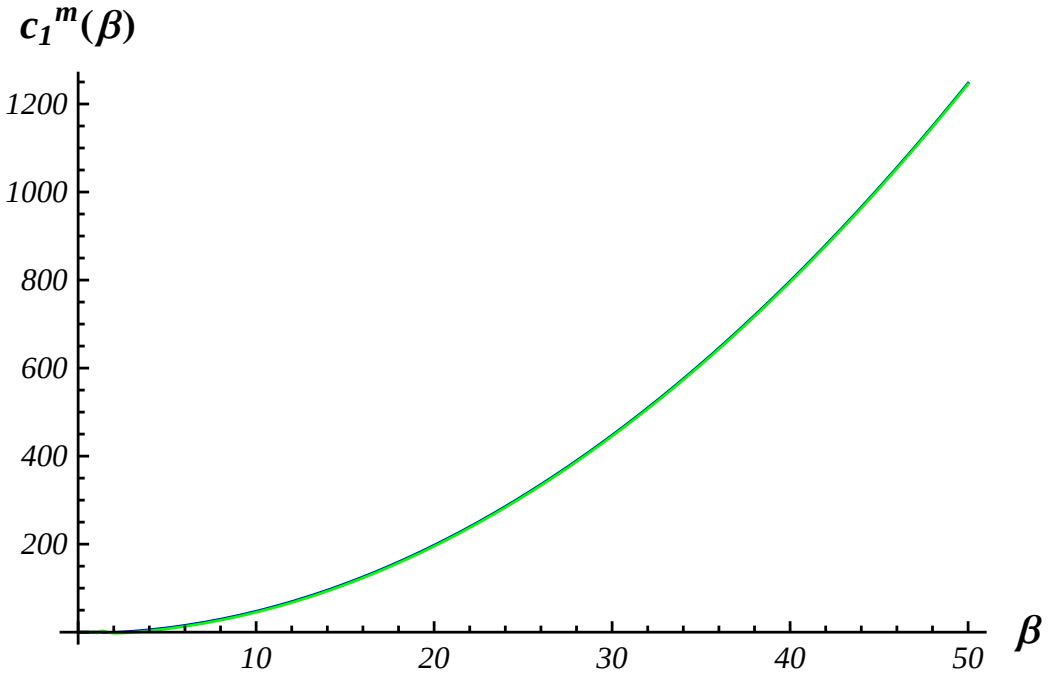

Figure 3.8: The solid curves represent the values of $c_1^{(5)}(\beta)$ (blue curve) and $c_1^{(10)}(\beta)$ (green curve), both calculated with eq.(3.13).

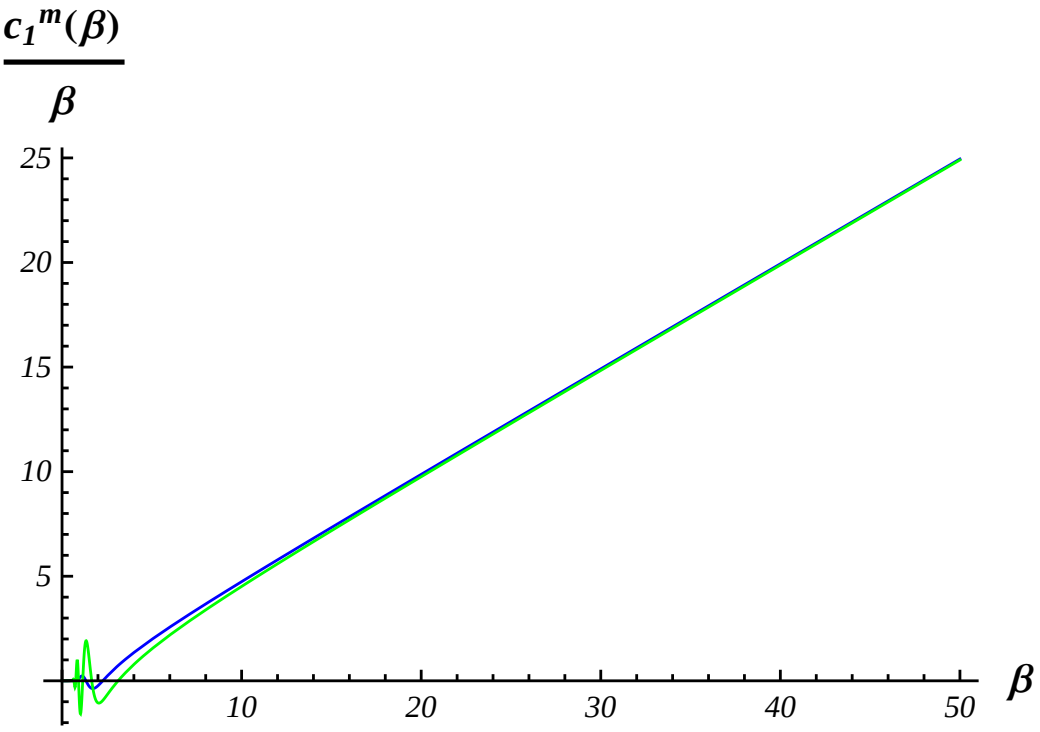

Figure 3.9: The plot represents $\frac{c_1^{(5)}(\beta)}{\beta}$ (the blue curve) and $\frac{c_1^{(10)}(\beta)}{\beta}$ (the green curve) obtained using eq.(3.13). They overlap for $\beta >> 1$, independently on their degree

3.5 Second order corrections

The second order term $c_2^{(m)}(\beta)$ in the expansion (3.9) can be obtained in the same way, by deriving eq.(3.12) one more time in x and setting $x = 0$ at the end of the calculation. The result reads:

$$\frac{\partial^2 Q_m(\beta, x)}{\partial x^2} = \sum_{j=1}^{m} g_j(\beta) h''_{m,j}(x), \tag{3.22}$$

where, from (3.12)

$$\begin{aligned} h''_{m,j}(x) = \frac{\partial^2 h_{m,j}(x)}{\partial x^2} =& \frac{1}{\prod_{i=1, i\neq j}^{m}(j-i)} \frac{\partial}{\partial x} \left(\sum_{\substack{k=1 \\ k\neq j}}^{m} \prod_{\substack{i=1 \\ i\neq j \\ i\neq k}}^{m} (x-i) \right) \\ =& \frac{1}{\prod_{\substack{i=1 \\ i\neq j}}^{m}(j-i)} \left[\sum_{\substack{k=1 \\ k\neq j}}^{m} \sum_{\substack{l=1 \\ l\neq j \\ l\neq k}}^{m} \prod_{\substack{i=1 \\ i\neq j \\ i\neq k \\ i\neq l}}^{m} (x-i) \right]. \end{aligned} \tag{3.23}$$

Thus, finally, the second order coefficient in eq.(3.9) is

$$\begin{aligned} c_2^{(m)}(\beta) = \left. \frac{\partial^2 Q_m(\beta, x)}{\partial x^2} \right|_{x=0} =& \sum_{j=1}^{m} g_j(\beta) \left. \frac{\partial^2 h_{m,j}(x)}{\partial x^2} \right|_{x=0} \\ =& \sum_{j=1}^{m} g_j(\beta) \frac{1}{\prod_{\substack{i=1 \\ i\neq j}}^{m}(j-i)} \left[\sum_{\substack{k=1 \\ k\neq j}}^{m} \sum_{\substack{l=1 \\ l\neq j \\ l\neq k}}^{m} \prod_{\substack{i=1 \\ i\neq j \\ i\neq k \\ i\neq l}}^{m} (-i) \right]. \end{aligned} \tag{3.24}$$

Fig. 3.10 shows that $c_2^{(m)}$ goes to 0 faster than $\frac{1}{\beta^2}$ when β is increased.

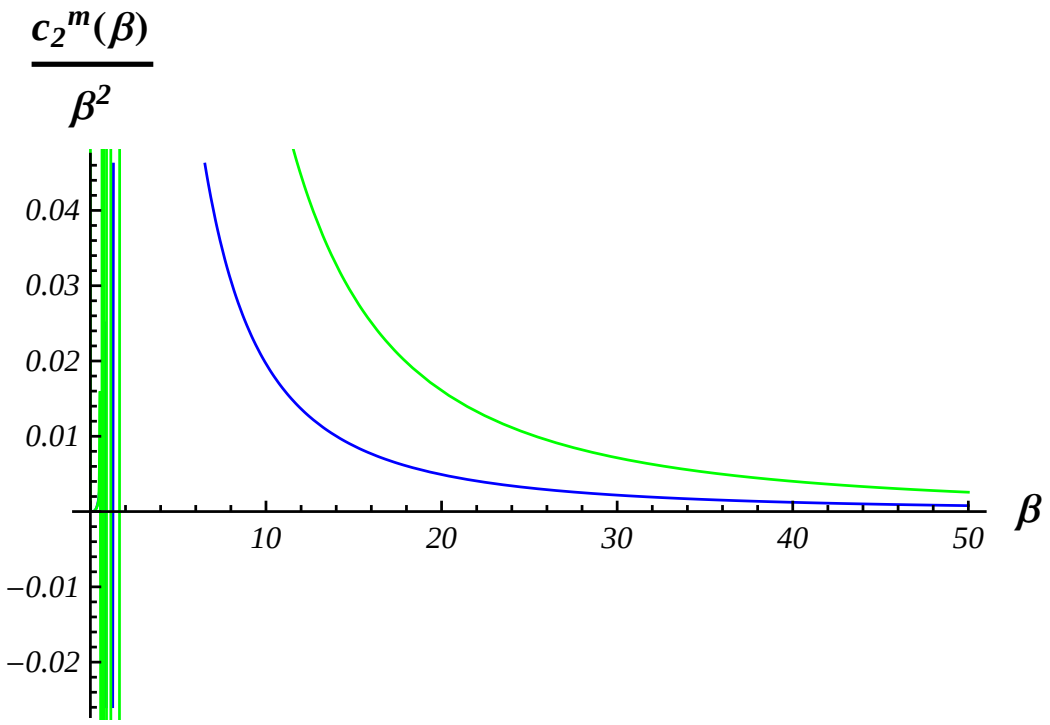

Figure 3.10: The curves represent the second order terms $c_2^{(m)}(\beta)$ (eq.(3.24)) that we find in equation (3.18). The blue curve is the coefficient $c_2^{(m)}(\beta)$ computed for $m = 5$ while the green curve is the coefficient with $m = 10$. Comparing their values with $c_1^{(m)}(\beta)$ computed for the same set of m, we conclude that we can neglect their contribution.

Comparing Fig. 3.10 with Fig. 3.9, we conclude that we can neglect the second order correction in eq.(3.9) for β large.

3.6 Conclusions

In Chapter 2, the polynomials $Q_m(x,\beta)$ (eq.(2.25)) were found to fail in approximating $\overline{\ln(Z_J(\beta))}$, if computed at $x = 0$ (Fig. 2.5).

In this chapter, we have then analyzed the behavior of $Q_m(x,\beta)$ when $x \neq 0$. Choosing a constant value of $x \neq 0$ we obtained the behavior shown in Fig. 3.2 and Fig. 3.3.

The behavior of $Q_m(x,\beta)$ computed along the curve $x(\beta)$ has been studied in Sec. 3.3. The curve $x(\beta)$ has been introduced in Sec. 3.2, by the comparison of $Q_m(x,\beta)$ and $\overline{\ln(Z_J(\beta))}$ over a region of the (x,β) plane. A numerical fit yielded eq.(3.3):

$$x(\beta) = \frac{\epsilon}{\sigma\beta} = \frac{\tilde{\epsilon}}{\beta} \quad \text{for } \beta \gg 1 \tag{3.25}$$

where, we expect that ϵ depends on the number of spins of the system, while $\tilde{\epsilon}$, being rescaled with respect to the standard deviation, should be constant for an arbitrary choice of N.

Substituting $x = x(\beta)$ into the first order approximation of $Q_m(x,\beta)$, for large β, gives a new class of functions which depend only on β, namely $\Theta_m(\beta)$ defined in (3.18). These functions have been truncated at the first order in the expansion, since, as stated in Sec. 3.3, Sec. 3.4 and Sec. 3.5, the second order correction is negligible. We finally obtained eq.(3.19) that gives a good approximation to $\overline{\ln(Z_J(\beta))}$, showed in Fig. 3.6. As stated in Sec. 2.1, we remark that we are interested in the ground state energy value of the system E_0 (2.7), i.e. in the limit slope of $\overline{\ln(Z_J(\beta))}$ for $\beta \gtrsim 1$. All the essential

information required are contained in the $c_1^{(m)}(\beta)$ term of eq.(3.19), while we are not interested in analyzing the constant offset between the solid curves and the red points in Fig. 3.6. This offset is due to the coefficient $c_0^{(m)}$ of eq.(3.18).

In the next chapter, an useful expression for $c_1^{(m)}(\beta)$ will be obtained, taking the limit of an infinite number of replicas. We will also give a physical interpretation of the constant $\tilde{\epsilon}$ introduced with (3.5), showing how it is linked to the value of the ground state energy.

It is interesting to note that, by taking a polynomial truncated at the first order, in the spirit of the discussion in Sec. 2.3, it is enough to use just the first replica to get a good approximation of the value of the ground state energy. Thus, to get the $n \to 0$ limit we must analyze the $n \to \infty$ limit.

Chapter 4

Ground State Energy

In the previous chapter, the calculation in Sec. 3.2, through equations (3.9) and (3.3), led us to write eq.(3.19), i.e. the asymptotic behavior of $\overline{\ln(Z_J(\beta))}$ for large β:

$$\overline{\ln(Z_J(\beta))} \sim \Theta_m(\beta) = c_0^{(m)} + c_1^{(m)}(\beta)\frac{\epsilon}{\sigma\beta} \quad \beta \text{ large.}$$

We are interested in the slope of this line, which should approximate the value of the ground state energy E_0, introduced in Chapter 2 (eq.(2.7)).
In this chapter, the exact calculation of the ground state energy E_0 for the $N = 3$ spin is given.
In the second section we analyze the first order term $c_1^{(m)}(\beta)$ in eq.(3.18) and we show how to obtain its dependence on β. Firstly, starting from equations (3.13) and (3.12), we present some useful calculation that enables us to write

$c_1^{(m)}(\beta)$ as a derivative of the pressure $g_n(\beta)$ with respect to the replica index n. In order to obtain this derivative, we consider the $n \to \infty$ limit and a saddle point approximation, obtaining the exact dependence on β. This procedure yields a method for the estimation of the value of E_0.

4.1 Ground State

As noted in Sec. 2.1, we can exploit equation (2.8) to calculate the quenched logarithm of the partition function and the free energy of the system for large β. We can write:

$$E_0 = \overline{\min_{\{s\}}[H_J(s)]}, \tag{4.1a}$$

$$\overline{\ln(Z_J(\beta))} = \overline{\ln \sum_{\{s\}} e^{-\beta H_J(s)}} \sim \overline{\ln e^{-\beta H_0}} = -\beta E_0, \quad \text{for } \beta \to \infty, \tag{4.1b}$$

$$\lim_{\beta\to\infty} \overline{f_J(\beta)} = -\frac{1}{N} \lim_{\beta\to\infty} \frac{1}{\beta} \overline{\ln(Z_J(\beta))} \sim \frac{1}{N} E_0. \tag{4.1c}$$

Due to the spin flip symmetry, there are four relevant configurations out of eight for the spin's set $\{s\}$. Consequently, we have four possible values of the Hamiltonian (2.1):

$$H_J(s) = \sum_i J_i s_i s_{i+1}. \tag{4.2}$$

The four possible values of the Hamiltonian are:

$$\begin{aligned}\{H_A, H_B, H_C, H_D\} =&\{J_1 + J_2 + J_3, J_1 - J_2 - J_3, \\ &- J_1 + J_2 - J_3, -J_1 - J_2 + J_3\},\end{aligned} \tag{4.3}$$

Which value is the smallest in a point of the $J_i's$ space depends on the value assumed by $\vec{J} = (J_1, J_2, J_3)$ in that point. We shall analyze all possible configurations of the $J_i's$, i.e., completely explore the space in which $\vec{J}$ lives, and understand in which part of this space a particular configuration results as that with the lowest energy.

For example, if $\vec{J} = \{0, 1, 2\}$ we have:

$$\{H_A, H_B, H_C, H_D\} = \{3, -3, -1, 1\}, \tag{4.4}$$

and, thus, the lowest energy is H_B.

This result leads us to divide the space of J_i's in four domains, that we call A,B,C and D, in such a way that $H_J(s)$ is minimized by H_A on A, by H_B on B, and so on. Finally, we must average on the disorder. The minimum of the Hamiltonian is the sum of these four terms:

$$\begin{aligned}E_0 &= \int d\vec{J} P(\vec{J}) H_0 = \int d\vec{J} P(\vec{J}) \min_s [H_J(s)] = \\ &= \int_A d\vec{J} P(\vec{J}) H_A + \int_B d\vec{J} P(\vec{J}) H_B + \\ &\quad + \int_C d\vec{J} P(\vec{J}) H_C + \int_D d\vec{J} P(\vec{J}) H_D.\end{aligned} \tag{4.5}$$

The domain A is obtained by requiring that H_A is the minimum in Eq.(4.3). We get:

$$\begin{cases} H_A \leq H_B \\ H_A \leq H_C \\ H_A \leq H_D \end{cases} \Rightarrow \begin{cases} J_1 + J_2 + J_3 \leq J_1 - J_2 - J_3 \\ J_1 + J_2 + J_3 \leq -J_1 + J_2 - J_3 \\ J_1 + J_2 + J_3 \leq -J_1 - J_2 + J_3 \end{cases} \tag{4.6}$$
$$\Rightarrow \begin{cases} J_3 \leq J_2 \leq -J_3 \\ J_1 \leq -J_2 \end{cases} \wedge \begin{cases} J_2 \leq J_3 \leq -J_2 \\ J_1 \leq -J_3. \end{cases}$$

This system gives the domain A where the Hamiltonian (4.2) is found to be minimized by $H_A = J_1 + J_2 + J_3$. This domain gives the integration limits for the first of the four integrals in eq.(4.5):

$$\begin{aligned} \int_A d\vec{J} P(\vec{J}) H_A = & \int_{-\infty}^{\infty} dJ_3 \int_{J_3}^{-J_3} dJ_2 \int_{-\infty}^{-J_2} dJ_1 P(\vec{J}) \, (J_1 + J_2 + J_3) \\ & + \int_{-\infty}^{\infty} dJ_2 \int_{J_2}^{-J_2} dJ_3 \int_{-\infty}^{-J_3} dJ_1 P(\vec{J}) \, (J_1 + J_2 + J_3) \\ & = 2 \int_{-\infty}^{\infty} dJ_3 \int_{J_3}^{-J_3} dJ_2 \int_{-\infty}^{-J_2} dJ_1 P(\vec{J}) \, (J_1 + J_2 + J_3), \end{aligned} \tag{4.7}$$

with

$$P(\vec{J}) = \left(\frac{3}{2\pi} \right)^{\frac{3}{2}} e^{-\frac{3}{2}(J_1^2 + J_2^2 + J_3^2)}. \tag{4.8}$$

Where we have exploited the symmetry with respect to the change of variables:

$$J_2 \longleftrightarrow J_3,$$

Step by step an exact result can be obtained. We proceed with the first integration:

$$\begin{aligned}
&\int_{-\infty}^{-J_2} e^{-\frac{3}{2}J_1^2}\,(J_1+J_2+J_3)\,dJ_1 \\
&= \int_{-\infty}^{-J_2} e^{-\frac{3}{2}J_1^2} J_1 dJ_1 + (J_2+J_3)\int_{-\infty}^{-J_2} e^{-\frac{3}{2}J_1^2} dJ_1 \\
&= -\left[\frac{1}{3}e^{-\frac{3}{2}J_1^2}\right]\Bigg|_{-\infty}^{-J_2} + (J_2+J_3)\left(\int_{-\infty}^{0} e^{-\frac{3}{2}J_1^2} dJ_1 - \int_{0}^{J_2} e^{-\frac{3}{2}J_1^2} dJ_1\right) \qquad (4.9)\\
&= -\frac{1}{3}e^{-\frac{3}{2}J_2^2} + (J_2+J_3)\left(\sqrt{\frac{\pi}{6}} - \int_{0}^{J_2} e^{-\frac{3}{2}J_1^2} dJ_1\right) \\
&= -\frac{1}{3}e^{-\frac{3}{2}J_2^2} + \sqrt{\frac{\pi}{6}}(J_2+J_3)\left(1-\operatorname{erf}\left(\sqrt{\frac{2}{3}}J_2\right)\right).
\end{aligned}$$

Where $\operatorname{erf}(x)$ is the error function, defined as follows:

$$\operatorname{erf}(x) = \frac{2}{\sqrt{\pi}}\int_0^x e^{-t^2} dt, \qquad (4.10)$$

We must now integrate the previous result eq.(4.9) on $J_2 \in [J_3, -J_3]$ and then on $J_3 \in [-\infty, \infty]$. Eq.(4.9) is made up by the sum of three terms. We shall show that the integration over the first and the third terms in eq.(4.9) yields zero. In fact, integrating these two terms on J_2, the results are both odd functions of J_3 and, since the final integration is made on $[-\infty, \infty]$, it gives zero as its result.

We proceed with the integration over J_2. The first term gives:

$$-\frac{1}{3}\int_{J_3}^{-J_3} dJ_2 e^{-3J_2^2} = -\frac{2}{3}\int_0^{J_3} dJ_2 e^{-3J_2^2} = -\frac{2}{3\sqrt{3}}\mathrm{erf}(\sqrt{3}J_3), \tag{4.11}$$

which vanishes after the integration over J_3 since $\mathrm{erf}(x)$ is an odd function of its argument, so:

$$\int_{-\infty}^{\infty} \mathrm{erf}(x)dx = 0. \tag{4.12}$$

The integration of the second term of eq.(4.9) over J_2 reduces to:

$$\begin{aligned}\int_{J_3}^{-J_3} e^{-\frac{3}{2}J_2^2}(J_2+J_3)dJ_2 =& \int_{J_3}^{-J_3}\left(J_2 e^{-\frac{3}{2}J_2^2}\right)dJ_2 + J_3\int_{J_3}^{-J_3} e^{-\frac{3}{2}J_2^2}dJ_2 \\ =& J_3\int_{J_3}^{-J_3} e^{-\frac{3}{2}J_2^2}dJ_2 = -2J_3\int_0^{J_3} e^{-\frac{3}{2}J_2^2}dJ_2.\end{aligned} \tag{4.13}$$

The integral of $J_2 e^{-\frac{3}{2}J_2^2}$ is zero since it is an odd function integrated over a symmetric domain. This quantity should be multiplied by $\sqrt{\frac{\pi}{6}}$ in the following. The integration on J_3 leads to:

$$\begin{aligned}&-2\sqrt{\frac{\pi}{6}}\int_{-\infty}^{\infty} dJ_3\left(e^{-\frac{3}{2}J_3^2}J_3\int_0^{J_3} e^{-\frac{3}{2}J_2^2}dJ_2\right) \\ =&-2\sqrt{\frac{\pi}{6}}\int_{-\infty}^{\infty} dJ_2 e^{-\frac{3}{2}J_2^2}\left(\int_{J_2}^{\infty} dJ_3\left(e^{-\frac{3}{2}J_3^2}J_3\right)\right) \\ =&-2\sqrt{\frac{\pi}{6}}\int_{-\infty}^{\infty} dJ_2 e^{-\frac{3}{2}J_2^2}\left[-\frac{1}{3}e^{-\frac{3}{2}J_3^2}\right]\Bigg|_{J_2}^{\infty} \\ =&-\frac{2}{3}\sqrt{\frac{\pi}{6}}\int_{-\infty}^{\infty} dJ_2 e^{-3J_2^2} = -\frac{2}{3}\sqrt{\frac{\pi}{6}}\sqrt{\frac{\pi}{3}} = -\frac{\sqrt{2}}{9}\pi.\end{aligned} \tag{4.14}$$

We are left with the calculation of the third term in the summation (4.9), that yields zero too. In fact, integrating over J_2 we get:

$$\begin{aligned}
&-\sqrt{\frac{\pi}{6}}\int_{J_3}^{-J_3} dJ_2 e^{-\frac{3}{2}J_2^2}(J_2+J_3)\mathrm{erf}\left(\sqrt{\frac{2}{3}}J_2\right)\\
=&-\sqrt{\frac{\pi}{6}}\int_{J_3}^{-J_3} dJ_2 e^{-\frac{3}{2}J_2^2}J_2\mathrm{erf}\left(\sqrt{\frac{2}{3}}J_2\right)\\
=&2\sqrt{\frac{\pi}{6}}\int_{0}^{J_3} dJ_2 e^{-\frac{3}{2}J_2^2}J_2\mathrm{erf}\left(\sqrt{\frac{2}{3}}J_2\right)\\
=&2\sqrt{\frac{\pi}{6}}\int_{0}^{J_3} dJ_2 e^{-\frac{3}{2}J_2^2}\left(J_2\int_0^{\sqrt{\frac{2}{3}}J_3} dx e^{-x^2}\right)\\
=&2\sqrt{\frac{\pi}{6}}\int_{0}^{J_3} dx\left(\int_{\sqrt{\frac{3}{2}}x}^{J_3} dJ_2\left(e^{-\frac{3}{2}J_2^2}J_2\right)e^{-x^2}\right)\\
=&2\sqrt{\frac{\pi}{6}}\int_{0}^{J_3} dx\left(\left[-\frac{1}{3}e^{-\frac{3}{2}J_2^2}\right]\Bigg|_{\sqrt{\frac{3}{2}}x}^{J_3} e^{-x^2}\right)\\
=&-\frac{2}{3}\sqrt{\frac{\pi}{6}}\int_0^{J_3} dx\left(e^{-\frac{3}{2}J_3^2-x^2}-e^{-2x^2}\right)\\
=&-\frac{\pi}{3\sqrt{6}}\left(e^{-\frac{3}{2}J_3^2}\mathrm{erf}(J_3)-\frac{1}{\sqrt{2}}\mathrm{erf}\left(\frac{J_3}{\sqrt{3}}\right)\right).
\end{aligned} \tag{4.15}$$

We have obtained the summation of two error functions of J_3 that, integrated on all the real axis, gives zero. Thus, only the second term in (4.9) has a non zero value after this two integration, i.e., (4.14). So, finally:

$$\int_{-\infty}^{\infty} dJ_3\int_{J_3}^{-J_3} dJ_2\int_{-\infty}^{-J_2} dJ_1 e^{-\frac{3}{2}(J_1^2+J_2^2+J_3^2)}\left(J_1+J_2+J_3\right)=-\frac{\sqrt{2}}{9}\pi. \tag{4.16}$$

This term must be multiplied by the normalization coefficient and a factor two, and finally yields:

$$\int_A d\vec{J} P(\vec{J}) H_A = -2 \left(\frac{3}{2\pi} \right)^{\frac{3}{2}} \frac{\sqrt{2\pi}}{9} = -\frac{1}{\sqrt{3\pi}}. \tag{4.17}$$

The same thing happens for the other three integrals in eq.(4.5).

In conclusion, the ground state reads:

$$E_0 = -\frac{4}{\sqrt{3\pi}} \simeq -1.30. \tag{4.18}$$

This result is exact, and we expect our simulations to be in agreement with it. In particular, from eq.(4.1c), we remark that, being $N = 3$:

$$\lim_{\beta \to \infty} \overline{f_J(\beta)} = \frac{1}{3} E_0. \tag{4.19}$$

In Fig. 4.1 we compare the analytical value (4.18) with the numerical results obtained for $\overline{f_J(\beta)}$, already reported in Fig. 2.2. The two trends are in agreement, but there is a tiny difference for large β that can be explained as follows.

The values of $\overline{f_J(\beta)}$ (the red points in Fig. 4.1) were obtained by numerical integration and the integrals present in $\overline{\ln(Z_J(\beta))}$ were calculated over a finite domain (eq.(2.6)). In particular, looking at eq.(2.31), we see that, for a fixed $\vec{J}$:

$$\ln(Z_J(\beta)) \geq \ln(Z_J(0)) = \ln(8), \quad \forall \beta, \tag{4.20}$$

thus, the argument of the integral in eq.(2.6) is positive defined. If we denote with J the space where the vector $\vec{J}$ lives ($\mathbb{R}^3$ for the 3 spin system), we have that the value of $\overline{\ln(Z_J(\beta))}$ computed over a finite domain $D \subset J$ will be smaller then the value of the same integral computed over all the J space:

$$\int_D d\vec{J} P(\vec{J}) \ln(Z_J(\beta)) \leq \int_J d\vec{J} P(\vec{J}) \ln(Z_J(\beta)). \tag{4.21}$$

Looking now at eq.(2.4), we see that, since:

$$\overline{f_J(\beta)} = -\frac{1}{N\beta} \overline{\ln(Z_J(\beta))}, \tag{4.22}$$

$\overline{f_J(\beta)}$ behaves in the opposite way, and thus we can write:

$$\left. \overline{f_J(\beta)} \right|_D \geq \left. \overline{f_J(\beta)} \right|_J . \tag{4.23}$$

In conclusion, by taking a larger integration domain, the agreement of the numerical results with the analytical value of E_0 will be improved.

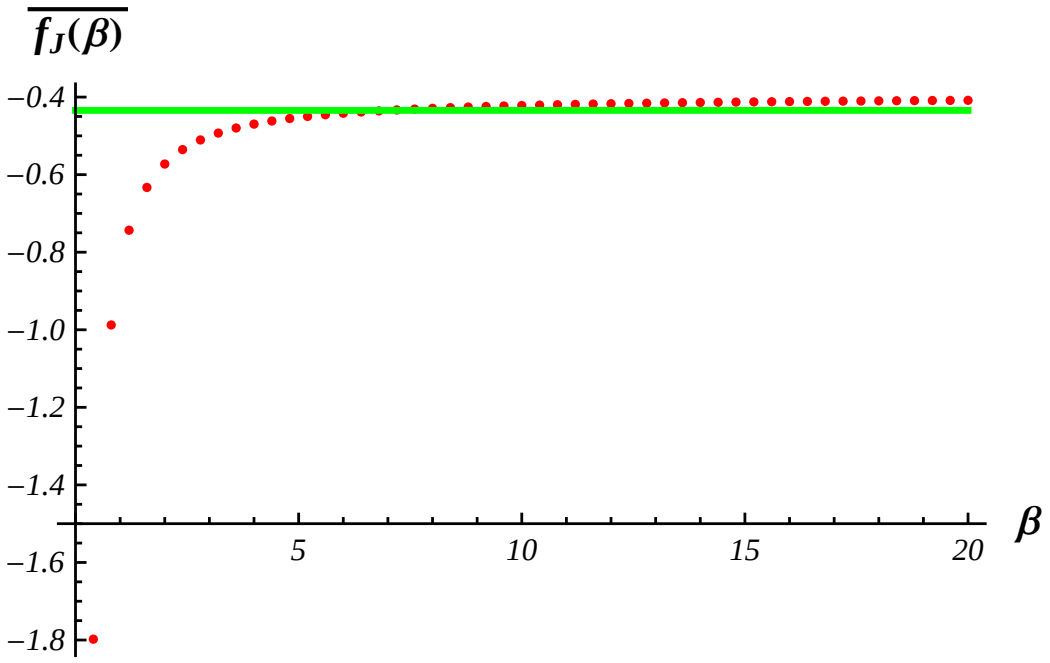

Figure 4.1: The red points are the values of $\overline{f_J(\beta)}$ computed with (2.6) and (2.4), while the green line is the value of $\frac{1}{3}E_0$ obtained from (4.5) to (4.18). The difference between the green line and the red points for great β arises because the values of $\overline{f_J(\beta)}$ have been computed numerically: the Gaussian integrals involved in eq.(2.6) have been computed on a finite domain of the $\vec{J}$ space, instead of the range $[-\infty, \infty]$.

4.2 $c_1^{(m)}(\beta)$ expansion

At the end of the previous chapter (Sec. 3.4), we introduced the function $\Theta_m(\beta)$ (eq.(3.18)):

$$\Theta_m(\beta) = c_0^{(m)} + \frac{\epsilon}{\sigma\beta} c_1^{(m)}(\beta), \tag{4.24}$$

which can be used for the estimation of $\overline{\ln(Z_J(\beta))}$ within the $\beta \to \infty$ limit:

$$\overline{\ln(Z_J(\beta))} \sim \Theta_m(\beta) \quad \text{for } \beta \text{ large.} \tag{4.25}$$

From eq.(3.13), eq.(3.12) and eq.(2.11) we know the expression for $c_1^{(m)}(\beta)$:

$$c_1^{(m)}(\beta) = \sum_{j=1}^{m} g_j(\beta) h'_{j,m}(0). \tag{4.26}$$

Eq.(4.25) is a good approximation for $\overline{\ln(Z_J(\beta))}$, for large values of β (see Fig. 3.6). In this section, we will give the explicit dependence of $c_1^{(m)}(\beta)$ on β. In eq.(4.26), we note that the dependence of $c_1^{(m)}$ on β is encoded in $g_j(\beta)$. It is possible to show that the value of $c_1^{(m)}(\beta)$ can be approximated by the largest term in the summation over j.

We note that the values of $h'_{j,m}(0)$, with $1 \leq j \leq m$, can be approximated by the stationary points of an oscillating Gaussian function, with its central peak centered on the value of $j = \frac{m}{2}$:

$$h'_{j,m}(0) \simeq e^{a_m} e^{-\frac{1}{2}\frac{(j-\frac{m}{2})^2}{b_m}} (-1)^j. \tag{4.27}$$

Thus, the highest term in (4.26) is the term with $j = \frac{m}{2}$. In Fig. 4.2, the red points are the values of $h'_{j,m}(0)$ computed for $m = 20$ and $j \in [1, 20]$, while the violet line is the expression found in eq.(4.27) with the constant a_m and b_m numerically computed for $m = 20$. We have found that the height of the central maximum grows exponentially with m (i.e. a_m is linear with respect to m). We compare the behavior of $h_{j,6}(0)$ with the trend of the pressure $g_j(\beta)$ for $j \in [1, 6]$ in Fig. 4.3, which is analogous to Fig. 4.2 but with the value of m set to 6. The blue curve is the value of the pressure $g_j(\beta)$ for $\beta = 1$. We observe that $g_j(\beta)$ grows slowly with j with respect to $h'_{j,m}(0)$, so we can consider its value as constant with respect to $h'_{j,m}(0)$ that strongly oscillates when j increases. The value of $g_j(\beta)$ can be taken out of the sum in eq.(4.26), with the value of j relative to the most important term of $h_{j,m}(0)$, that is $j = \frac{m}{2}$.[1] We then write:

$$c_1^{(m)}(\beta) \simeq g_{\frac{m}{2}}(\beta) \sum_{j=1}^{m} h'_{j,m}(0). \tag{4.28}$$

But this approximation fails since:

$$\sum_{j=1}^{m} h'_{j,m}(0) = 0. \tag{4.29}$$

[1] If m is odd, the maximum value is achieved for $j = \frac{m-1}{2}$

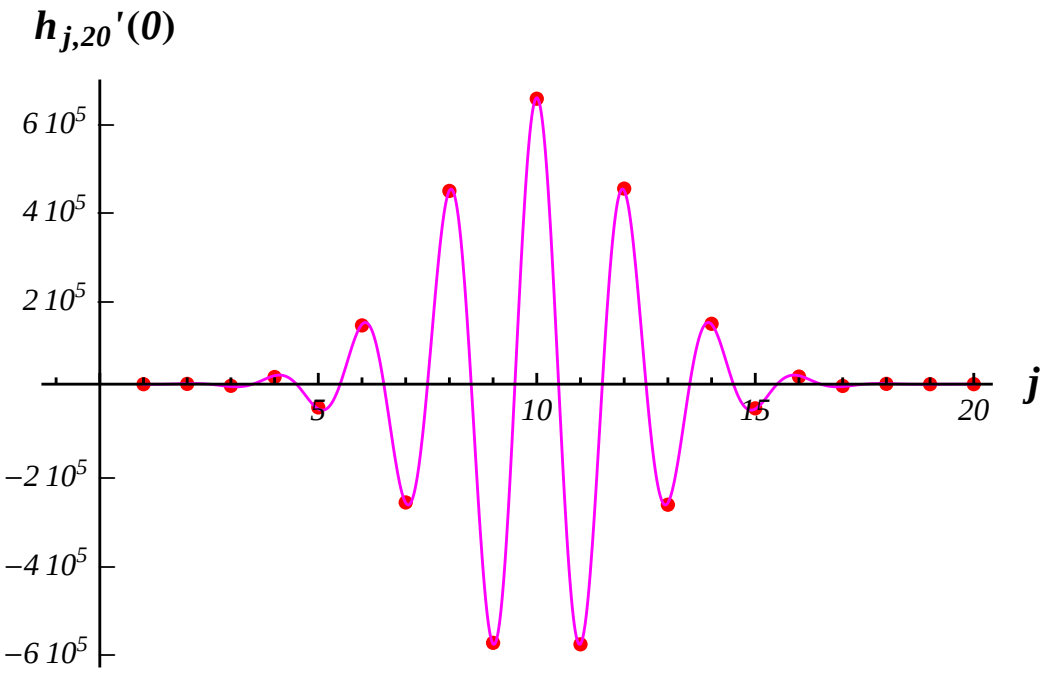

Figure 4.2: The red points are the various value of $h'_{j,m}(x)$ defined in eq.(3.12), with $m = 20$, the violet line is the oscillating Gaussian approximation eq.(4.27).

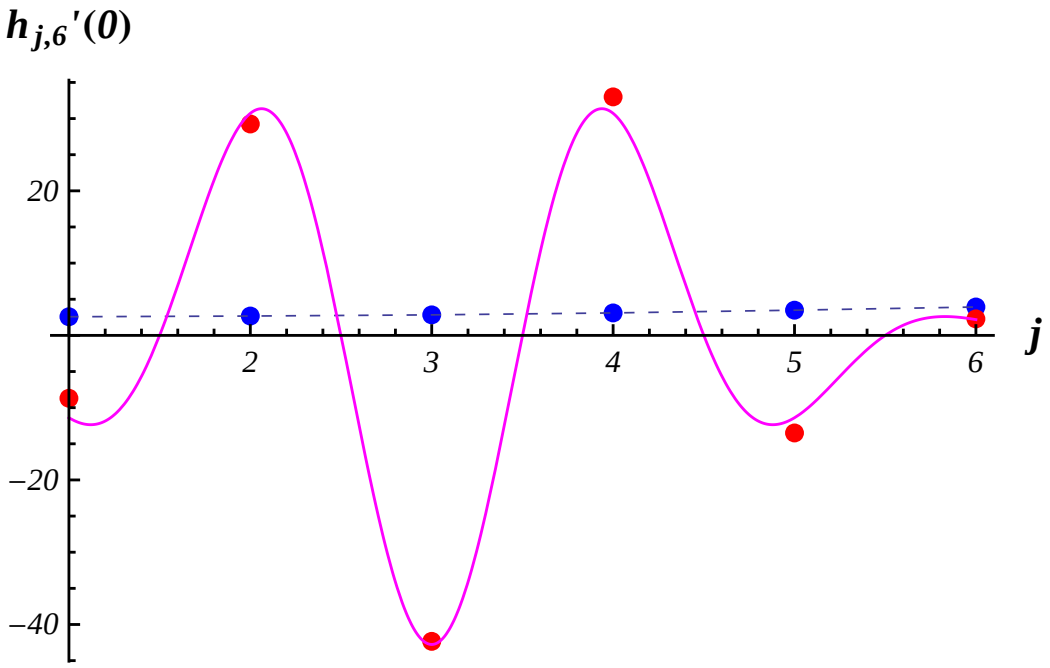

Figure 4.3: The red points are the various value of $h'_{j,m}(x)$ (defined in eq.(3.12)), with $m = 6$, the violet line is the oscillating Gaussian approximation (eq.(4.27)) and the blue points are the values of $g_j(\beta)$ (eq.(2.11) computed for $\beta = 1$ and $j \in [1, 6]$.

Indeed:

$$\begin{aligned} h'_{j,m}(0) &= \frac{1}{\prod_{i\neq j}(j-i)} \sum_{\substack{k=1\\k\neq j}}^{m} \prod_{\substack{i=1\\i\neq k\\i\neq j}}^{m} (-i) \\ &= \frac{1}{\prod_{i\neq j}(j-i)} \sum_{\substack{k=1\\k\neq j}}^{m} \frac{(-1)^m m!}{kj} \\ &= \frac{(-1)^m m!}{\prod_{i\neq j}(j-i)} \sum_{\substack{k=1\\k\neq j}}^{m} \frac{1}{kj} = \frac{(-1)^m m!}{\prod_{i\neq j} j(j-i)} \sum_{\substack{k=1\\k\neq j}}^{m} \frac{1}{k}. \end{aligned} \tag{4.30}$$

We can use for the denominator:

$$\begin{aligned} \prod_{i\neq j}^{m} j(j-i) &= j(j-1)(j-2)\dots(j-j+1)(j-j-1)\dots(j-m) = \\ &= (-1)^{m-j} j!(m-j)!. \end{aligned} \tag{4.31}$$

So $h'_{j,m}(0)$ becomes:

$$\begin{aligned} h'_{j,m}(0) &= (-1)^m (-1)^{-m+j} m! \frac{1}{j!(m-j)!} \sum_{\substack{k=1\\k\neq j}}^{m} \frac{1}{k} \\ &= (-1)^j \binom{m}{j} \sum_{\substack{k=1\\k\neq j}}^{m} \frac{1}{k} = (-1)^j \binom{m}{j} \left(\sum_{k=1}^{m} \frac{1}{k} - \frac{1}{j} \right). \end{aligned} \tag{4.32}$$

Now we sum over the index j:

$$\sum_{j=1}^{m} h'_{j,m}(0) = \left(\sum_{k=1}^{m} \frac{1}{k} \right) \left(\sum_{j=1}^{m} (-1)^j \binom{m}{j} \right) - \sum_{j=1}^{m} \frac{(-1)^j}{j} \binom{m}{j}. \tag{4.33}$$

Exploiting the binomial formula (cfr: (A.1)):

$$\sum_{j=0}^{m}(-1)^j\binom{m}{j}=0\Rightarrow\sum_{j=1}^{m}(-1)^j\binom{m}{j}=-1. \tag{4.34}$$

Thus, the previous expression becomes:

$$\sum_{j=1}^{m}h'_{j,m}(0)=-\sum_{j=1}^{m}\frac{1}{j}\left(1+(-1)^j\binom{m}{j}\right). \tag{4.35}$$

By induction, we can show that:

$$\sum_{j=1}^{m}\frac{1}{j}\left(1+(-1)^j\binom{m}{j}\right)=0. \tag{4.36}$$

Indeed the previous equation holds for $m=1$. Supposing that it is true for $m-1$ we can write:

$$\sum_{j=1}^{m}\frac{1}{j}\left(1+(-1)^j\binom{m}{j}\right)=\sum_{j=1}^{m-1}\frac{1}{j}\left(1+(-1)^j\binom{m}{j}\right)+\frac{1+(-1)^m}{m}. \tag{4.37}$$

We show that the first term of the previous equation is the opposite of the second. Keeping in mind that:

$$\binom{k}{l}=\binom{k-1}{l}+\binom{k-1}{l-1}, \tag{4.38}$$

we obtain:

$$\begin{aligned}\sum_{j=1}^{m-1}\frac{1}{j}\left(1+(-1)^j\binom{m}{j}\right) =& \sum_{j=1}^{m-1}\frac{1}{j}\left(1+(-1)^j\binom{m-1}{j}+(-1)^j\binom{m-1}{j-1}\right)\\ =& \sum_{j=1}^{m-1}\frac{(-1)^j}{j}\binom{m-1}{j-1}\\ =& \frac{1}{m}\sum_{j=1}^{m-1}\frac{(-1)^j}{j}\binom{m}{j}\\ =& \frac{1}{m}\left(\sum_{j=1}^{m}\frac{(-1)^j}{j}\binom{m}{j}-(-1)^m\right)\\ =& -\frac{1}{m}\left(1+(-1)^m\right).\end{aligned} \tag{4.39}$$

We have shown that eq.(4.29) holds, thus we cannot exploit eq.(4.28) to obtain the dependence of $c_1^{(m)}(\beta)$ on β.

We then, cannot take the value of $g_{\frac{m}{2}}(\beta)$ out of the sum (4.26), since the value of $h'_{j,m}(0)$ is strongly oscillating with mean 0. We can instead carry out the derivative of the pressure $g_j(\beta)$ with respect to j in the point $j=\frac{m}{2}$:

$$g_j(\beta)\simeq g_{\frac{m}{2}}+\left.\frac{\partial g_j(\beta)}{\partial j}\right|_{j=\frac{m}{2}}\left(j-\frac{m}{2}\right), \tag{4.40}$$

and, by inserting this result in eq.(4.26), we have that:

$$\begin{aligned} c_1^{(m)}(\beta) =& \sum_{j=1}^{m} g_j(\beta) h'_{j,m}(0) \simeq \sum_{j=1}^{m} \left(g_{\frac{m}{2}}(\beta) + \left.\frac{\partial g_j(\beta)}{\partial j}\right|_{j=\frac{m}{2}} \left(j - \frac{m}{2}\right) \right) h'_{j,m}(0) \\ =& \left(g_{\frac{m}{2}}(\beta) - \frac{m}{2} \left.\frac{\partial g_j(\beta)}{\partial j}\right|_{j=\frac{m}{2}} \right) \sum_{j=1}^{m} h'_{j,m}(0) + \left.\frac{\partial g_j(\beta)}{\partial j}\right|_{j=\frac{m}{2}} \sum_{j=1}^{m} j h'_{j,m}(0) \\ =& \left.\frac{\partial g_j(\beta)}{\partial j}\right|_{j=\frac{m}{2}} \sum_{j=1}^{m} j h'_{j,m}(0), \end{aligned} \tag{4.41}$$

where, in the last line, we have used eq.(4.29). Now, the function $j\, h'_{j,m}(0)$ still oscillates, but with mean 1. Using eq.(4.32), it is straightforward to show that:

$$\sum_{j=1}^{m} j h'_{j,m}(0) = \left(\sum_{k=1}^{m} \frac{1}{k} \right) \left(\sum_{j=1}^{m} (-1)^j j \binom{m}{j} \right) - \sum_{j=1}^{m} (-1)^j \binom{m}{j} = 1, \tag{4.42}$$

since

$$\sum_{j=1}^{m} (-1)^j j \binom{m}{j} = 0. \tag{4.43}$$

Indeed, again by induction, being the last equation true for $m = 2$, if we assume:

$$\sum_{j=1}^{m-1} (-1)^j j \binom{m-1}{j} = 0, \tag{4.44}$$

we obtain:

$$\begin{aligned}
\sum_{j=1}^{m}(-1)^j j\binom{m}{j} &= \sum_{j=1}^{m-1}(-1)^j j\binom{m}{j} + (-1)^m m \\
&= \sum_{j=1}^{m-1}(-1)^j j\left(\binom{m-1}{j} + \binom{m-1}{j-1}\right) + (-1)^m m \\
&= \sum_{j=1}^{m-1}(-1)^j j\binom{m-1}{j} + \sum_{j=1}^{m-1}(-1)^j j\binom{m-1}{j-1} + (-1)^m m \\
&= \sum_{j=1}^{m-1}(-1)^j j\binom{m-1}{j-1} + (-1)^m m \\
&= \sum_{j=0}^{m-1}(-1)^{j+1}(j+1)\binom{m-1}{j} - (-1)^m m + (-1)^m m \\
&= \sum_{j=0}^{m-1}(-1)^{j+1} j\binom{m-1}{j} + \sum_{j=0}^{m-1}(-1)^{j+1}\binom{m-1}{j} = 0.
\end{aligned} \tag{4.45}$$

We then have that eq.(4.41) becomes:

$$c_1^{(m)}(\beta) \simeq \frac{\partial g_j(\beta)}{\partial j}. \tag{4.46}$$

In this way we can express equations (4.24) and (4.25) as follows:

$$\Theta_m(\beta) = c_0^{(m)} + \frac{\epsilon}{\sigma\beta}\frac{\partial g_n(\beta)}{\partial n}, \tag{4.47}$$

$$\overline{\ln(Z_J(\beta))} \sim c_0^{(m)} + \frac{\epsilon}{\sigma\beta}\frac{\partial g_n(\beta)}{\partial n}, \quad \text{for } \beta \text{ large.} \tag{4.48}$$

Where, we should set $\sigma = \frac{1}{\sqrt{3}}$ from eq.(1.11).

Now, recalling eq.(4.1b) from Sec. 4.1 we have that:

$$E_0 \sim -\frac{1}{\beta}\overline{\ln(Z_J(\beta))}, \qquad \text{for } \beta \to \infty. \tag{4.49}$$

We can thus write:

$$\begin{aligned} E_0 =& -\frac{1}{\beta}\left(c_0^{(m)} + c_1^{(m)}(\beta)\left(\frac{\epsilon}{\sigma\beta}\right)\right) \\ =& -\frac{1}{\beta}c_0^{(m)} - \frac{\epsilon}{\sigma\beta^2}c_1^{(m)}(\beta) \\ =& -\frac{1}{\beta}c_0^{(m)} - \frac{\epsilon}{\sigma\beta^2}\frac{\partial g_n(\beta)}{\partial n}. \end{aligned} \tag{4.50}$$

Recalling that $c_0^{(m)}$ is the constant value reached by $c_0^{(m)}(\beta)$ within the $\beta \to \infty$ limit, see eq.(3.11), while $c_1^{(m)}(\beta)$ behaves quadratically (see Fig. 2.5 and Sec. 3.4), in the following we will write the ground state energy value E_0 as follows:

$$E_0 = -\frac{\epsilon}{\sigma\beta^2}\frac{\partial g_n(\beta)}{\partial n}. \tag{4.51}$$

We must express what we mean by $\frac{\partial g_n(\beta)}{\partial n}$, since n is a discrete variable. We can use a finite difference for this:

$$\begin{aligned} \frac{\partial(g_n(\beta))}{\partial n} &\equiv g_{n+1}(\beta) - g_n(\beta) \\ &= \frac{1}{n+1}\ln\left(\overline{Z_J(\beta)^{n+1}}\right) - \frac{1}{n}\ln\left(\overline{Z_J(\beta)^n}\right). \end{aligned} \tag{4.52}$$

We shall take the $n \to \infty$ limit. In this limit eq.(4.41) is esaier to handle because we can use the saddle point method in eq.(4.52) for the estimation of $g_n(\beta)$.

4.3 The $n \to \infty$ limit

Eq.(2.22) and eq.(2.21) stated that:

$$\begin{aligned}\overline{Z_J(\beta)^n} &= 2^n \sum_{|k|\leq n} \binom{n}{\vec{k}} e^{\frac{\beta^2\sigma^2}{2} r^2(n,\vec{k})} \\ &= 2^n \sum_{|k|\leq n} \frac{n!}{k_1!k_2!k_3!(n-|\vec{k}|)!} e^{\frac{\beta^2\sigma^2}{2} r^2(n,\vec{k})},\end{aligned} \tag{4.53}$$

$$r^2(n,\vec{k}) = (n-2k_1-2k_2)^2 + (n-2k_1-2k_3)^2 + (n-2k_2-2k_3)^2, \tag{4.54}$$

where $\vec{k} = (k_1, k_2, k_3)$ and $|\vec{k}| = k_1 + k_2 + k_3$ were defined in Chapter 2.
We will show that, for large values of n, we can approximate eq.(4.53) with the leading term in the summation over $|\vec{k}|$. The leading term corresponds to $\vec{k} = (0,0,0)$. For this task, we introduce the scaled variables x, y and z, such that:

$$\begin{aligned} k_1 = nx \quad k_2 = ny \quad k_3 = nz, \\ \vec{k} = n\vec{t} \quad \text{with} \quad \vec{t} = (x,y,z). \end{aligned} \tag{4.55}$$

We rewrite $\overline{Z_J(\beta)^n}$ as:

$$\begin{aligned}\overline{Z_J(\beta)^n} &= 2^n \sum_{|t|\leq 1} \frac{n!}{(nx)!(ny)!(nz)!(n(1-|\vec{t}|))!} e^{\frac{\beta^2\sigma^2 n^2}{2} w^2(\vec{t})} \\ &= 2^n \sum_{|t|\leq 1} \binom{n}{n\vec{t}} e^{\frac{\beta^2\sigma^2 n^2}{2} w^2(\vec{t})},\end{aligned} \tag{4.56}$$

where:

$$\begin{gathered}|\vec{t}| = x + y + z \quad \text{and} \\ w^2(\vec{t}) = (1-2x-2y)^2 + (1-2x-2z)^2 + (1-2y-2z)^2.\end{gathered} \tag{4.57}$$

By using Stirling's approximation, we show that, as $n \to \infty$, the behavior of the multinomial coefficient can be neglected in eq.(4.56). Indeed, from :

$$\ln n! \simeq n \ln n - n + \frac{1}{2} \ln 2\pi n, \quad \text{for } n \to \infty, \tag{4.58}$$

we have:

$$\begin{aligned}
\ln \binom{n}{n\vec{t}} =& \ln \left(\frac{n!}{(nx)!(ny)!(nz)!(n(1-|\vec{t}|))!} \right) \\
\simeq& n \ln n - n + \frac{1}{2} \ln 2\pi n \\
& - nx \ln nx + nx - \frac{1}{2} \ln(2\pi nx) \\
& - ny \ln ny + ny - \frac{1}{2} \ln(2\pi ny) \\
& - nz \ln nz + nz - \frac{1}{2} \ln(2\pi nz) \\
& - n(1-|\vec{t}|) \ln n(1-|\vec{t}|) + n(1-|\vec{t}|) - \frac{1}{2} \ln 2\pi n(1-|\vec{t}|) \\
=& - n(x \ln x + y \ln y + z \ln z) - \frac{1}{2} \ln \frac{1}{(2\pi n)^3 xyz(1-|\vec{t}|)}.
\end{aligned} \tag{4.59}$$

So, we get:

$$\begin{aligned}
\lim_{n\to\infty} \binom{n}{n\vec{t}} &= \frac{1}{\sqrt{(2\pi n)^3 xyz(1-|\vec{t}|)}} e^{-n(x \ln x + y \ln y + z \ln z)} \\
&\equiv \frac{1}{\sqrt{(2\pi n)^3 xyz(1-|\vec{t}|)}} e^{-nS(x,y,z)},
\end{aligned} \tag{4.60}$$

where we have introduced:

$$S(x,y,z) = x \ln(x) + y \ln(y) + z \ln(z). \tag{4.61}$$

In the limit of an infinite number of replicas n, the multinomial factor $\binom{n}{n\vec{t}}$ does not grow as n^n, but as a negative exponential of n. Eq.(4.56) becomes:

$$\overline{Z_J(\beta)^n} \simeq \sum_{|\vec{t}|\leq 1} \frac{1}{\sqrt{(2\pi n)^3 xyz(1-|\vec{t}|)}} e^{-nS(x,y,z)} e^{\frac{\beta^2\sigma^2 n^2}{2} w^2(\vec{t})}, \quad \text{for } n \to \infty. \tag{4.62}$$

The largest term in $\overline{Z_J(\beta)^n}$ is the exponential of $\frac{\beta^2\sigma^2n^2}{2}w^2(\vec{t})$. We can replace the summation over $|\vec{t}|$ in eq.(4.56) with this term, by choosing $x = y = z = 0$. With this choice we have that, from equations (4.61) and (4.57):

$$\begin{gathered} \lim_{(x,y,z)\to\{0,0,0\}} S(x,y,z) = 0, \\ \text{and} \quad w^2(\vec{0}) = 3. \end{gathered} \tag{4.63}$$

In this way, setting $\vec{k} = (0,0,0)$ in eq.(4.53), $\overline{Z_J(\beta)^n}$ becomes:

$$\overline{Z_J(\beta)^n} \simeq 2^n e^{\frac{\beta^2\sigma^2n^2}{2}w^2(\vec{0})} = 2^n e^{\frac{3\sigma^2}{2}\beta^2 n^2}. \tag{4.64}$$

And eq.(4.52) finally becomes:

$$\begin{aligned} \lim_{n\to\infty} \frac{\partial(g_n(\beta))}{\partial n} &= \lim_{n\to\infty} \left[\frac{1}{n+1} \ln\left(\overline{Z_J(\beta)^{n+1}}\right) - \frac{1}{n} \ln\left(\overline{Z_J(\beta)^n}\right) \right] \\ &= \frac{1}{n+1} \ln\left(2^{n+1} e^{\frac{3\sigma^2}{2}\beta^2(n+1)^2}\right) - \frac{1}{n} \ln\left(2^n e^{\frac{3\sigma^2}{2}\beta^2 n^2}\right) \\ &= \frac{3\sigma^2}{2}\beta^2(n+1) - \frac{3\sigma^2}{2}\beta^2 n = \frac{3\sigma^2}{2}\beta^2. \end{aligned} \tag{4.65}$$

We can conclude the discussion began in Sec(4.2) for the explicit calculation of the β dependence of the first order coefficient $c_1^{(m)}(\beta)$ of the equation (4.24). From equations (4.26),(4.41),(4.42) and (4.65):

$$\begin{aligned} c_1^{(m)}(\beta) &= \sum_{j=1}^{m} g_j(\beta) h'_{j,m}(0) \\ &\simeq \frac{\partial g_j(\beta)}{\partial j} \sum_{j=1}^{m} j h'_{j,m}(0) \\ &= \frac{\partial g_j(\beta)}{\partial j} \simeq \frac{3\sigma^2}{2}\beta^2. \end{aligned} \tag{4.66}$$

Eq.(4.25), introduced in Sec. 3.4 then becomes:

$$\begin{aligned} \overline{\ln(Z_J(\beta))} &\sim c_0^{(m)} + \frac{\epsilon}{\sigma\beta} c_1^{(m)}(\beta) \\ &= c_0^{(m)} + \frac{\epsilon}{\sigma\beta} \frac{\partial g_n(\beta)}{\partial n} \\ &= c_0^{(m)} + \frac{3}{2}\sigma\beta\epsilon, \quad \text{for } \beta \text{ large}, \end{aligned} \tag{4.67}$$

with ϵ defined at the end of Sec. 3.2, while, for the ground state energy E_0 we have:

$$E_0 = -\frac{\epsilon}{\sigma\beta^2} \frac{\partial g_n(\beta)}{\partial n} = -\frac{\epsilon}{\sigma\beta^2} \frac{3\sigma^2}{2}\beta^2 = -\frac{3\epsilon\sigma}{2}. \tag{4.68}$$

4.4 Conclusions

In this chapter we have exactly computed the ground state energy for a system described by the Hamiltonian (4.2):

$$E_0 = -\frac{4}{\sqrt{3\pi}}. \tag{4.69}$$

We have then shown that the exact dependence of $c_1^{(m)}(\beta)$ (first order coefficient in eq.(3.18)) on β can be obtained with a saddle point approximation within the $n \to \infty$ limit. Eq.(3.18) can be rearranged, looking at (4.67) as follows:

$$\begin{aligned} \Theta_m(\beta) &= c_0^{(m)} + c_1^{(m)}(\beta) \\ &= c_0^{(m)} + \frac{\partial g_n(\beta)}{\partial n} \\ &= c_0^{(m)} + \frac{3\sigma}{2}\epsilon\beta. \end{aligned} \tag{4.70}$$

From section (3.2) we remark that $\Theta_m(\beta)$ has been obtained in the spirit of eq.(3.6),

$$\overline{\ln(Z_J(\beta))} = Q_m(x(\beta), \beta), \tag{4.71}$$

with $x(\beta)$ obtained from eq.(3.3). The asymptotic expression of $\overline{\ln(Z_J(\beta))}$ for large β can be obtained from equations (3.19), (3.18) and (4.66):

$$\overline{\ln(Z_J(\beta))} \sim c_0^{(m)} + \frac{3\sigma}{2}\epsilon\beta, \quad \text{for } \beta \text{ large.} \tag{4.72}$$

Moreover, looking at eq.(4.1b) we can write:

$$\overline{\ln(Z_J(\beta))} = -\beta E_0. \tag{4.73}$$

Merging the latter results we have that (4.68):

$$E_0 = -\frac{\epsilon}{\sigma\beta^2}\frac{\partial g_n(\beta)}{\partial n} = -\frac{\epsilon}{\sigma\beta^2}\frac{3\sigma^2}{2}\beta^2 = -\frac{3\epsilon\sigma}{2}. \tag{4.74}$$

Having neglected the terms $\frac{c_0^{(m)}(\beta)}{\beta}$ which result to be negligible in the $\beta \to \infty$ limit. We are able now to compare the numerical calculation made for $\overline{f_J(\beta)}$, the exact value of the ground state energy E_0 with our results for the free energy density in the $\beta \to \infty$ limit. In Fig(4.4) we show the free energy density (the red points, as in Fig.(2.1)) plus the value of $\frac{E_0}{3}$ (green line, see Fig. 4.1). The blue line is the value obtained from eq.(4.68), having set $\sigma = \frac{1}{\sqrt{3}}$. This yields to: $-\frac{\epsilon}{2\sqrt{3}} = -0.39$.

We have found that the following equation gives a good approximation for the value of the free energy density within the limit of low temperatures for a 3-spin system:

$$\lim_{\beta\to\infty} \overline{f_J(\beta)} = -\frac{\sigma}{2}\epsilon = -\frac{1}{2\sqrt{3}}\epsilon, \tag{4.75}$$

where we have set $\sigma = \frac{1}{\sqrt{3}}$. Now, we must see if this equation is valid in general. In the next chapter we will investigate the behavior of a system with a number of spins $N > 3$.

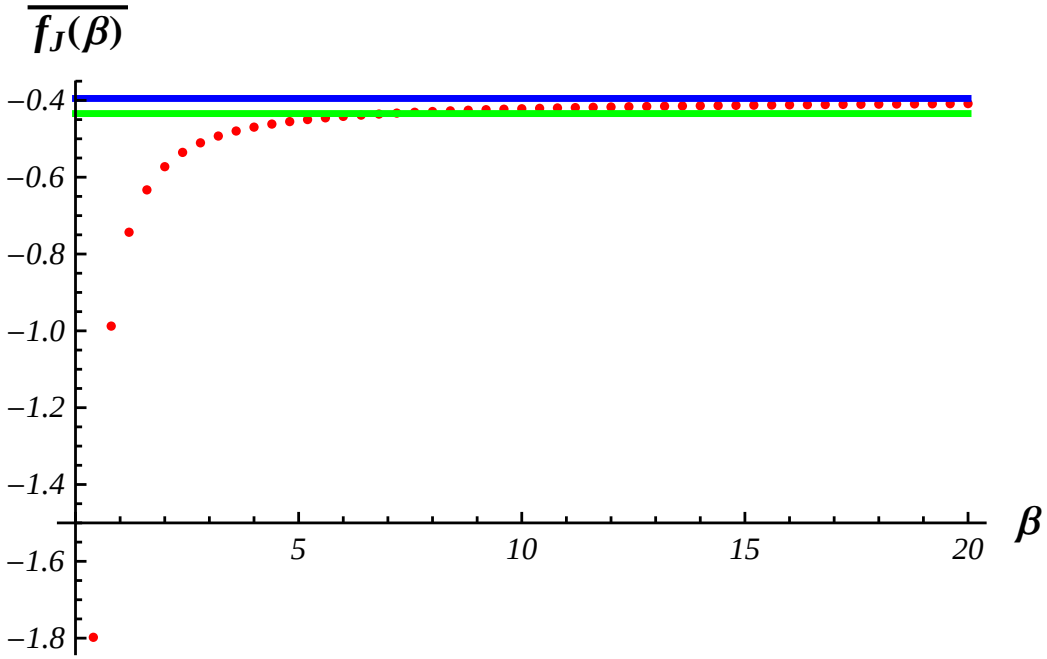

Figure 4.4: As in Fig. 4.1, the red points represent the values of $\overline{f_J(\beta)}$ computed with (2.6) and (2.4), while the green line is the value of $\frac{1}{3}E_0$ obtained from (4.5) to (4.18).
The blue line instead, represent the value obtained with eq.(4.75)

Chapter 5

Larger Systems

In this chapter, we generalize the methods introduced in the previous chapter eq.(4.75) for the estimation of the free energy density $\overline{f_J(\beta)}$ and, hence, within the $\beta \to \infty$ limit, of the ground state energy value E_0 of a finite size spin glass.

We present the exact calculation of the pressure $g_n(\beta)$ (eq.(2.11)) for a system with 4 spins, by covering the procedure used in the second chapter (Sec. 2.2). Exploiting the results achieved in Sec. 4.2 and Sec. 4.3, we show that is possible to obtain a relationship that estimates the ground state energy for a system of $N = 4$ spins using the constant $\tilde{\epsilon}$ introduced with eq.(3.5).

In the last section, this approach is generalized to a spin glass system with an arbitrary number of spins N.

5.1 4-spin system

Let us consider a system of $N = 4$ spins, interacting with each other according to the following Hamiltonian:

$$\begin{aligned} H_J(s) = \sum_{\langle i,j \rangle} J_{i,j} s_i s_j = & J_1 s_1 s_2 + J_2 s_1 s_3 + J_3 s_1 s_4 \\ & + J_4 s_2 s_3 + J_5 s_2 s_4 + J_6 s_3 s_4, \end{aligned} \tag{5.1}$$

where the summation over $\langle i, j \rangle$ is made on all distinct pairs of spins. In (5.1) we have called for simplicity:

$$\begin{aligned} & J_{1,2} \equiv J_1, \quad J_{1,3} \equiv J_2, \quad J_{1,4} \equiv J_3, \\ & J_{2,3} \equiv J_4, \quad J_{2,4} \equiv J_5, \quad J_{3,4} \equiv J_6. \end{aligned}$$

The probability distribution function $P(J)$, introduced in eq.(1.3), becomes:

$$\begin{aligned} P(J_1, \ldots, J_6) &= \left(\frac{1}{2\pi\sigma^2} \right)^{\frac{1}{2}\frac{N(N-1)}{2}} \exp\left\{ -\frac{J_1^2 + J_2^2 + J_3^2 + J_4^2 + J_5^2 + J_6^2}{2\sigma^2} \right\} \\ &= \left(\frac{1}{2\pi\sigma^2} \right)^{3} \exp\left\{ -\frac{J_1^2 + J_2^2 + J_3^2 + J_4^2 + J_5^2 + J_6^2}{2\sigma^2} \right\}, \end{aligned} \tag{5.2}$$

having set $N = 4$. We shall study numerically the free energy ground state of the system. As in eq.(2.4) we have:

$$\overline{f_J(\beta)} = -\frac{1}{\beta N} \overline{\ln(Z_J(\beta))}. \tag{5.3}$$

Where $Z_J(\beta)$ is the partition function of the system and the symbol $\overline{(\dots)}$ denotes the quenched average introduced in Sec. 1.2.

The Hamiltonian (5.1) is symmetric with respect to the spin flip operator eq.(1.12), hence, the relevant spin configurations are $2^{N-1} = 8$ and, since a mean field interaction is adopted, the number of interactions between spins is equal to the number of pairs, i.e. $\frac{N(N-1)}{2} = 6$. The partition function $Z_J(\beta)$ can be expressed as:

$$\begin{aligned} Z_J(\beta) = \sum_{\{s\}} e^{-\beta H_J(s)} = 2 \times \big(& e^{-\beta(J_1+J_2+J_3+J_4+J_5+J_6)} + e^{-\beta(J_1+J_2-J_3+J_4-J_5-J_6)} \\ & + e^{-\beta(J_1-J_2+J_3-J_4+J_5-J_6)} + e^{-\beta(-J_1+J_2+J_3-J_4-J_5+J_6)} \\ & + e^{-\beta(-J_1-J_2-J_3+J_4+J_5+J_6)} + e^{-\beta(J_1-J_2-J_3-J_4-J_5+J_6)} \\ & + e^{-\beta(-J_1+J_2-J_3-J_4+J_5-J_6)} + e^{-\beta(-J_1-J_2+J_3+J_4-J_5-J_6)} \big) , \end{aligned} \tag{5.4}$$

where $\{s\}$ denotes the sum over all the spin configurations and with $H_J(s)$ introduced with eq.(5.1).

Now, using the probability distribution function (5.2), we can average over the disorder.

$$\overline{\ln(Z_J(\beta))} = \left(\frac{1}{2\pi\sigma^2}\right)^3 \int dJ_1 \dots dJ_6 P(J_1, \dots, J_6) \left(\sum_{\{s\}} e^{-\beta H_J(s)} \right), \tag{5.5}$$

We show in Fig. 5.1 how $\overline{\ln(Z_J(\beta))}$ behaves when β varies between 0 and 1. It has a trend similar to the behavior $\overline{\ln(Z_J(\beta))}$ computed for the $N = 3$ spin

system (see Fig. 2.1). Also in this case, as already carried out in Sec. 4.1, the saddle point approximation will be used for the estimation of the ground state energy value of the system:

$$\begin{aligned} \overline{\ln(Z_J(\beta))} =& \overline{\ln \sum_{\{s\}} e^{-\beta H_J(s)}} \simeq \overline{\ln e^{-\beta H_0}} = -\beta E_0, \\ \text{with} \quad & E_0 = \overline{\min_{\{s\}}[H_J(s)]}. \end{aligned} \tag{5.6}$$

5.2 The replica approach

Also for the $N = 4$ spin system we can exploit the replica procedure encountered in Chapter 2. We rewrite equations (2.11) and (2.12) for our system:

$$g_n(\beta) \equiv \frac{1}{n} \ln \overline{Z_J(\beta)^n}, \tag{5.7}$$

$$\overline{f_J(\beta)} = -\frac{1}{N\beta} \lim_{n \to 0} g_n(\beta). \tag{5.8}$$

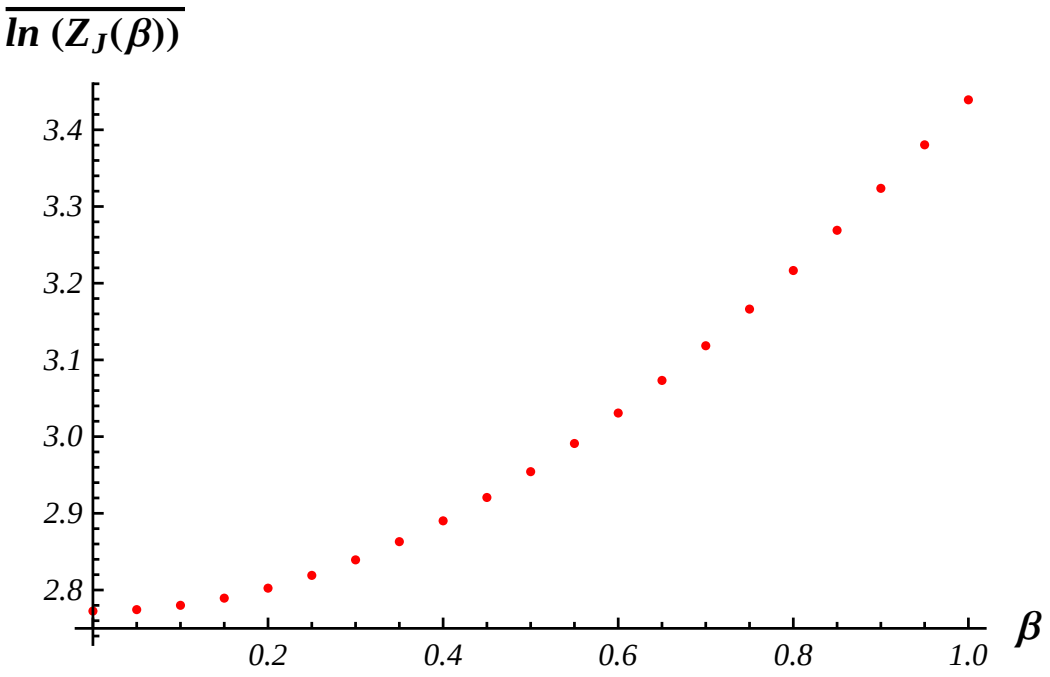

Figure 5.1: The red points are the values numerically computed for $\overline{\ln(Z_J(\beta))}$. The behavior is linear for $\beta \gtrsim 0.8$. The slope is the value of the energy ground state according to (2.8)

We shall set $N = 4$ in eq.(5.8). The n^{th} power of the partition function (5.4) can be calculated using the Multinomial Theorem (A.2):

$$\begin{aligned} Z_J(\beta)^n = \left(\sum_{\{s\}} e^{-\beta H_J(s)} \right)^n = 2^n \sum_{|\vec{K}|=n} \frac{n}{k_1!k_2!k_3!k_4!k_5!k_6!k_7!k_8!} \\ \times e^{-\beta(J_1+J_2+J_3+J_4+J_5+J_6)k_1} e^{-\beta(J_1+J_2-J_3+J_4-J_5-J_6)k_2} \\ \times e^{-\beta(J_1-J_2+J_3-J_4+J_5-J_6)k_3} e^{-\beta(-J_1+J_2+J_3-J_4-J_5+J_6)k_4} \\ \times e^{-\beta(-J_1-J_2-J_3+J_4+J_5+J_6)k_5} e^{-\beta(J_1-J_2-J_3-J_4-J_5+J_6)k_6} \\ \times e^{-\beta(-J_1+J_2-J_3-J_4+J_5-J_6)k_7} e^{-\beta(-J_1-J_2+J_3+J_4-J_5-J_6)k_8}, \end{aligned} \tag{5.9}$$

where the vector $\vec{K}$ has been introduced:

$$\vec{K} = (k_1, k_2, k_3, k_4, k_5, k_6, k_7, k_8).$$

The summation in eq.(5.9) is made on all the configurations of $\vec{K}$:

$$|\vec{K}| = \sum_{i=1}^{8} k_i = n. \tag{5.10}$$

This constraint is satisfied imposing the following condition:

$$\begin{aligned} |\vec{K}| = \sum_{i=1}^{8} k_i = \sum_{i=1}^{7} k_i + k_8 = n \Rightarrow \\ \sum_{i=1}^{7} k_i = n - k_8 \leq n, \end{aligned} \tag{5.11}$$

since k_8 can assume all the values between 0 and n. Introducing:

$$\begin{aligned} \vec{k} &= (k_1, k_2, k_3, k_4, k_5, k_6, k_7) \\ \text{with} \quad |\vec{k}| &= \sum_{i=1}^{7} k_i, \end{aligned} \tag{5.12}$$

the n^{th} power of eq.(5.4) can be written as follows:

$$\begin{aligned} Z_J(\beta)^n = \left(\sum_{\{s\}} e^{-\beta H_J(s)} \right)^n &= 2^n \sum_{|\vec{k}| \leq n} \binom{n}{\vec{k}} \\ &\times e^{-\beta(J_1+J_2+J_3+J_4+J_5+J_6)k_1} e^{-\beta(J_1+J_2-J_3+J_4-J_5-J_6)k_2} \\ &\times e^{-\beta(J_1-J_2+J_3-J_4+J_5-J_6)k_3} e^{-\beta(-J_1+J_2+J_3-J_4-J_5+J_6)k_4} \\ &\times e^{-\beta(-J_1-J_2-J_3+J_4+J_5+J_6)k_5} e^{-\beta(J_1-J_2-J_3-J_4-J_5+J_6)k_6} \\ &\times e^{-\beta(-J_1+J_2-J_3-J_4+J_5-J_6)k_7} e^{-\beta(-J_1-J_2+J_3+J_4-J_5-J_6)(n-|\vec{k}|)} \\ =2^n \sum_{|\vec{k}| \leq n} \binom{n}{\vec{k}} & e^{\beta J_1(2k_4+2k_5+2k_7-n)} e^{\beta J_2(2k_3+2k_5+2k_6-n)} \\ &\times e^{-\beta J_3(2k_1+2k_3+2k_4-n)} e^{-\beta J_4(2k_1+2k_2+2k_5-n)} \\ &\times e^{\beta J_5(2k_2+2k_4+2k_6-n)} e^{\beta J_6(2k_2+2k_3+2k_7-n)}, \end{aligned} \tag{5.13}$$

where:

$$\binom{n}{\vec{k}} = \frac{n}{k_1! \ldots k_7!(n-k_1-\ldots-k_7)!} \tag{5.14}$$

is the multinomial coefficient. Let us proceed by averaging eq.(5.13) over the disorder, using eq.(5.2):

$$
\begin{aligned}
\overline{Z_J(\beta)^n} =& \int P(J_1,\ldots,J_6) Z_J(\beta)^n dJ_1 \ldots dJ_6 \\
=& \left(\frac{1}{2\pi\sigma^2}\right)^3 \int e^{-\frac{1}{2\sigma^2}(J_1^2+J_2^2+J_3^2+J_4^2+J_5^2+J_6^2)} Z_J(\beta)^n dJ_1 \ldots dJ_6 \\
=& \left(\frac{1}{2\pi\sigma^2}\right)^3 2^n \sum_{|\vec{k}|\le n} \binom{n}{\vec{k}} \int_{-\infty}^{\infty} e^{-\frac{J_1^2}{2\sigma^2}} e^{\beta J_1(2k_4+2k_5+2k_7-n)} dJ_1 \\
& \times \int_{-\infty}^{\infty} e^{-\frac{J_2^2}{2\sigma^2}} e^{\beta J_2(2k_3+2k_5+2k_6-n)} dJ_2 \\
& \times \int_{-\infty}^{\infty} e^{-\frac{J_3^2}{2\sigma^2}} e^{-\beta J_3(2k_1+2k_3+2k_4-n)} dJ_3 \\
& \times \int_{-\infty}^{\infty} e^{-\frac{J_4^2}{2\sigma^2}} e^{-\beta J_4(2k_1+2k_2+2k_5-n)} dJ_4 \\
& \times \int_{-\infty}^{\infty} e^{-\frac{J_5^2}{2\sigma^2}} e^{\beta J_5(2k_2+2k_4+2k_6-n)} dJ_5 \\
& \times \int_{-\infty}^{\infty} e^{-\frac{J_6^2}{2\sigma^2}} e^{\beta J_6(2k_2+2k_3+2k_7-n)} dJ_6 \\
=& 2^n \sum_{|\vec{k}|\le n} \binom{n}{\vec{k}} e^{\frac{\sigma^2}{2}\beta^2(2k_4+2k_5+2k_7-n)^2} e^{\frac{\sigma^2}{2}\beta^2(2k_3+2k_5+2k_6-n)^2} \\
& \times e^{\frac{\sigma^2}{2}\beta^2(2k_1+2k_3+2k_4-n)^2} e^{\frac{\sigma^2}{2}\beta^2(2k_1+2k_2+2k_5-n)^2} \\
& \times e^{\frac{\sigma^2}{2}\beta^2(2k_2+2k_4+2k_6-n)} e^{\frac{\sigma^2}{2}\beta^2(2k_2+2k_3+2k_7-n)^2} \\
=& 2^n \sum_{|\vec{k}|\le n} \binom{n}{\vec{k}} e^{\frac{\sigma^2}{2}\beta^2 r^2(n,\vec{k})}.
\end{aligned}
\tag{5.15}
$$

Here we have performed a Gaussian integration (see eq.(2.19)), and introduced:

$$
\begin{aligned}
r^2(n,\vec{k}) =& (2k_4+2k_5+2k_7-n)^2 + (2k_3+2k_5+2k_6-n)^2 \\
& + (2k_1+2k_3+2k_4-n)^2 + (2k_1+2k_2+2k_5-n)^2 \\
& + (2k_2+2k_4+2k_6-n)^2 + (2k_2+2k_3+2k_7-n)^2,
\end{aligned}
\tag{5.16}
$$

that is the analogous of $r^2(n, \vec{k})$ encountered for the $N = 3$ spin system in eq.(2.21). As before, $r^2(n, \vec{k})$ is the summation of $\frac{N(N-1)}{2}$ terms, each deriving from a Gaussian integral and containing a n^2 term.

The pressure for a system of 4 spins is then:

$$\begin{aligned} g_n(\beta) &= \frac{1}{n} \ln \left(\overline{Z_J(\beta)^n} \right) \\ &= \frac{1}{n} \ln \left(2^n \sum_{|\vec{k}| \leq n} \binom{n}{\vec{k}} e^{\frac{\sigma^2}{2} \beta^2 r^2(n, \vec{k})} \right). \end{aligned} \tag{5.17}$$

Comparing this result with eq.(2.22) encountered at the end of Sec. 2.2, it can be noted the analogy with the case $N = 3$. Indeed, apart from the number of terms in the summation, the pressure has the same form, and in the $n \to \infty$ limit we can approximate $g_n(\beta)$ with the leading term of the summation, achieved at $\vec{k} = (0, 0, 0, 0, 0, 0, 0)$.

5.3 The $n \to \infty$ and $\beta \to \infty$ limits

In this section, we estimate the behavior of $\overline{\ln(Z_J(\beta))}$ and of $\overline{f_J(\beta)}$ within the $\beta \to \infty$ limit, following the same method used in the previous chapters. In short, knowing from Fig. 5.1 that $\overline{\ln(Z_J(\beta))}$ assumes a linear behavior for $\beta \gtrsim 0.6$, we write an asymptotic equation similar to (3.19) for $\overline{\ln(Z_J(\beta))}$:

$$\overline{\ln(Z_J(\beta))} \sim c_0^{(m)} + \left(\frac{\tilde{\epsilon}}{\beta} \right) c_1^{(m)}(\beta), \quad \text{for } \beta \text{ large}, \tag{5.18}$$

where, $c_0^{(m)}$ is a constant value, while for the first order coefficient $c_1^{(m)}(\beta)$, we suppose that eq.(4.46) still holds for a system of 4 spins, hence, it can be expressed as a partial derivative of the pressure (5.17) with respect to n:

$$c_1^{(m)}(\beta) \simeq \frac{\partial(g_n(\beta))}{\partial n}. \tag{5.19}$$

In eq.(5.18) we have utilized $\tilde{\epsilon} = \frac{\epsilon}{\sigma}$ instead of ϵ (cfr. (3.5)) since we have supposed that the value of $\tilde{\epsilon}$ is independent of the number of spins. It is possible to write:

$$\tilde{\epsilon} = \frac{\epsilon_N}{\sigma} = \sqrt{N}\epsilon, \tag{5.20}$$

with $\sigma = \frac{1}{\sqrt{N}} = \frac{1}{\sqrt{4}}$ from eq.(1.11). Thus, for $N = 4$ we can introduce a new constant:

$$\epsilon_4 = \sigma\tilde{\epsilon} = \frac{\tilde{\epsilon}}{\sqrt{4}} = \frac{2.38}{2} = 1.19. \tag{5.21}$$

Gathering these results and, using eq.(5.6), we obtain that:

$$\overline{\ln(Z_J(\beta))} \sim c_0^{(m)} + \left(\frac{\epsilon_4}{\sigma\beta}\right)\frac{\partial g_n(\beta)}{\partial n}, \quad \text{for } \beta \text{ large}, \tag{5.22a}$$

$$\begin{aligned} E_0 &= -\lim_{\beta\to\infty}\frac{1}{\beta}\overline{\ln(Z_J(\beta))} = -\lim_{\beta\to\infty}\frac{\epsilon_4}{\sigma\beta^2}c_1^{(m)}(\beta) \\ &\simeq -\lim_{\beta\to\infty}\frac{\epsilon_4}{\sigma\beta^2}\frac{\partial g_n(\beta)}{\partial n}. \end{aligned} \tag{5.22b}$$

having neglected the term containing $c_0^{(m)}(\beta)$ in eq.(5.22b), since it behaves like $\frac{1}{\beta}$ in the $\beta \to \infty$ limit.

Also for $N = 4$ spins, we seek the expression of $\frac{\partial g_n(\beta)}{\partial n}$, by taking the $n \to \infty$ limit. In this limit, $g_n(\beta)$ can be approximated by the leading term in the summation (5.17).

This can be done by recalling all the calculations performed in Sec. 4.3, from eq.(4.53) to eq.(5.28). It is necessary to consider the expression of $\overline{Z_J(\beta)^n}$ calculated in eq.(5.15), to rewrite it in a scaled form with respect to n and then to take the $n \to \infty$ limit:

$$\begin{aligned}\overline{Z_J(\beta)^n} =& 2^n \sum_{|\vec{k}|\leq n} \binom{n}{\vec{k}} e^{\frac{\sigma^2}{2}\beta^2 r^2(n,\vec{k})} \\ =& 2^n \sum_{|\vec{t}|\leq n} \binom{n}{n\vec{t}} e^{\frac{\sigma^2}{2}\beta^2 n^2 w^2(n,\vec{k})},\end{aligned} \tag{5.23}$$

where the vector $\vec{t}$ has been introduced, such that:

$$\begin{aligned}&\vec{t} = (t_1, \ldots, t_7) \quad \text{with} \quad t_i = \frac{k_i}{n} \quad \forall i \\ &\text{and} \quad |\vec{t}| = \sum_{i=1}^{7} t_i = \frac{1}{n}|\vec{k}| \leq 1.\end{aligned} \tag{5.24}$$

With this choice, using the Stirling approximation in the $n \to \infty$ limit, we have:

$$\begin{aligned}
\ln \binom{n}{n\vec{t}} =& \ln \left(\frac{n!}{(n(1-t))! \prod_{i=1}^{7} (nt_i)!} \right) \\
\simeq& n \ln n - n + \frac{1}{2} \ln 2\pi n \\
& - \sum_{i=1}^{7} \left(nt_i \ln(nt_i) - nt_i + \frac{1}{2} \ln(2\pi n t_i) \right) \\
& - n(1-t) \ln n(1-t) + n(1-t) - \frac{1}{2} \ln 2\pi n(1-t) \\
=& - n \sum_{i=1}^{7} t_i \ln(t_i) - \frac{1}{2} \ln \frac{1}{(2\pi n)^7 \prod_{i=1}^{7} t_i (1-t)}.
\end{aligned} \tag{5.25}$$

So, we get:

$$\lim_{n \to \infty} \binom{n}{n\vec{t}} = \frac{1}{\sqrt{(2\pi n)^7 \prod_{i=1}^{7} t_i (1-t)}} e^{-nS(\vec{t})}, \tag{5.26}$$

where we have introduced:

$$S(\vec{t}) = \sum_{i=1}^{7} t_i \ln(t_i). \tag{5.27}$$

In the limit of an infinite number of replicas n, the Eq.(5.23) becomes:

$$\overline{Z_J(\beta)^n} \simeq \sum_{|\vec{t}| \leq 1} \frac{1}{\sqrt{(2\pi n)^3 \prod_{i=1}^{7} t_i (1-t)}} e^{-nS(\vec{t})} e^{\frac{\beta^2 \sigma^2 n^2}{2} w^2(\vec{t})}, \quad \text{for } n \to \infty. \tag{5.28}$$

The leading term in (5.17) is achieved by choosing:

$$\vec{k} = (0, 0, 0, 0, 0, 0, 0), \tag{5.29}$$

where, the function $r^2(n, \vec{k})$ reaches its maximum value while the multinomial coefficient is equal to 1:

$$r^2(n, \vec{0}) = 6n^2, \tag{5.30}$$

$$\binom{n}{\vec{k}} = 1. \tag{5.31}$$

Thus, in the limit $n \to \infty$, the quenched n^{th} power of the partition function becomes:

$$\begin{aligned} \lim_{n\to\infty} \overline{Z_J(\beta)^n} &= \lim_{n\to\infty} 2^n \sum_{|\vec{k}|\leq n} \binom{n}{\vec{k}} e^{\frac{\sigma^2}{2}\beta^2 r^2(n,\vec{k})} \\ &\simeq \lim_{n\to\infty} 2^n e^{\frac{\sigma^2}{2}\beta^2 6n^2}. \end{aligned} \tag{5.32}$$

The pressure becomes:

$$\begin{aligned} \lim_{n\to\infty} g_n(\beta) &= \lim_{n\to\infty} \frac{1}{n} \ln(\overline{Z_J(\beta)^n}) \\ &= \lim_{n\to\infty} \frac{1}{n} \ln\left(2^n e^{\frac{\sigma^2}{2}\beta^2 6n^2}\right) \\ &= \ln(2) + \frac{1}{n} 3\sigma^2\beta^2 n^2 \Rightarrow \\ &\Rightarrow \quad g_n(\beta) \simeq 3\sigma^2\beta^2 n, \quad \text{when } n \to \infty. \end{aligned} \tag{5.33}$$

We can use eq.(5.33) and obtain a simple expression of $\overline{\ln(Z_J(\beta))}$, $\overline{f_J(\beta)}$ and E_0. Looking respectively at the equations (5.22a), (5.3) and (5.22b), we have

that:

$$\overline{\ln(Z_J(\beta))} \sim c_0^{(m)} + \frac{\epsilon_4}{\sigma\beta}\frac{\partial g_n(\beta)}{\partial n} = c_0^{(m)} + 3\sigma\epsilon_4\beta \quad \text{, for } \beta \text{ large,} \tag{5.34a}$$

$$E_0 \simeq -\lim_{\beta\to\infty}\frac{\epsilon_4}{\sigma\beta^2}\frac{\partial g_n(\beta)}{\partial n} = -\lim_{\beta\to\infty} 3\sigma\epsilon = -3\sigma\epsilon_4, \tag{5.34b}$$

$$\lim_{\beta\to\infty}\overline{f_J(\beta)} = -\frac{1}{N}\lim_{\beta\to\infty} -\frac{1}{\beta}\overline{\ln(Z_J(\beta))} = -\frac{3\sigma\epsilon_4}{N}. \tag{5.34c}$$

In Fig. 5.2, we show the agreement between the numerical value computed for $\overline{\ln(Z_J(\beta))}$ and the value obtained from eq.(5.34a), having set $\sigma = \frac{1}{\sqrt{N}} = \frac{1}{2}$,

$$\overline{\ln(Z_J(\beta))} \sim \frac{3}{2}\epsilon_4\beta = 1.79\beta, \quad \text{for } \beta \text{ large.} \tag{5.35}$$

The numerical result for the slope of $\overline{\ln(Z_J(\beta))}$ is 1.81. The difference between these two values is about 1.1%.

Fig. 5.2 is analogous to Fig. 3.6. The difference is that here we have dropped the 0^{th} term $c_0^{(m)}(\beta)$ in eq.(3.18), that is nonessential to calculation the free energy ground state.

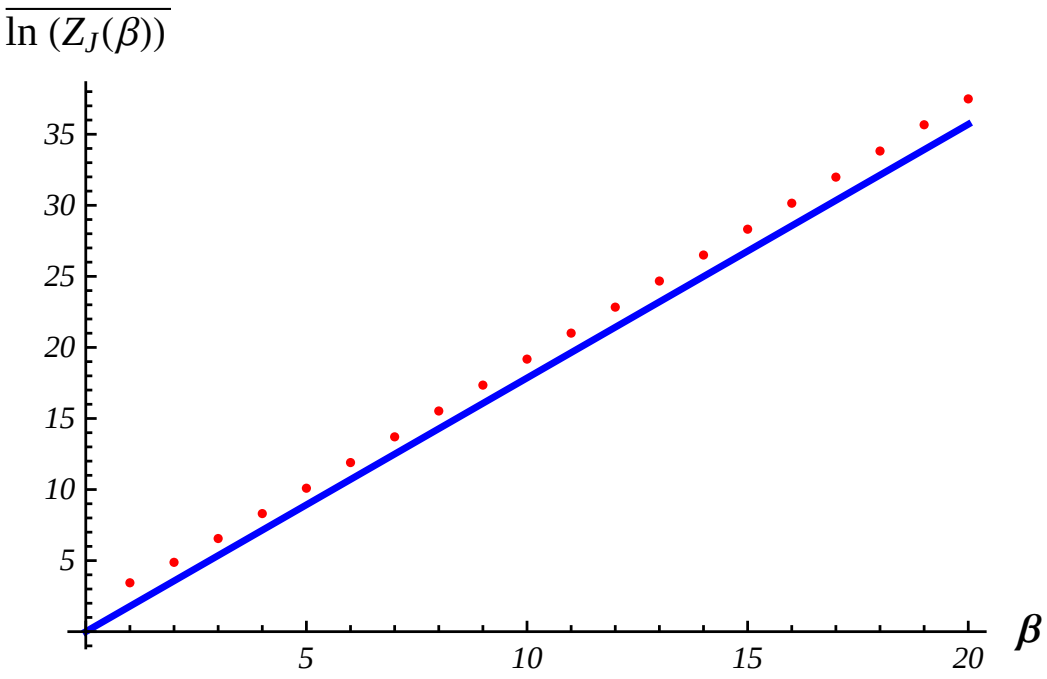

Figure 5.2: The red points are the numerical values computed for $\overline{\ln(Z_J(\beta))}$ (eq.(5.5) and Fig. 5.1. The blue line has slope $\frac{3}{2}\epsilon_4\beta = 1.79\beta$ as in eq.(5.34a)

5.4 N-spin systems

For a system of N spins, we can generalize what was stated in the last section. The Hamiltonian, the partition function and the quenched free energy density are, respectively:

$$H_J(s) = \sum_{\langle i,j \rangle} J_{ij} s_i s_j, \tag{5.36}$$

$$Z_J(\beta)_J(\beta) = \sum_{\{s\}} e^{-\beta H_J(s)}, \tag{5.37}$$

$$\overline{f_J(\beta)} = -\frac{1}{\beta N} \overline{\ln(Z_J(\beta))}, \tag{5.38}$$

where the summation over $\langle i, j \rangle$ is made over all the distinct pairs of spins and the symbol $\overline{(\dots)}$ denotes the quenched average introduced in Sec. 1.2. We shall write $Z_J(\beta)$ instead of $Z_J(\beta)$ hereafter.

The Hamiltonian is symmetric with respect to the spin flip operator (1.12), hence, the relevant spin configurations are 2^{N-1} and the number of interactions between spins is equal to the number of couplings, i.e.:

$$N_c = \frac{N(N-1)}{2}.$$

The probability distribution introduced in eq.(1.3) reads:

$$P(J_1, \dots, J_{N_c}) = \left(\frac{1}{2\pi\sigma^2} \right)^{\frac{N_c}{2}} \exp\left\{ -\frac{J_1^2 + J_2^2 + \cdots + J_{N_c}^2}{2\sigma^2} \right\}. \tag{5.39}$$

We introduce the pressure:

$$g_n(\beta) = \frac{1}{n}\overline{\ln(Z_J(\beta)^n)}, \tag{5.40}$$

and we know that $g_n(\beta)$ can be expressed in a form similar to eq.(2.22) and to eq.(5.17):

$$g_n(\beta) = \frac{1}{n}\ln\left(2^n \sum_{|\vec{k}|\leq n} \binom{n}{\vec{k}} e^{\frac{\sigma^2}{2}\beta^2 r^2(n,\vec{k})}\right), \tag{5.41}$$

where, the summation is done over all the configuration of the vector $\vec{k}$:

$$\vec{k} = (k_1, k_2, \ldots, k_{N_s}), \quad \text{with } N_s = 2^{N-1} - 1,$$

such that:

$$|\vec{k}| = \sum_{i=1}^{N_s} k_i \leq n. \tag{5.42}$$

$r^2(n,\vec{k})$, instead, is the summation of N_c terms, each of them containing a n^2 term which derives from a Gaussian integral (see Sec. 2.2 and Sec. 5.2). Let us now assume that, as an educated guess, within the $n \to \infty$ limit, we can approximate the summation over $|\vec{k}|$, in the previous equation, with an unique term obtained by choosing $\vec{k} = (0, 0, \ldots, 0)$:

$$r^2(n,\vec{k}) = N_c n^2.$$

With this choice of $\vec{k}$ the multinomial factor is:

$$\binom{n}{\vec{k}} = \frac{n!}{\prod_{i=1}^{N_s} k_i!(n - \sum_{i=1}^{N_s} k_i)!} = 1,$$

and, neglecting the $\ln(2)$, we have:

$$\lim_{n\to\infty} \overline{Z_J(\beta)^n} \simeq e^{\frac{\sigma^2\beta^2}{2} r^2(n,\vec{0}).} \tag{5.43}$$

The pressure behaves then as follows:

$$g_n(\beta) \simeq \frac{1}{n} \ln\left(e^{\frac{\sigma^2\beta^2}{2} r^2(n,\vec{0})}\right) = \frac{1}{n}\frac{\sigma^2\beta^2}{2} r^2(n,\vec{0}) = \frac{\sigma^2\beta^2}{2} N_c n. \tag{5.44}$$

We then rewrite eq.(5.22b), eq.(5.34a) and eq.(5.34c) for a generic N-spin system:

$$\begin{aligned} E_0 &\simeq -\frac{\epsilon_N}{\sigma} \lim_{\beta\to\infty} \frac{1}{\beta^2} \frac{\partial g_n(\beta)}{\partial n} \\ &= -\frac{\epsilon_N}{\sigma} \lim_{\beta\to\infty} \frac{1}{\beta^2} \frac{\sigma^2\beta^2}{2} N_c = \frac{\epsilon_N N_c}{2}\sigma, \end{aligned} \tag{5.45a}$$

$$\overline{\ln(Z_J(\beta))} \sim \frac{\epsilon_N}{\sigma\beta} \frac{\partial g_n(\beta)}{\partial n} = \frac{N_c}{2}\sigma\epsilon_N\beta, \quad \text{for large } \beta, \tag{5.45b}$$

$$\begin{aligned} \overline{f_J(\beta)} &= -\frac{\epsilon_N}{N\sigma\beta^2} \frac{\partial g_n(\beta)}{\partial n} = -\frac{(N-1)}{4}\sigma\epsilon_N \\ &= -\frac{(N-1)}{4}\sigma^2\tilde{\epsilon} = -\frac{(N-1)}{4N}\tilde{\epsilon}. \end{aligned} \tag{5.45c}$$

$\overline{f_J(\beta)}$ becomes independent of N (as it must be, look at Sec. 1.2 for large values of N, if we set $\sigma^2 = \frac{1}{N}$. The total *free energy* is, for $N >> 1$

$$F = N\overline{f_J(\beta)} \simeq -\frac{N}{4}\tilde{\epsilon}, \tag{5.46}$$

with $\tilde{\epsilon} = 2.38$ from eq.(3.5). This equation depends only on the dimension of the system and has been derived by using the proprieties of the probability distribution function eq.(1.3). It is independent of β, because this dependence disappears within the limit of low temperature. We remark that all the previous expressions have been obtained without explicitly computing the partition function.

Conclusions

In this thesis, we have succeeded in finding a good estimation for the computation of the ground state energy value (5.46) for a finite size spin glass described by the Hamiltonian (4.2) with a probability distribution function for the coupling constants given by (1.3).

Since the system is disordered all thermodynamic functions must be averaged over the disorder (cfr. Sec. 1.2) and this makes the calculations difficult. The free energy is:

$$\overline{f_J(\beta)} = -\frac{1}{N\beta}\overline{\ln(Z_J(\beta))},$$

where $Z_J(\beta)$ is the partition function of the system (see eq.(1.4)) and $\overline{(\dots)}$ denotes the quenched average discussed in Sec. 1.2. To simplify the problem, the replica trick was introduced in Chapter 1 (see eq.(1.23)):

$$\overline{\ln(Z_J(\beta))} = \lim_{n\to 0}\frac{1}{n}\ln(\overline{Z_J(\beta)^n}).$$

The first step has been to define the pressure $g_n(\beta)$ (eq.(2.11)) for an $N = 3$ spin system, i.e., the quenched free energy of the system in the replica

approximation, scaled with respect to the number of spins N and to the temperature $\frac{1}{\beta}$:

$$g_n(\beta) = \frac{1}{n} \ln(\overline{Z_J(\beta)^n}),$$

in such a way that:

$$\overline{f_J(\beta)} = -\frac{1}{N\beta} \lim_{n\to 0} g_n(\beta).$$

In Sec. 2.3, we introduced the polynomials $Q_m(x, \beta)$ as interpolating functions for the pressure $g_n(\beta)$ (eq.(2.25)). They were defined in such a way that they assume the same value of the pressure $g_n(\beta)$ when $x = n$, n being an integer index:

$$Q_m(x, \beta) = \sum_{j=1}^{m} g_j(\beta) \prod_{\substack{i=1 \\ i\neq j}} \frac{(x-i)}{(j-i)},$$

$$Q_m(n, \beta) = g_n(\beta), \quad \forall n \in \mathbb{N},$$

(see Sec. 2.3). We expected to gain some insight into the behavior of $g_n(\beta)$ when n goes to 0 by analyzing the polynomials $Q_m(x, \beta)$ with $x = 0$. Instead, these polynomial were found to fail in the approximation of $\overline{\ln(Z_J(\beta))}$ (See Fig. 2.5).

Consequently, in the third chapter we analyzed the behavior of $Q_m(x, \beta)$ with $x \neq 0$. In Sec. 3.3 the polynomials $Q_m(x, \beta)$ were rewritten showing their explicit dependence on x (eq.(3.9)):

$$Q_m(x, \beta) = \sum_{i=0}^{m} c_i^{(m)}(\beta) x^i.$$

In Sec. 3.2, by solving numerically eq.(3.1):

$$\overline{\ln(Z_J(\beta))} = Q_m(x, \beta),$$

we have found eq.(3.3):

$$x(\beta) = \frac{\tilde{\epsilon}}{\beta} = \frac{\epsilon_N}{\sigma\beta}, \quad \beta \gg \eta,$$

with ϵ_N dependent on the dimension of the system. Substituting in the first order approximation of $Q_m(x, \beta)$ the value of x obtained with the function $x(\beta)$ for large β, we get a new class of functions, namely $\Theta_m(\beta)$, that has been introduced by eq.(3.18):

$$\Theta_m(\beta) = c_0^{(m)} + c_1^{(m)}(\beta)\frac{\epsilon_N}{\sigma\beta},$$

in such a way that:

$$\overline{\ln(Z_J(\beta))} \sim \Theta_m(\beta), \quad \text{when } \beta \to \infty.$$

The 0^{th} order coefficient can be obtained from the second of equations (3.11), while, a sensible expression for the first order coefficient $c_1^{(m)}(\beta)$ has been found in Sec. 4.2, eq.(4.46):

$$c_1^{(m)}(\beta) \simeq \frac{\partial g_n(\beta)}{\partial n}.$$

In Sec. 4.3, the $n \to \infty$ limit was analyzed, and the following expression for $g_n(\beta)$ was found:

$$g_n(\beta) \simeq \frac{\sigma^2\beta^2}{2n} r^2(n, \vec{0}) = \frac{\sigma^2\beta^2}{2} N_c n,$$

since $r^2(n, \vec{0}) = N_c n^2$, with N_c denoting the number of couplings between spins, i.e. $N_c = \frac{N(N-1)}{2}$.

In this way, the following expressions, within the limit $\beta \to \infty$ were obtained:

$$\overline{\ln(Z_J(\beta))} \sim \frac{\epsilon}{\sigma\beta} \frac{\partial g_n(\beta)}{\partial n} = \frac{N_c}{2} \sigma \epsilon_N \beta, \quad \text{for large } \beta,$$

$$\overline{f_J(\beta)} = -\frac{\epsilon_N}{N\sigma\beta^2} \frac{\partial g_n(\beta)}{\partial n} = -\frac{(N-1)}{4N} \tilde{\epsilon},$$

$\tilde{\epsilon}$ being numerically found to be independent on the dimension of the system found in Sec.(3.2). The total free energy was found to be, for $N >> 1$:

$$F = N\overline{f_J(\beta)} \simeq -\frac{N}{4}\tilde{\epsilon}$$

Moreover, from (4.1b):

$$\overline{\ln(Z_J(\beta))} = \overline{\ln \sum_{\{s\}} e^{-\beta H_J(s)}} \simeq \overline{\ln e^{-\beta H_0}} = -\beta E_0$$
$$\text{with} \quad E_0 = \overline{\min_{\{s\}}[H_J(s)]} \qquad ,$$

we obtained a useful expression for the evaluation of the ground state energy value of the system E_0. The dependence of $\overline{\ln(Z_J(\beta))}$ on β is linear for $\beta \to \infty$, as was already evident from the figures (2.1) and (5.1). Gathering the latter results, we obtained:

$$E_0 - \lim_{\beta\to\infty} \frac{\sigma\epsilon_N}{\beta^2} c_1^{(m)}(\beta) \simeq - \lim_{\beta\to\infty} \frac{\sigma\epsilon_N}{\beta^2} \frac{\partial g_n(\beta)}{\partial n} = - \lim_{\beta\to\infty} \frac{\epsilon_N}{\beta^2} \frac{N(N-1)}{4} \sigma\beta^2,$$

having neglected the term containing $c_0^{(m)}(\beta)$ which reaches a constant value when β goes to ∞ (see Sec. 2.4). The free energy density becomes:

$$\overline{f_J(\beta)} = -\frac{\sigma\epsilon_N}{N\beta^2} \frac{\partial g_n(\beta)}{\partial n} = -\frac{(N-1)}{4} \sigma\epsilon_N.$$

The $\tilde{\epsilon}$ parameter has been introduced and determined through numerical computation in Sec. 3.2 and has been found to be:

$$\tilde{\epsilon} = \sqrt{N}\epsilon_N \simeq 2.38.$$

ϵ_N has thus a precise meaning, it is a coefficient that links the energy density of the system $\overline{f_J(\beta)}$ with its dimension N. Its value depends on the probability distribution function used ($P(J)$, eq.(1.3)), thus on the kind of interaction analyzed. By choosing $\sigma^2 = \frac{1}{N}$, the free energy density $\overline{f_J(\beta)}$ becomes independent on the dimension of the system N.

Let us briefly comment on short range systems.

As we have noted in Chapter 2, for a 3-spin system there is no difference between a short and a long-range model. When we take larger systems this difference becomes evident. By changing the probability distribution function $P(J)$, it changes the way of averaging, thus all the quantity computed are different (eq.(1.7)).

Moreover, the number of interaction does no longer grow as

$$\frac{N(N-1)}{2}$$

but grows in a way which is dependent on the strength of the interaction between spins. We wonder whether it would be possible to write a formula like eq.(3.18) also in this case, and hence, to adopt the same technique introduced here.

Appendix A

Multinomial Theorem

A.1 Binomial Theorem

The n^{th} power of a binomial can be written as:

$$\begin{aligned}(x+y)^n =& \underbrace{(x+y)\dots(x+y)}_{\text{n times}} \\ =& x^n + a_{n,1}x^{n-1}y + a_{n,2}x^{n-2}y^2 + \dots a_{1,n-1}xy^{n-1} + y^n,\end{aligned} \tag{A.1}$$

where $a_{i,j}$ represents the number of times that the element

$$e_1 e_2 \dots e_n$$

appears in the sum, in which each e_k can be x or y, with x repeated i times and y repeated j times, and with $i + j = n$.

We have to compute the number of possible way of placing the elements of a

string made of n elements (equals to x or to y) in such a way to have i times x and j times y, without ordering. This is the number of disposition of k elements in a class on n elements, divided by the number of permutation of the k elements to account for all repetitions, i.e. the binomial coefficient:

$$a_{n-k,k} = \binom{n}{k} = \frac{n!}{k!(n-k)!}. \tag{A.2}$$

The previous formula becomes:

$$\begin{aligned}(x+y)^n &= x^n + \binom{n}{1}x^{n-1}y + \binom{n}{2}x^{n-2}y^2 + \dots \binom{n}{n-1}xy^{n-1} + y^n = \\ &= \sum_{k=0}^{n}\binom{n}{k}x^{n-k}y^k.\end{aligned} \tag{A.3}$$

This result is known as the Binomial Theorem.

A.2 Multinomial Theorem

The multinomial theorem states that:

$$(\sum_{i=1}^{m} x_i)^n = \sum_{\sum_{i=1}^{m} k_i = n} \binom{n}{k_1 k_2 \dots k_m} \prod_{i=1}^{m} x_i^{k_i}, \tag{A.4}$$

where the term:

$$\binom{n}{k_1 k_2 \dots k_m} = \frac{n!}{k_1! k_2! \dots k_m!}, \tag{A.5}$$

is the Multinomial Coefficient and reduces to the Binomial Coefficient (A.2) for $m = 1$:

$$\binom{n}{k} \equiv \frac{n!}{k!(n-k)!} \tag{A.6}$$

Proof. The theorem can be proved in different ways. Here we give a proof obtained by induction, using the Binomial Theorem.

By setting $m = 1$, we see that eq.(A.4) is trivially verified:

$$x_1^n = \sum_{k_1=n} \binom{n}{k_1} x_1^{k_1} = \binom{n}{n} x_1^n = x_1^n, \tag{A.7}$$

since:

$$\binom{n}{n} = 1. \tag{A.8}$$

Let us now suppose that eq.(A.4) holds for m, we shall show that it is true for $m + 1$:

$$\begin{aligned} (\sum_{i=1}^{m+1} x^i)^n &= \sum_{i=1}^{m-1} (x^i + (x_m + x_{m+1}))^n \\ &= \sum_{\sum_{i=1}^{m-1} k_i + p = n} \binom{n}{k_1 \dots k_{m-1} p} \prod_{i=1}^{m-1} x_i^{k_i} \cdot (x_m + x_{m+1})^p. \end{aligned} \tag{A.9}$$

By using the Binomial Theorem (A.3) for the last term:

$$(x_m + x_{m+1})^p = \sum_{q=0}^{p} \binom{p}{q} x_m^{p-q} x_{m+1}^q, \tag{A.10}$$

we obtain:

$$
\begin{aligned}
(\sum_{i=1}^{m+1} x^i)^n &= \sum_{\sum_{i=1}^{m-1} k_i + p = n} \binom{n}{k_1 \dots k_{m-1} p} \prod_{i=1}^{m-1} x_i^{k_i} \cdot \left(\sum_{q=0}^{p} \binom{p}{q} x_m^{p-q} x_{m+1}^q \right) \\
&= \sum_{\sum_{i=1}^{m-1} k_i + p = n} \sum_{q=0}^{p} \binom{n}{k_1 \dots k_{m-1} p} \binom{p}{q} \prod_{i=1}^{m-1} x_i^{k_i} \cdot x_m^{p-q} x_{m+1}^q
\end{aligned}
\tag{A.11}
$$

Since:

$$
\begin{aligned}
\binom{n}{k_1 \dots k_{m-1} p} \binom{p}{q} &= \frac{n!}{k_1! \dots k_{m-1}! p!} \, \frac{p!}{q!(p-q)!} \\
&= \frac{n!}{k_1! \dots k_{m-1}! \, q! \, (p-q)!} \\
&= \binom{n}{k_1 \dots k_{m-1} \, q \, (p-q)}
\end{aligned}
\tag{A.12}
$$

Now, by calling $p - q \equiv k_m$ and $q \equiv k_{m+1}$, we have that $p = k_m + k_{m+1}$, and:

$$
\sum_{i=1}^{m-1} k_i + p = \sum_{i=1}^{m+1} k_i = n. \tag{A.13}
$$

(A.11) is then:

$$
(\sum_{i=1}^{m+1} x^i)^n = \sum_{\sum_{i=1}^{m+1} k_i = n} \binom{n}{k_1 \dots k_{m+1}} \prod_{i=1}^{m+1} x_i^{k_i} \tag{A.14}
$$

q.e.d. $\square$

Bibliography

[1] P.W. Anderson and S.F. Edwards. Theory of spin glasses. *J. Phys.*, F 5(965), 1975.

[2] K. Binder and A.P. Young. Spin glasses: Experimental facts, theoretical concepts and open questions. *Rev. Mod. Phys.*, 58:801–976, 1986.

[3] V. Dotsenko. *An Introduction to the Theory of Spin Glasses and Neural Network*. World Scientific, 1994.

[4] M. Mezard, G. Parisi, and M. A. Virasoro. *Spin Glasses and beyond*. World Scientific Publishing, Singapore, 1987.

[5] H. Nishimori. *Statistical Physics of Spin Glasses and Information Processing, An Introduction*. Clarendon Press, Oxford, 2001.

[6] E. Orlandini, M.C. Tesi, and S.G. Whittington. Self-averaging in statistical mechanics of some lattice models. *J. Phys. A: Math*, (35):4219–4227, Gen. 2002.

[7] G. Parisi. Toward a mean field theory for spin glasses. *Phys. Lett.*, 73 A(3), 1979.

[8] G. Parisi. Magnetic properties of spin glasses in a new mean field theory. *J. Phys. A: Math*, 13, Gen. 1980.

[9] G. Parisi. The order parameter for spin glasses: A function on the interval 0-1. *J. Phys. A: Math*, 13, Gen. 1980.

[10] G. Parisi. A sequence of approximated solution to the s-k model for spin glasses. *J. Phys. A: Math*, 13(115), 1980.

[11] R. Rammal, G. Toulouse, and M. A. Virasoro. Ultrametricity fot physicists. *Rev. Mod. Phys.*, 58:765, 1986.

[12] D. Sherrington and S. Kirkpatrick. Solvable model of a spin glass. *Phys. Rev. Lett*, 35(26), Dec. 1975.

[13] D. Sherrington and S. Kirkpatrick. Infinite-ranged models of spin-glasses. *Phys. Rev. B*, 17(11), 1978.

[14] D.J. Thouless, R.G. Palmer, and P.W. Anderson. Solution of solvable model of spin glass. *Philosophical Magazine*, 35:593, 1977.

[15] E.C. Titchmarsh. *The theory of functions.* Oxford University Press, 1939.

[16] G. Toulouse. Theory of the frustration effect in spin glasses: I. *Communications in Physics 2*, 1977.